City University of Applied Sciences Bremen

Faculty 5 - Nature and Engineering

Aerospace Technologies (M.Sc.)

**Deutsches Zentrum
DLR für Luft- und Raumfahrt**
German Aerospace Center

HSB
Hochschule Bremen
City University of Applied Sciences

Master Thesis

Experimental Development of a Lunar Water Simulant and System Control of a Related Lunar Water Purification System

Victoria Pesch

Start Date:	27. January 2023
Submission Date:	30. June 2023
First Examiner:	Prof. Dr.-Ing. Uwe Apel
Second Examiner:	Prof. Dr.-Ing. Sven Oppermann

Abstract

This master thesis deals with the selection of a lunar water simulant based on the results of dissolution experiments and the system control via *LabVIEW* of a related lunar water purification system. The research questions are: What is the required composition for a lunar water simulant using lunar regolith simulant? How can the related lunar water purification system be controlled using a *LabVIEW* program?

Dissolution experiments are conducted to investigate possible contaminants of extracted water from the lunar surface. To determine a lunar water simulant, the methodology of the dissolution experiments and the results are described. For the dissolution experiments, ultrapure water or buffer solution with a pH of 5.6 are tested with the lunar regolith simulants LHS-1 and LMS-1 by *Exolith Lab*. This further includes lunar regolith simulant LHS-1D in an ambient and in a nitrogen atmosphere. These results provide new insights into the influences of pH, simulant to aqueous solution ratio, bulk chemistry, and simulant particle size on dissolution experiments. A lunar water simulant is selected, portraying the worst-case regarding released ions with a chosen lunar regolith simulant, simulant to aqueous solution ratio, and aqueous solution from all conducted dissolution experiments within the Synergetic Material Utilization (SMU) research group of the German Aerospace Center (DLR) Bremen.

It is further investigated how to control a related lunar water purification system via a *LabVIEW* program. For the lunar water purification system, the methodology, including control technology, selected measuring instruments, and sedimentation experiments, is explained. The results of the sedimentation experiments, the *LabVIEW* program and the first test of the lunar water purification system lead to estimates of the purification ability and optimisations of the lunar water purification system and the *LabVIEW* program.

These results can be used to test the lunar water purification system on Earth and to adapt the purification system to a fully automatic application with extracted lunar water.

Declaration of Authorship

I hereby certify that I have written this thesis independently and have not used any sources or aids other than those indicated. The passages in the work that have been taken from other works in terms of wording or meaning are indicated by the source.

This declaration also applies to graphics, sketches and illustrations contained in the thesis as well as to sources from the Internet.

I have not yet submitted the work in the same or similar form, even in part, as part of an examination or course assignment.

I certify that the submitted electronic version of the work is completely consistent with the print version.

<div align="center">

Victoria Pesch

5198023

28.6.2023

victoria.pesch@web.de

</div>

Contents

List of Abbreviations

ASTM	American Society for Testing and Materials
DAQ	Data Acquisition System
DLR	German Aerospace Center
EC	Electric Conductivity
ECLSS	Environmental Control and Life Support System
EU	European Union
g	gaseous
ICP-OES	Inductively Coupled Plasma Optical Emission Spectrometry
ICP/MS	Inductively Coupled Plasma Mass Spectronomy
IHOP	ISRU-derived water purification and Hydrogen Oxygen Production
ISRU	In-Situ Resource Utilization
ISS	International Space Station
l	liquid
LabVIEW	Laboratory Virtual Instrument Engineering Workbench
LCROSS	Lunar Crater Observation and Sensing Satellite
LS	Life Support
LUWEX	Validation of Lunar Water Extraction and Purification Technologies for In-Situ Propellant and Consumables Production
NASA	National Aeronautics and Space Administration
NI	National Instruments
NTU	Nephelometric Turbidity Unit
PEM	Polymer Electrolyte Membrane
PSR	Permanently Shadowed Region
RPM	Rotations Per Minute
SMU	Synergetic Material Utilization
SOEL	Solid Oxide Electrolyser

SOFIA Stratospheric Observatory For Infrared Astronomy

VISA Virtual Instrument Software Architecture

WHO World Health Organisation

XRF X-Ray Fluorescence

List of Symbols

$\dot{n}_{H2}$	Hydrogen Production Rate	$[\frac{mol}{s}]$
Δs	Standard Deviation	$[\frac{mg}{g_{solid}}/\frac{mg}{l_{aqueous}}]$
$\overline{x}$	Sample Mean Average	$[\frac{mg}{g_{solid}}/\frac{mg}{l_{aqueous}}]$
A_{cell}	Effective Cell Area	$[cm^2]$
F	Faraday Constant	$[\frac{C}{mol}]$
i_{cell}	Current Density	$[\frac{A}{cm^2}]$
I_{cell}	Stack Current	$[A]$
n	Sample Size	$[-]$
T	Temperature	$[^{\circ}C]$
$Wt.\%$	Weight Percentage	$[-]$
x	Sample Value	$[\frac{mg}{g_{solid}}/\frac{mg}{l_{aqueous}}]$
z	Number of Moles of Electrons Transferred in Reaction	$[-]$
c	Molarity	$[\frac{mol}{l}]$
EC	Electric Conductivity	$[\frac{\mu S}{cm}]$
t	Time	$[h/min/s]$
V	Volume	$[l/ml]$

List of Figures

List of Tables

XII

1 Introduction

The existence of water molecules on the Moon was explored with Stratospheric Observatory For Infrared Astronomy (SOFIA) [1]. The existence of water was then confirmed with Lunar Crater Observation and Sensing Satellite (LCROSS) [2]. This has researchers determined to look into further uses for lunar water as the resources brought along with spacecrafts to the Moon are limited. The overall goal for long-duration missions, like with the Artemis program, is to generate a sustainable infrastructure using the celestial body's materials - in other words: In-Situ Resource Utilization (ISRU) [3]. Local materials are used for the three main tasks of ISRU: generating propellant, sustaining life support and generating construction materials. The decomposition of water (H_2O) into hydrogen (H_2) and oxygen (O_2) via water electrolysis provides breathable oxygen for the life support systems, as well as hydrogen and oxygen as propellant for space vehicles [4].

"Dust is still a principal limiting factor in returning to the lunar surface for missions of any extended duration. However, viable technology solutions have been identified, but need maturation to be available to support both lunar and Mars missions" [5, p.1]. In the context of ISRU the lunar dust is a critical problem for the feasibility of the water electrolysis [5]. Current technologies require ultrapure water [4], while dust can contaminate extracted water [5]. Therefore, a filtration of the extracted water is required before conversion [5]. A filtration system for the extracted lunar water is consequently a necessary contribution to the lunar ISRU effort.

The SMU research group of the DLR Bremen focusses on the lunar water extraction and water purification for a $H_2O - H_2 - O_2$ system. It shall combine the treatment of extracted lunar water with the recycling of water brought along a mission. The lunar water extraction and water purification shall enable water electrolysis. The decomposition of water then provides hydrogen and oxygen. The project Validation of Lunar Water Extraction and Purification Technologies for In-Situ Propellant and Consumables Production (LUWEX) by the SMU research group targets this topic and has been selected in the framework of a competition by the European Union (EU) for funding. This thesis is part of the SMU research, which closely cooperates with LUWEX.

This master thesis deals with the selection of a lunar water simulant based on the results

of dissolution experiments, and the system control via a *Laboratory Virtual Instrument Engineering Workbench (LabVIEW)* program of a related lunar water purification system. The research questions of this thesis are:

1. What is the required composition for a lunar water simulant using lunar regolith simulant?

2. How can the related lunar water purification system be controlled using a *LabVIEW* program?

The results can be used to test the lunar water purification system on Earth and adapt the purification system to an fully automatic application with extracted lunar water.

To determine the possible contaminants in extracted lunar water, various dissolution experiments with lunar regolith simulant LHS-1 and LMS-1 from the *Exolith Lab* are conducted. Using the results from further dissolution experiments done within the SMU research group, a lunar water simulant is experimentally developed. This lunar water simulant enables testing individual processes inside the ISRU process chain for water extraction on the Moon, like the water purification. The lunar water simulant is then exposed to the related lunar water purification system to investigate its contaminant retention. For the system control of the lunar water purification system, a *LabVIEW* program is presented. Lastly, possible optimisations regarding the lunar water purification system structure and the *LabVIEW* program are given.

2 Project Overview

This chapter gives an overview of the DLR as working environment, the SMU research group of DLR Bremen and the LUWEX project.

2.1 DLR

The DLR consists of 55 research institutes and facilities. The DLR is present in 30 locations in Germany with over 10,000 employees. The Institute of Space Systems in Bremen was found in 2006 and has around 140 employees. Recent, well-known missions of the institute are the MASCOT asteroid lander and the EDEN ISS Antarctic Greenhouse. [6]

2.2 Synergetic Material Utilization Research Group

The SMU research group is a DLR Bremen research group internally founded in 2021. It researches and develops ISRU technologies for Moon and Mars exploration.
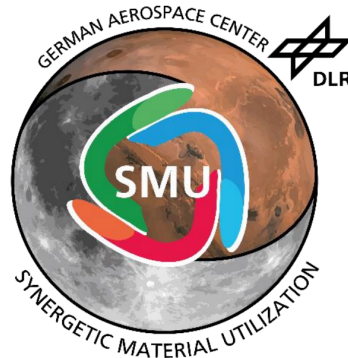
Figure 2.1: *SMU Research Group Logo*

The SMU group of the DLR is focussing explicitly on ISRU with one Ph.D. candidate focussing on the lunar water extraction and another Ph.D. focussing on the lunar water purification to develop an $H_2O - H_2 - O_2$ system for the space habitats, e.g. on the Moon. Additional support is provided by multiple students in the form of internships, bachelor and master thesis. This thesis is written in the framework of the SMU research group. A schematic of the shared infrastructure can be seen in figure 2.2. The shared

$H_2O - H_2 - O_2$ infrastructure combines water recycling and lunar water extraction to minimise the water mass brought from Earth. Unpurified water consisting of extracted lunar water and water from Environmental Control and Life Support System (ECLSS) is given into the water treatment and the water recycling, which interact. Clean water is then stored and supplies ISRU processes, ECLSS processes, and the electrolysis with water. The products of the water electrolysis, hydrogen and oxygen, are stored and can be used as propellant. Moreover, the products can be used for ISRU and ECLSS processes. [7]
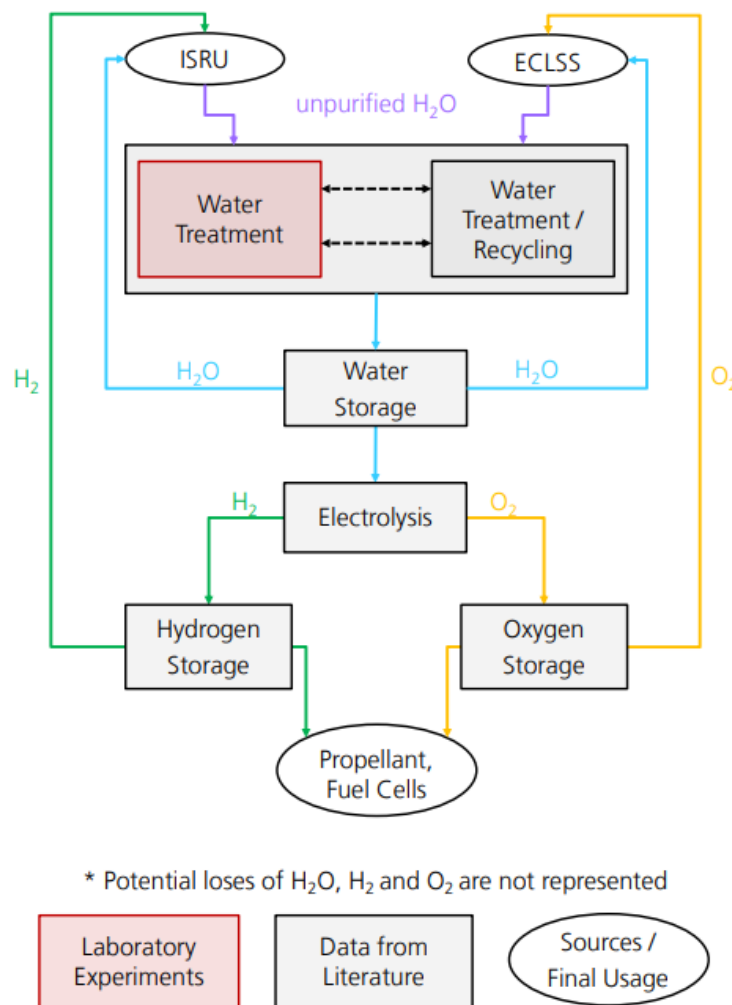
Figure 2.2: *Schematic of the $H_2O - H_2 - O_2$ Infrastructure [7, p.1]*

Figure 2.3 explains the process chain of ISRU water extraction from water ice deposits on the Moon for an $H_2O - H_2 - O_2$ system. At first the water from the water ice deposits is extracted in the form of water vapour by heating the icy regolith. Afterwards, the unpurified gaseous water with contaminants is undergoing a liquefaction process. The liquid water is then purified, resulting in dirt residues and potable water for the Life Support (LS) and purified water for the subsequential water electrolysis. After the

electrolysis the hydrogen and oxygen are used for energy storage, propellant production and life support. The hydrogen is used for energy storage and propellant production. The oxygen is used for propellant production and for the life support.

This master thesis is part of the SMU research group and contributes information to the purification and the liquefaction as highlighted with red boxes. As a water simulant with known composition is developed it can be used to determine the functionality and quality of a process, like the water purification and liquefaction by comparing results and the input water composition.
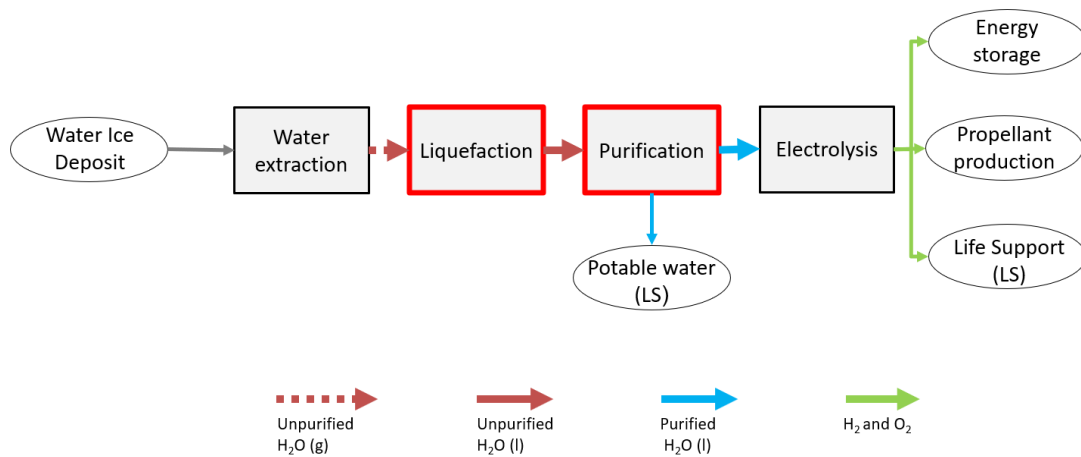
Figure 2.3: *Process Chain of ISRU for Water Extraction on the Moon*

2.3 LUWEX

LUWEX is a project by DLR, *Technical university of Braunschweig, Liquifer Systems Group, Thales Alenia Space, Wrocław University of Science and Technology* and *Scanway*, which is funded by the EU. The possibility using ISRU technology is to enable a long stay on another celestial body for future space missions, e.g. on the Moon. This shall be reached by extracting and purifying lunar water in preparation for hydrogen and oxygen production via water electrolysis. Furthermore, it reaches for milestone technologies. It is desired to design and manufacture technologies for the water extraction, liquefaction, purification and storage. This can be seen on the project scope overview in figure 2.4. The red boxes highlight to which parts of the project this master thesis is contributing information to. The lunar water simulant which is experimentally developed in this thesis supports developing the purification and the liquefaction technology. Since the composition of the lunar water simulant is known the quality of the liquefaction and purification can be determined for the technologies designed within the LUWEX project. [6]
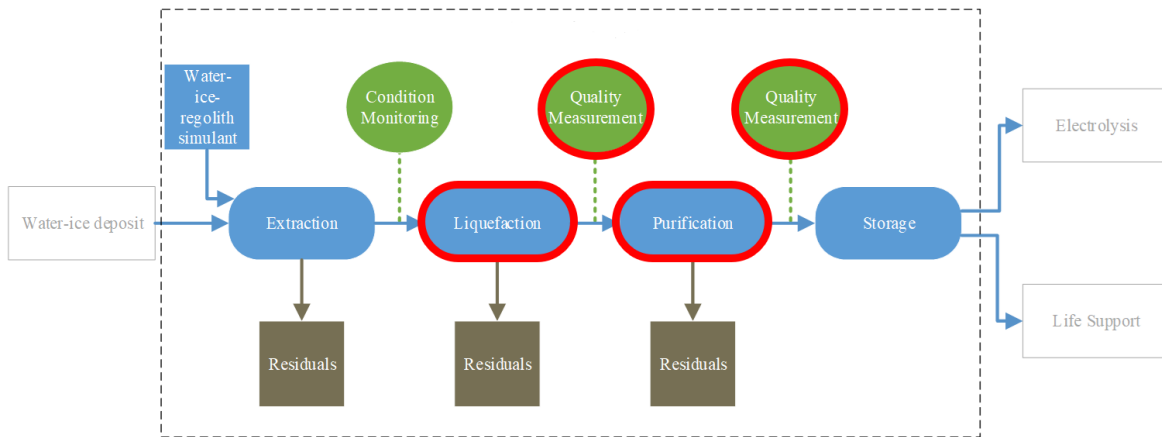
Figure 2.4: *LUWEX Project Scope [6, p.8]*

The corresponding project schedule can be seen in figure 2.5. The project is started in November 2022 and is funded until November 2024. It is divided into three phases: the preliminary design, the critical design review, the validation of the design. During the first phase, which lasts a time period of four months, the requirements are defined and the preliminary design of subsystems and experiments is set. During the second phase a detailed design is worked on, as well as manufacturing processes and the development of icy regolith and a lunar water simulant. This critical design review phase has a duration of 13 months. During the third phase, which lasts seven months, the technology validation campaign and an evaluation of the experiments shall be finished. The design is validated and an investigation regarding future terrestrial and space applications shall be done. This master thesis is contributing information for the first and second phase, highlighted in red. [6]

Figure 2.5: *Project Schedule of LUWEX [6, p.10, with additional text]*

3 Theoretical Background

Chapter 3 presents the theoretical background of the thesis. The properties of the lunar environment are described first, focussing on lunar regolith, lunar regolith simulant, and the existence of water on the Moon. Next, each process of the process chain of ISRU water extraction is explained. Additionally, the water electrolysis and state-of-the-art ISRU electrolysis technologies are highlighted. The state-of-the-art of dissolution experiments is presented lastly.

3.1 Lunar Environment

Within the following section the lunar environment is outlined regarding regolith and water occurrence. The lunar regolith, its properties and its composition, and the properties of lunar regolith simulant are described. Lastly, the existence of water on the moon is described. This information helps to understand the possibilities of regolith simulant and the difficulties in simulating the lunar environment.

3.1.1 Lunar Regolith

Lunar regolith is the grey, clastic, fine-grained $4\ m$ to $15\ m$ thick layer of unconsolidated solid material covering the bedrock of the Moon. The lunar regolith particles have irregular and jagged shapes. The average particle size on the Moon is $5\ \mu m$ [8]. This makes them a risk to human health and mechanical equipment. Concerning human health, the particles are respirable and their sharp edges are dangerous. Those characteristics cause damage to DNA of e.g. neuronal and lung cells, which may lead to cancer [9]. Concerning mechanical equipment, they can cause clogging, scratching, and wear and tear. This results in a hindrance of processes up to functional failure. On Earth particles are shaped round naturally over time due to erosion of wind and water. The regolith is not exposed to natural erosion processes wearing the particles down due to a lack of atmosphere. ([10]; [11])

The Moon can be divided into highland and mare regions. The mare regions are dark grey areas on the lunar surface, mainly found on the side of the Moon facing the earth, and make up 20 % of the lunar surface. The mare regions consist of mostly volcanic rocks and are consequently relatively young compared to the highland regions. During impacts craters are formed and in a volcanic episode then filled with magma. Because

7

the Moon's crust is thicker on the side facing the Earth, it is more difficult for magma to permeate the lunar mantle there. The name "mare" comes from the fact that centuries ago people saw the darker areas, which characterise the mare regions, and thought of them being seas of water. Highland regions are light grey areas on the moon which are cratered and mountainous and make up the remaining 80 % of the lunar surface. They consist of calcium- and aluminium-rich feldspars, which is a mineral group also existing on Earth. In the mare regions the regolith is generally about $4-5 \ m$ thick and in the highland regions about $10-15 \ m$. In picture 3.1 an example of the highland and mare region is given. ([12]; [13]; [10])
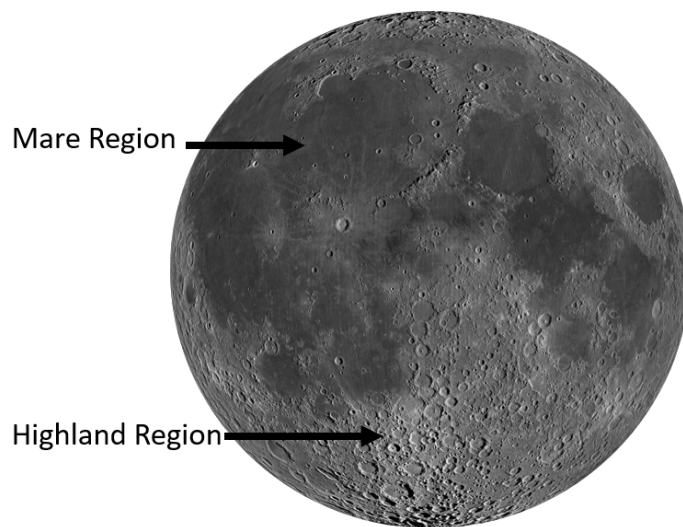
Figure 3.1: *Picture of the Moon with Highlighted Highland and Mare Region, Image Credit: NASA/GSFC/Arizona State University*

Lunar regolith is clastic - lunar regolith particles are formed due to impacts melting and crushing regolith particles. The types of particles are agglutinates, impact glasses, ropy glasses, shocked minerals, and spherules. Agglutinates make up 60 to 70 % of the lunar regolith. The impact of a micrometeorite melts regolith, which forms agglutinates. They form irregular cluster and are particles bond together due to impact-melted glass. A picture of an agglutinate can be seen in figure 3.2. Due to its forming process it can only be found on planets without an atmosphere, like the Moon. Its diameter size is millimeters down to sub-microns. Additionally, fine metallic iron droplets can be found inside agglutinates. ([14]; [10])
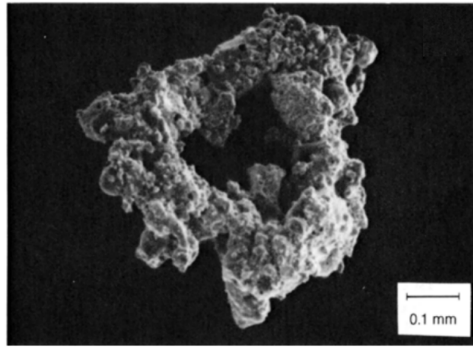
Figure 3.2: *Scanning Electron Photomicrograph of Doughnut-Shaped Agglutinate (NASA Photo S87-38812) [10, p.296, without picture numbering]*

Impact glasses make up approximately 3-5% of lunar regolith. They can be characterised as small beads or as irregular glass pieces. They are created during an impact melting glasses together.

Ropy glasses are distributed throughout lunar regolith. They occur as twisted glasses and are therefore distinctive. Regolith grains are enclosed inside them. A picture of a ropy glass can be seen in figure 3.3. [10]
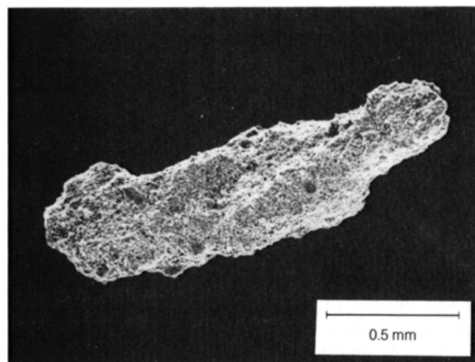
Figure 3.3: *Scanning Electron Micrograph of Ropy Glass from Apollo 12 Sample 12033 (NASA Photo S71-24593) [10, p.303, without picture numbering]*

Shocked minerals are formed by mineral metamorphism. This conversion is caused by shock waves during impacts [10].

Volcanic glasses can be recognised by their uniform chemical composition. Additionally, the surface is coated by volatile elements, and siderophile elements are absent. The most common volcanic glasses are green and orange glass spherules. A picture of an orange spherule can be seen in figure 3.4. Spherules can be formed when melt, caused by an impact, or lava is thrown up and solidifies before it hits the lunar surface. ([10]; [14])
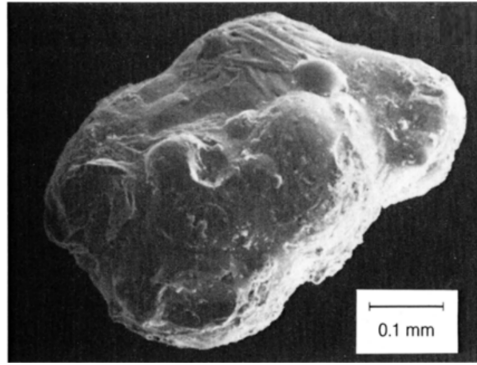
Figure 3.4: *Scanning Electron Micrograph of Volcanic Glass from Apollo 17 core 74001/2 [10, p.303, without picture numbering]*

With a few exceptions, the minerals found on the Moon can be also found on Earth. Minerals are defined by four properties. A mineral occurs naturally and has a chemical composition that does vary within a defined range or not vary at all. It has a crystalline structure and a mineral can be mechanically separated from other minerals. Glasses on the other hand are solids but do not have a crystalline structure, but may have a similar compositions to minerals. The lunar minerals can be divided into five types: silicate minerals, oxide minerals, sulfide minerals, native iron, and phosphate minerals. For this thesis pyroxene, plagioclase feldspar, olivine, glass-rich basalt, anorthosite, and ilmenite are relevant, further minerals are not considered. [10]

Pyroxene, plagioclase feldspar, and olivine are silicate minerals. Pyroxene with the chemical formula $(Mg, Ca, Fe)SiO_3$ is the most chemically complex silicate within lunar regolith. Plagioclase feldspar is defined as $NaAlSi_3O_8$ to $CaAl_2Si_2O_8$. Olivine with the chemical formula $(Mg, Fe)_2(SiO_4)$ is a silicate mineral in an olive colour.

Glass-rich basalts contain mostly silicate minerals.

Anorthosite is described as $CaAl_2Si_2O_8$ and contains mainly plagioclase feldspar.

Ilmenite is an oxide mineral with the formula $FeTiO_3$. It makes up the largest part of oxide minerals within lunar regolith and is a black, opaque mineral. [10]

3.1.2 Lunar Regolith Simulant

Since regolith samples from the Moon are rare while the demand is high for research and testing, companies on Earth have made it their mission to provide materials with similar properties as the regolith found on the Moon. These materials are called regolith simulants. The regolith simulant preparation is done using materials of terrestrial origin. To get the desired composition, crushing and mixing of minerals is varied depending on the simulated surface region of the Moon. These simulants are generated for various planets, as well as asteroids and comets.

The company *Exolith Lab* provides lunar regolith simulants for the mare and the highland

region and a global lunar simulant. These vary in composition and particle size, from larger particle sizes - 1000 μm - down to dust particles - < 0.04 μm. For this thesis the dissolution of ions is investigated with experiments with the lunar mare simulant LMS-1, the lunar highland simulant LHS-1, and the lunar highland dust simulant LHS-1D. According to a test of different lunar simulants done by the *Hopkins University*, the lunar regolith by *Exolith Lab* shows a good match to real lunar regolith [15]. The regolith simulant test evaluated bulk chemistry, production and post-testing [15].

3.1.3 Water Occurence on the Moon

In 1961 the existence of water ice in the coldest places on the Moon was first proposed by Watson et al. ([16]; [17]). These coldest places on the lunar surface are found within a Permanently Shadowed Region (PSR) which is characterised as an area where sunlight never reaches ([16]; [18]). Consequently these areas are often found at the floor of a lunar crater [18], which mainly occur on the south pole of the Moon. During the LCROSS mission a rocket struck a PSR inside a south pole crater, ejecting debris, dust, and vapour [2]. A second spacecraft analysed the debris and the vapour confirming the existence of water vapour inside the ejected material with an estimated water concentration in lunar regolith of 5.6 ± 2.9 % by mass [2]. The existence of water was further supported by the SOFIA mission detecting water ice at the polar PSR [1]. According to SOFIA's and the Moon Mineralogy Mapper's M(3) observations, water can be found as structurally bound as hydroxyls on the lunar surface, or trapped inside glasses on the lunar surface, or as molecular water inside the lunar regolith inside a PSR ([19]; [20]; [21]; [17]). The water ice detection results from the Moon Mineralogy Mapper comparing north and south pole can be seen in figure 3.5.
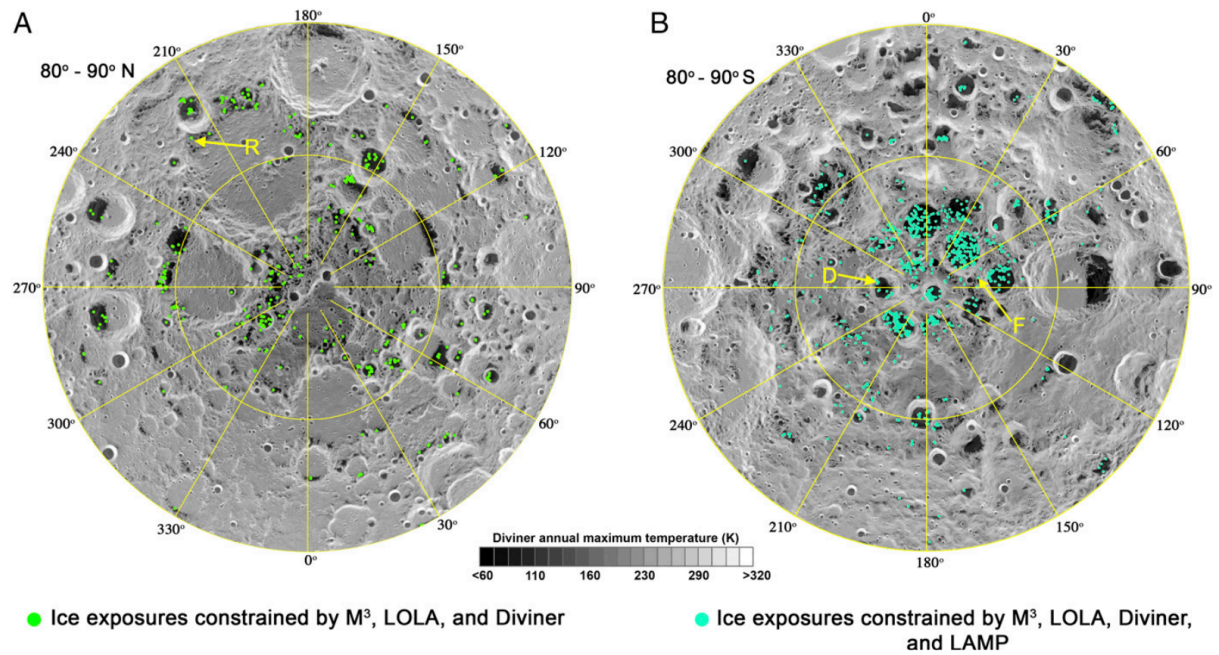
Figure 3.5: *"Distribution of water-ice-bearing pixels (green and cyan dots) overlain on the Diviner annual maximum temperature for the (A) northern- and (B) southern polar regions. Ice detection results are further filtered by maximum temperature (<110 K), LOLA albedo (>0.35) [22], and LAMP off and on band ratio (>1.2, only applicable in the south) [23]. Each dot represents an M (3) pixel, ≈ 280 m × 280 m."* [18, p.5]

The overall favoured hypothesis is that water is present as water ice in permanently shadowed regions in craters on the Moon in relatively high quantities ([2]; [24]; [17]). The structure of water ice and the lunar regolith is only partly investigated, possible structures can be seen in figure 3.6. This artwork is done by the *Colorado School of Mines*, a university dedicated to engineering and applied science, including the study of terrestrial and extraterrestrial minerals. Prof. Angel Abbud-Madrid, the director of the center of space recources of the *Colorado School of Mines* is also part of the LUWEX external advisory board.
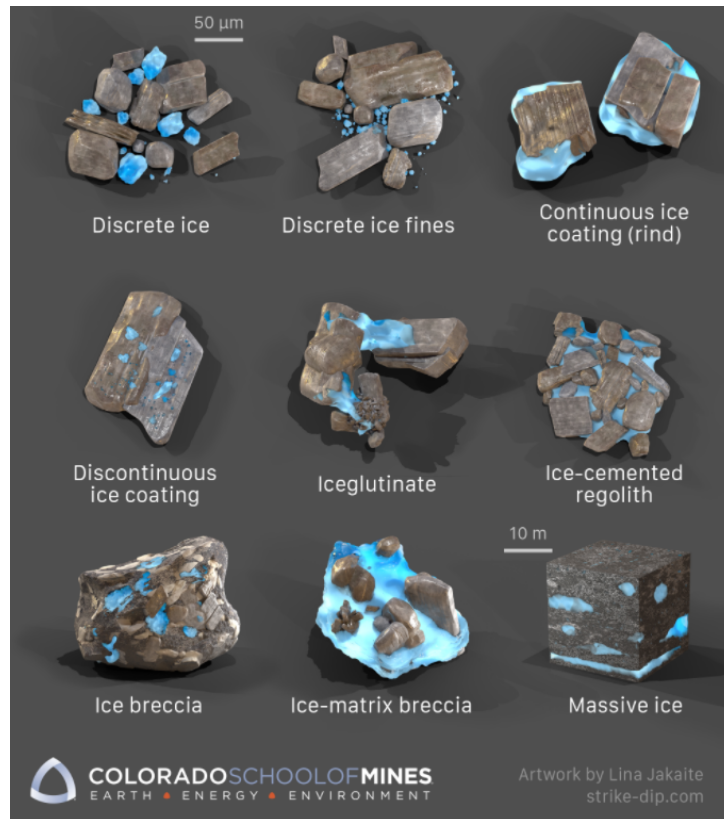
Figure 3.6: *Possible Structures of Regolith and Water on the Moon [6]*

Multiple laboratory-based studies have led to the hypothesis that the Moon contains water under its surface, some even suggest underground water reservoirs ([25]; [26]; [27]; [17]). The lower end of the estimated amount of water on the Moon is 600,000,000,000 kg [28]. This estimation was made by NASA with the radar data from Chandrayaan-1 [28]. Since the Artemis mission started, the scientific community hopes to gain knowledge about the actual water composition of regolith on the Moon [29]. The suspected amount of water is a reason for the Artemis mission's destination: thirteen landing sites are currently candidates for the lunar landing of Artemis III, with each of them being located within six degrees of latitude of the lunar south pole [29].
While the origin of water on the Moon is unclear, possible origins are asteroids, comets, volcanism and solar wind ([30]; [31]).

3.2 Process Chain of ISRU Lunar Water Extraction

In this section the process chain of ISRU for water extraction on the Moon is explained - including water extraction from the lunar surface, water capturing, water liquefaction, water purification and water electrolysis, water classifications and ISRU water electrolysis technology.

3.2.1 Water Extraction and Liquefaction

To extract liquid water from the icy lunar regolith, the water needs to be thermally extracted, in the form of vapour from the regolith, captured and liquefied.

Liu et al. proposed a thermal method combined with a drill for water extraction from icy lunar regolith. A drill apparatus was developed, where the hollow drill rod could be heated and then guides water vapour from the icy regolith through its hollow interior to a water capturing system. A test in a pilot-scale unit was done on Earth, including all process steps of water extraction consisting of drilling, heating, water evapouration, condensation and collection and was successfully performed on Earth. [32]

Kiewiet et al. simulated two methods of lunar water extraction, an in-situ extraction and an excavated extraction. They were simulated with alternating parameters, like heating power, water weight percentage in regolith, power density, in order to determine the accessibility, lifetime, complexity, reliability, development cost, and robustness of the extraction methods. A schematic of these methods can be seen in 3.7. The in-situ extraction device was simulated to be put directly onto the regolith. It was designed with a heated dome and a surface heater or heating rods which were designed to be placed into the regolith. For the excavated extraction the regolith was simulated to be filled into a crucible by an excavator and heated to evapourate the water. [33]
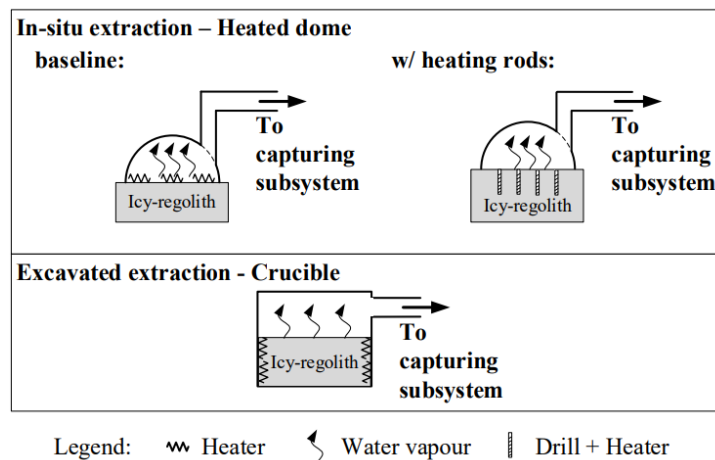
Figure 3.7: *Schematic of Water Extraction Methods Proposed by Kiewiet et al. [33, p.2]*

After the simulation and comparison of the methods the excavated method was stated to perform best due to its closed and insulated system. Additionally, the losses of this method were expected to be much lower than with the in-situ method. Even though the excavated extraction was characterised as more complex and with a lower lifetime than compared methods it had a better accessibility to the product, the water vapour. [33]

3.2.2 Water Capturing

When the water is extracted, the produced water vapour needs to be captured and liquefied. Using the cold trap the water vapour shall be collected by a cold area where the vapour deposits. For the liquefaction the ice shall be molten within the cold trap device. [33]

Jurado designed a cold trap to deposit water vapour from icy lunar regolith. The ice growth at the cold trap was tested and a thermal delamination process by heating the cold plate to remove the water ice. A picture of the cold trap can be seen in figure on the left and the thermal delamination process on the right. [34]
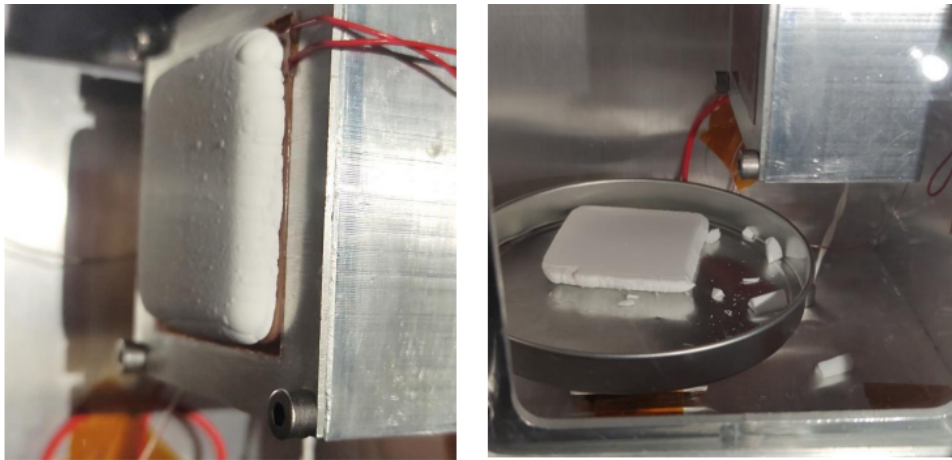
Figure 3.8: *Water Ice on Cold Trap (left) and Thermal Delamination (right) [34, p.41]*

Holquist et al. simulated the cold trap and gave estimates regarding possible contaminants the lunar water still holds after using a cold trap. They assumed a heated dome as extraction method, hence water vapour as product of the water extraction. The described cold trap concept is e.g. used for the ISRU-derived water purification and Hydrogen Oxygen Production (IHOP), which is developed by *Paragon Space Development Corporation CR and Giner INC.* [35]

Holquist et al. then conducted experiments with a manufactured cold trap. Water vapour containing volatiles according to the LCROSS mission were trapped in evacuated and actively chilled glass bottles. The resulting water ice was investigated regarding its contaminant retention. The cold trap operated with relevant temperatures, pressures, water content, and contaminant concentrations to mimic the lunar environment. It was taken care that the water in the cold trap shall be deposited directly and not condensate and then freeze. The most reasonable estimates of the test batches were stated to lead to the assumption that the described process would provide expected performance on the Moon. [36]

3.2.3 Water Purification Caused by Capturing Process

As the water gets in contact with lunar regolith it can be easily contaminated resulting in dissolved salts, metals, volatiles and compounds [5]. Some contaminants of the lunar water can sublimate with the water vapour created in the extraction process while others cannot. When the water vapour deposits using a cold trap the water ice contains less contaminants due to the freeze distillation. It selectively deposits water ice from water vapour while rejecting contaminants. [36].

As mentioned in subsection 3.2.1 Holquist et al. simulated the cold trap and made a prediction for the retaining contaminants in lunar water ice using Henry's law. [35]

Holquist et al. tried to prove the prediction by conducting cold trap experiments and observing the purification abilities of a cold trap. Water vapour containing volatiles according to the LCROSS mission was trapped in evacuated, actively chilled glass bottles. A simulation for a cold trap experiment on Earth was generated and the deviations between experiment and simulation were put into a ratio. Using this ratio the estimates for a best and a worst case for conducting cold trap experiments on the Moon were calculated from simulations under lunar conditions. It is stated that the simulations using the Henry's Law are a conservative estimate for contaminant retention. [36]

3.2.4 Water Electrolysis

Splitting a chemical compound using electric current is called electrolysis. For the electrolysis, two electrodes, an electrolyte, and a container to collect each product, are needed. One of the electrodes is charged negatively so it attracts anions and is called anode. The other electrode is charged positively and attracts cations - the cathode. The electrolyte is a liquid or solid, which can conduct electricity. It is needed for the ions to easily travel to the desired electrode. The decomposition of water - $H_2 0$ - with electrolysis results in hydrogen - H_2 - and oxygen - O_2.

The water electrolysis exists in three systems: The Polymer Electrolyte Membrane (PEM) electrolysis, the alkaline electrolysis and the Solid Oxide Electrolyser (SOEL) electrolysis. In the alkaline electrolysis an electric current flows through an alkaline solution such as potassium hydroxide (KOH) or sodium dioxide ($NaOH$) from a nickel-based anode to cathode, displayed in figure 3.9. At the cathode water reduces to hydrogen gas and hydroxide ions and at the anode the water forms oxygen gas and water. [4]
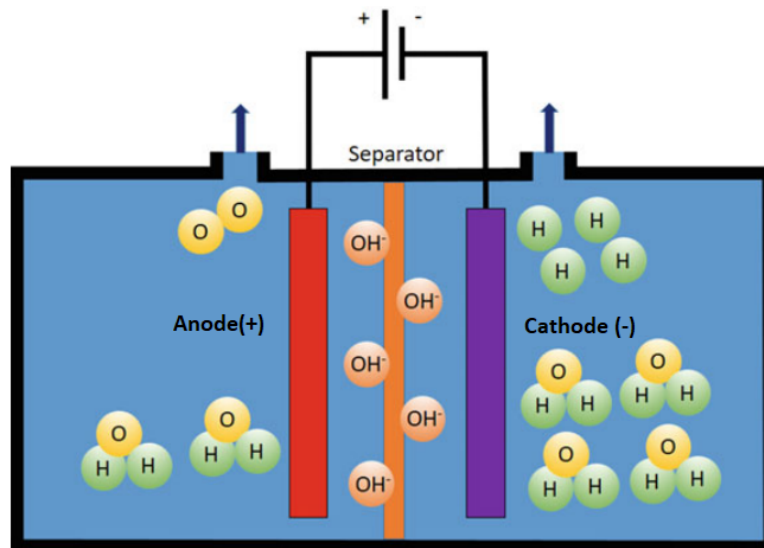
Figure 3.9: *Schematic of Alkaline Electrolysis [4, p.188, with additional text]*

The process of the PEM electrolysis can be seen in figure 3.10. The anode, e.g. the iridium catalyst, is fed water, where the oxygen gas and the H molecules are split at. The oxygen gas can be collected at the outlet of the anode and the hydrogen molecules pass the $20 - 300 \ \mu m$ thick proton-exchange membrane [37] and combine with electrons at the cathode, e.g. a platinum catalyst, to form hydrogen gas. The thin membrane allows a thin electrolyte resulting in a quick response to power input. [4]
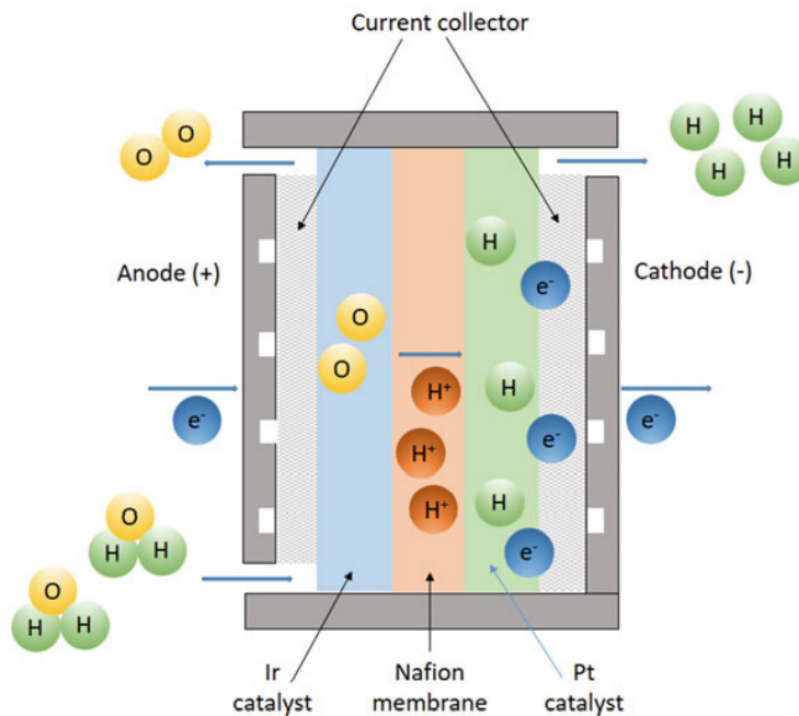
Figure 3.10: *Schematic of PEM Electrolysis [4, p.189, with additional text]*

Figure 3.11 is a schematic of the SOEL electrolysis. The water steam and the power are fed the porous cathode. The molecules are then reduced to oxygen and hydrogen, whereas hydrogen is collected at the cathode. The ceramic membrane allows only oxygen molecules to pass and form oxidant molecules at the anode. SOEL electrolysis requires less power than PEM or alkaline electrolysis due to the increased efficiencies, because of the higher operating temperatures and has a higher hydrogen production rate. [4]
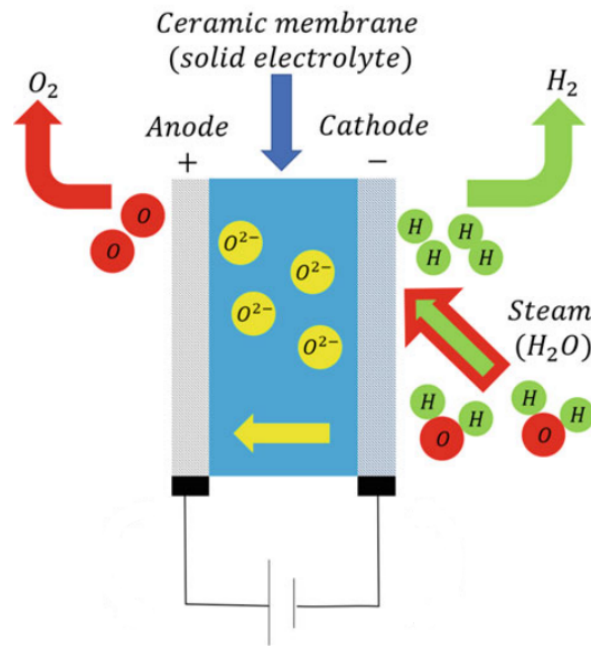
Figure 3.11: *Schematic of SOEL Electrolysis [4, p.190]*

The reaction of the water electrolysis is explained in the following.
An oxidation process is happening at the anode. Oxygen is produced. The following equation 3.1 is applied to the anode. [4]

$$Anode: 2H_2O \rightarrow O_2 + 4H^+ + 4e^- \tag{3.1}$$
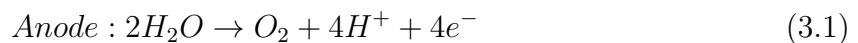
At the cathode, a reduction process occurs and hydrogen is produced. Equation 3.2 is the chemical reaction at the Cathode. [4]

$$Cathode: 2H_2O + 2e^- \rightarrow H_2 + 2OH^- \tag{3.2}$$
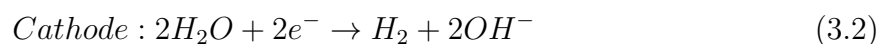
The net ionic equation for the electrolysis is the equation 3.3. It can be seen that from the electrolysis of two water atoms two hydrogen atoms and one oxygen atom are received. Moreover, the liquid (l) water decomposes into two gaseous (g) components. [4]

$$2H_2O(\text{l}) \rightarrow 2H_2(\text{g}) + O_2(\text{g}) \tag{3.3}$$

The hydrogen production rate $\dot{n}_{H2}$ in $\frac{mol}{s}$ is given by equation 3.4. F is the Faraday constant in $\frac{C}{mol}$, i_{cell} describes the current density in $\frac{A}{cm^2}$ and A_{cell} is the effective cell area in cm^2. The number of moles of electrons transferred in the reaction is z and has the value 2 for hydrogen. The Faraday constant F is $9.6485 \cdot 10^4 \frac{C}{mol}$. The stack current is I_{cell} in A. [4]

$$\dot{n}_{H2} = \frac{\eta_F \cdot i_{cell} \cdot A_{cell}}{z \cdot F} = \frac{\eta_F \cdot I_{cell}}{z \cdot F} \qquad (3.4)$$

From equation 3.4, it can be seen that the hydrogen production rate is linearly proportional to the current of the cell. This is important when determining possibilities to increase the hydrogen production rate.

An overview of the different electrolysis technologies regarding operating temperature, efficiency, technology method, the required state of feedstock water, and purity requirements for feedstock water is shown in table 3.1. The summed-up water electrolysis technologies are alkaline electrolysis, PEM and SOEL.

Table 3.1: *Overview of Alkaline, PEM and SOEL Water Electrolysis*

Parameter	Alkaline	PEM	SOEL
Operating Temperature	<90°C [4]	<100°C [4]	700 - 1000°C [4]
Efficiency	59-70% [38]	65-82% [38]	40-60% [38]
Method	Electric Current Flows through Alkaline Solution, at Cathode Water Forms, at Anode Oxygen and Water [4]	At Anode Oxygen Gas and Hydrogen are Split, Hydrogen Molecules pass 20-300µm Thick Membrane and Combine with Electrons at Cathode to Hydrogen Gas [4]	Water Steam is Fed Porous Cathode where it Reduces to Oxygen Gas and Hydrogen, Oxygen Passes Ceramic Membrane and Forms Oxidant Molecules at Anode [4]
State of Input Water	Liquid [4]	Liquid [4]	Vapour [4]
Requirement Input Water	ASTM Type I or II [4]	ASTM Type I or II [4]	ASTM Type I or II [4]

Advantages and disadvantages of the different electrolysis technologies can be see in table

3.2. The advantages are highlighted in green, the neutral aspects in orange and the disadvantages in red. The highlighted parameters are catalysts, efficiency, if they are applicable to renewable energy, lifetime, and maturity. The catalysts, lifetime, renewable energy applicability, and life time are important for applications with limited resources. The efficiency, and maturity are important to determine the amount of output which can be generated and efficiency and renewable energy applicability are important parameters to determine needed space for such an electrolysis system. If the system is applicable for renewable energy is evaluated on the fact whether it functions using lower loads [4].

Table 3.2: *Advantages and Disadvantages of Alkaline, PEM and SOEL Water Electrolysis*

Parameter	Alkaline	PEM	SOEL
Catalysts	Inexpensive Catalysts, Non-precious Metal [4]	Expensive Catalysts [4]	Inexpensive Catalysts [4]
Efficiency	Medium Efficiency [38]	High Efficiency [38]	Low Efficiency [38]
Renewable Energy Applicable	No [4]	Yes [4]	No [4]
Lifetime	Long Lifetime [4]	Long Lifetime [4]	Long Lifetime [4]
Maturity	Mature Technology [4]	Mature Technology [4]	Immature Technology [4]

3.2.5 Water Classifications

To evaluate the results of the lunar water purification system different water classifications are given in the following section. The requirements for the electrolysis input water according to American Society for Testing and Materials (ASTM) are given, a NASA standard for potable water on the ISS. The WHO requirements for drinking water are given. The estimates for the lunar water contamination after a cold trap are given according to Holquist et al.'s experiments described in subsections 3.2.1 and 3.2.3 [36]. In addition, the concentrations of compounds of lunar water measured during the LCROSS mission [2] are given in table 3.6. A density of 1 $\frac{kg}{l}$ is assumed for litre of water.

The required water conductivity for the individual electrolysis technology system is strongly dependent on the manufacturer of the electrolysis system. The water classification by theASTM is a general guideline for electrolysis input water with the classification of type

I and type II. The ASTM sets requirements, which can be seen in table 3.3, for the conductivity, resistivity, the total organic carbon, sodium, silica, and chloride. Water according to type II can be used for electrolysis but type I is preferred [4].

Table 3.3: *Requirements for ASTM Water Type I and Type II [4]*

Requirements	Type I	Type II
Conductivity in $\frac{\mu S}{cm}(25°C)$	<0.056	<1
Resistivity in $M\Omega cm(25°C)$	>18	>1
Total Organic Carbon in $\frac{\mu g}{L}$	<50	<50
Sodium in $\frac{\mu g}{L}$	<1	<5
Silica in $\frac{\mu g}{L}$	<3	<3
Chloride in $\frac{\mu g}{L}$	<1	<5

In table 3.4 the limits of released ions for the International Space Station (ISS) can be seen. The requirements is the standard of potable water for 100 up to 1,000 days by NASA.

Table 3.4: *Requirements for Potable Water for 100 up to 1,000 Days on the ISS by NASA [39]*

Chemical	Unit	Limit
Ammonia	mg/l	1
Antimony	mg/l	2
Barium	mg/l	10
Cadmium	mg/l	0.022
Manganese	mg/l	0.3
Nickel	mg/l	0.3
Silver	mg/l	0.4
Total Iodine	mg/l	0.2
Zinc	mg/l	2
Total Organic Carbon	mg/l	3
Acetone	mg/l	15
Alkylamines (Di)	mg/l	0.3
Alkylamines (Mono)	mg/l	2
Alkylamines (Tri)	mg/l	0.4
Benzene	mg/l	0.07
Caprolactam	mg/l	100
Chloroform	mg/l	6.5
Di(2-ethylhexyl)phthalate	mg/l	20
Di-n-butyl phthalate	mg/l	40
Dichloromethane	mg/l	15
Ethylene Glycol	mg/l	4
Formaldehyde	mg/l	12
Formate	mg/l	2500
2-Mercaptobenzothiazole	mg/l	30
Methanol	mg/l	40
Methyl Ethyl Ketone (MEK)	mg/l	54
n-Phenyl-beta-naphthylamine	mg/l	260
Propylene Glycol	mg/l	1700

Other sources, like the official World Health Organisation (WHO) guideline for limits of released ions for drinking water as seen in table 3.5, can be used to further evaluate the usability of the water samples. This guideline includes aluminium, calcium, iron, magnesium, and manganese, after which the water samples are analysed.

Table 3.5: *Requirements for Drinking Water by the WHO [40]*

Ion	Limit in mg/l
Aluminium	0.10
Ammonium	0.35
Calcium	100
Chloride	200
Copper	2
Iron	0.02
Magnesium	500
Manganese	0.05
Sulphate	250
Sodium	200

In 2009 National Aeronautics and Space Administration (NASA)'s project LCROSS was launched. A rocket struck a PSR at the south pole, where water existence was generally suspected. The ejected debris, dust, and vapour were observed and confirmed the existence of water vapour and water ice in the ejected material. The state-of-the-art regarding the water composition on the Moon are the data of the LCROSS mission. The compound concentration inside the $3148kg \pm 787kg$ regolith mass, the ejected material, can be seen in table 3.6 in $\frac{mg}{L}$. Those concentrations are transferred from the unit of $\frac{mol}{L}$ using the molar weight shown in table 3.6. [2]

The estimates for a worst and best case using a cold-trap by Holquist et al. can be seen [36] in table 3.6 as well. Further information regarding Holquist et al.'s experiment is given in section 3.2.3. This table is shown to give a general estimate of the contamination of the lunar water, respectively after the cold trap.

Table 3.6: *Concentrations of Compounds in $\frac{mg}{L}$ Measured During LCROSS Mission [2] and Estimates Using Cold Trap [36]*

Compound	Chemical Formula	Molar Weight in $\frac{g}{mol}$	Concentration in $\frac{mg}{l}$		
			LCROSS	Best Case	Worst Case
Water	H_2O	18.00			
Hydrogen Sulfide	H_2S	34.08	1.38E+05	9.47E-04	4.17E-03
Ammonia	NH_3	17.04	2.50E+04	1.67E-01	8.79E-01
Sulfur Dioxide	SO_2	64.06	5.00E+04	2.49E-03	7.83E-02
Ethylene	C_2H_4	28.06	2.14E+04	1.56E-04	9.35E-04
Carbon Dioxide	CO_2	44.01	2.32E+04	7.34E-04	7.34E-03
Methanol	CH_3OH	32.05	1.25E+04	3.74E-02	2.66E+00
Methane	CH_4	16.05	2.50E+03	2.68E-06	2.68E-05
Hydrogen	H_2	2.02	2.50E+05	1.46E-04	3.03E-04
Carbon Monoxide	CO	28.01	1.25E+05	3.11E-05	4.67E-04

3.2.6 ISRU Electrolysis Technologies

Technologies specifically designed for ISRU projects are of interest for the SMU research group and LUWEX which are focussing on ISRU technology. ISRU lunar water electrolysis is a small area of research. Combined with technologies still being under development ([41]; [42]; [43]; [44]) and companies withholding intellectual property [45] only limited information can be provided.

The photocatalytic electrolysis is designed for renewable energies. A solar cell is used to power an electrochemical cell which produces hydrogen and oxygen. [41]

A dirty water alkaline electrolysis system is designed by the *Teledyne Company*. A water purification and a robust electrolysis system are combined. It is unclear whether both, hydrogen and oxygen, are products of this electrolysis process. [42]

The company *Enapter* developed a PEM technology, using a bipolar plate where only hydrogen passes through. This combines PEM technology and high purity hydrogen of 99.999 % resulting in lower costs compared to other technologies with the same hydrogen purity. A disadvantage is that only the hydrogen is captured while the oxygen remains dissolved in water. Meaning two of the main tasks of ISRU are not fulfilled: sustaining life support and propellant production. The state of the input water is liquid. [45]

The *Paragon Company* is developing an ISRU-derived water purification and hydrogen and oxygen production technology. It is a PEM technology which is developed specifically for space applications. The state of water for input, output of the electrolysis, as well as the product's purity at the outlet remain unclear. The technology is developed for IHOP and stated as scalable and durable. ([44]; [43])

3.3 Dissolution Experiments

Dissolution experiments examine which ions are dissolved from solid material into an aqueous solution. The dissolution of ions is a function of, among other things, pH, aqueous solution to solid ratio, and particle size or surface area [46]. To expand the knowledge regarding the influences on dissolving particles dissolution experiments are done. In the following sections the definition of a surface controlled reaction and diffuse controlled reaction are given and dissolution experiments with lunar simulant are summarised, including the dissolution experiments done prior by the SMU research group.

3.3.1 Surface- and Diffusion-Controlled Reaction

Surface-controlled and diffusion-controlled reactions are different transporting mechanisms for molecules. For both mechanisms particles can be imagined as surrounded by solution. [47]

The surface-controlled reaction is describing the process of solution molecules migrating to the surface of a particle and vice versa. During this process molecules of the particle are transferred to the solution – molecules are dissolved into the surrounding solution. The limiting factor of the surface-controlled reaction is the total surface area of the particle. A surface-controlled reaction can be seen as parabolic progression when looking at ion concentrations over time. ([48]; [47])

With the diffusion-controlled reaction the solution molecules diffuse into the subsurface of the particle and vice versa. Simultaneously, molecules from the particle dissolve into the surrounding solution. This process continues until a stoichiometric equilibrium is achieved. The limiting factor of the diffusion-controlled reaction is the rate of transport within the particle, the diffusion. Diffusion-controlled reactions in the form of ion concentration over time can be characterised as linear. ([48]; [47])

3.3.2 Dissolution Experiments with Lunar Simulant

Eick et. al. examined the influences of pH and organic acids on lunar glass simulant. The dissolution of ions was examined over time in different aqueous solutions with the pH levels of three, five and seven and a variation of citric and oxalic acid. The experiments

were done at 298 K, analysing silicon, aluminium, iron, manganese, calcium, magnesium, titanium and chromium. Silicate glasses were stated as probably being the most reactive materials in aqueous environments. The dissolution of ions was divided in two stages. In the first stage with a time period of 24 days the ions were released rapidly. The ion concentration was characterised as parabolic progression over time. Eick et al. concluded that the initial release was limited by a surface-controlled reaction. During the second stage, which was from 24 days up to 365 days, the release rate of the ions was more linear. The ions diffused from greater depths - a diffuse-controlled reaction. The ion concentration over time of silicon was characterised as linear from the beginning. Since only trace quantities of titanium, chromium, and manganese were released they were not considered. [48]

Eick et al. conducted further dissolution experiments with analysing the same ions as before. The experiments regarding the ion concentration over time with the lunar simulant MLS-1 (Minnesota Lunar Simulant - Mare Simulant) were done at 298K. The different aqueous solutions, where the simulant was mixed into, had the pH level three, five, and seven, and different amounts of organic anions. The dissolution of ions was accelerated by a reduced pH level and citrate and oxalate anions. The following ions were released in an ascending order: Fe $\approx$ Mg > Si > Al $\approx$ Ca. The following minerals are listed in ascending order of their relative abundance in the basalt, which was experimented with: olivine > pyroxene > feldspar > ilmenite. The dissolved ions were directly linked to the solubility of the minerals present in MLS-1. The order of dissolved ions was a direct consequence of their amount present in minerals and the solubility of minerals present in MLS-1. Most importantly, a higher ion dissolution from simulant into water at lower pH was reported. [49]

Karl et al. mixed feldspar lunar regolith simulants and deionised water or pH buffer solution. Next, the dissolved ions from the mixture were determined. The mixture was formed and using fusion drying bricks were built and tested for its compressive strength. For the feldspar, WH and K30 were selected. WH is a K-feldspar from the company *Weierhammer* and K30 is a Na-Feldspar. 20 *ml* of feldspar - WH or K30 - were mixed into 40 *g* of distilled water or a pH 4 buffer solution within centrifuge tubes. The tubes were then sealed and shaken approximately every five hours for three days. Using Inductively Coupled Plasma Optical Emission Spectrometry (ICP-OES), the dissoluted ions were determined. With WH and K30 having different particle size distributions it was stated that the small particle size distribution is proportional to ion dissolution because of its surface volume ratio [50]. The pH 4 buffer showed higher dissolved ion concentrations. Calcium, silicon, and aluminium were dissolved into water, but dissolved at a higher magnitude into buffer

solution. Potassium ions were dissolved by WH into both aqueous solutions and none from K30, even though WH had a smaller potassium content in weight percentage. No statement was made for magnesium and nitrogen. Karl et al. stated a lower pH resulting in higher ion dissolution from simulant into aqueous solution. According to Whitney et al. it was further stated that mineral dissolution is inversely proportional to the particle size [46]. [51]

3.3.3 Dissolution Experiments with LHS-1D

The dissolution experiments inside the SMU research group prior this thesis were performed by Freer. They were done to determine the contaminants that dissolve into an aqueous solution as is gets contaminated with lunar regolith simulant. It was tested for short term contamination of lunar water with a time period of 3 to 7 days and experimented with the lunar highland dust simulant LHS-1D. It has a mean particle size of $7\ \mu m$, a median particle size of $5\ \mu m$ and a particle size range of $<\ 0.04\ -\ 35\ \mu m$. The procedure fundamentals were oriented at [52], [53] and [54].

It was determined that the higher the mass of simulant is the higher the amount of contaminants in ultrapure water and the more the pH increases. Secondly, a correlation between low pH and higher ion solubility in $\frac{mg}{g_{solid}}$ was observed by the comparison of 1:100 and 1:500 in ultrapure water. Using a ratio of 1:500 caused a higher amount of released ions in water in $\frac{mg}{g_{simulant}}$ than using 1:100 since 1:500 causes a lower pH. In the buffer solution on the other hand the pH was 5.6 using the ratio 1:100 and 1:500. Therefore, the ion dissolution in $\frac{mg}{g_{solid}}$ was assumed equal for 1:100 and 1:500 and that already dissolved ions had no influence on ions that continued to dissolve. Parabolic curves were observed with regards to the pH and the released ions over time. The greatest increase in ions was observed within the first two minutes. It was suggested that even in the event of short-term water contamination, treatment should take place to remove not only solid particles but also dissolved ions. The amount of released iron, manganese, and titanium ions did not exceed the detection limit in ultrapure water. The additional extraction time of seven days lead to nearly the same ion concentration as after three days. Due to these results and the low probability of contamination for more than three days in a space habitat the extraction time of seven days was proposed to be left out for further experiments. [7]

A second series of experiments was performed under an atmosphere of 95% nitrogen and 5% hydrogen inside a glovebox. To test the influence of oxygen on ion dissolution and investigate the differences between the environment of the Moon and the Earth, dissolved oxygen is removed from the aqueous solutions at the beginning of the experiment. To remove dissolved oxygen from the aqueous solutions, the aqueous solutions are bubbled with 80% nitrogen and 20% carbon dioxide prior to running the experiment. In this

process, the amount of dissolved oxygen was reduced to $< 1 \frac{mg}{L}$. In the experiments under nitrogen atmosphere, only a slight influence of dissolved oxygen was detected. The experiments resulted in only slightly increased levels of dissolved ions in $\frac{mg}{g_{solid}}$ compared to the experiments in ambient atmosphere. Based on these results Freer et al. decided that further experiments will be conducted in ambient atmosphere. [7]

4 Lunar Water Simulant

To extend the knowledge of the contamination of water by lunar regolith, dissolution experiments will be carried out with the simulants LHS-1 and LMS-1. With the knowledge gained from the experiments carried out in the SMU research group, a lunar water simulant is determined. Using this lunar water simulant, individual processes that take place in the ISRU process chain for water extraction on the Moon can be carried out, like the water purification.

4.1 Methodology

In this section, the selection of the lunar regolith simulant is explained and the experimental procedure of the dissolution experiments is described.

4.1.1 Lunar Regolith Simulant Selection

In this thesis, the simulant LMS-1 for the mare regions and simulant LHS-1 for the highland regions is experimented with. Since the lunar highland dust simulant LHS-1D was used for prior experiments conducted within the SMU research group it is considered as well for the discussion. The simulants from *Exolith Lab* like LHS-1 and LMS-1 are deemed to be a good match to real lunar regolith [15]. This is stated in an overall test of different simulants from different companies regarding bulk chemistry, production, and post-testing by the *Hopkins University* [15].

In table 4.1 the median particle size, the mean particle size and the particle size range can be seen. It can be noted that LMS-1 provides a bigger surface per volume simulant as its median, mean particle size and particle size range is smaller. The same applies for LHS-1D having a smaller particle size than both LHS-1 and LMS-1.

Table 4.1: *Median Particle Size, Mean Particle Size and Particle Size Range of LHS-1, LHS-1D and LMS-1 ([55]; [56]; [57])*

Simulant	Median Particle Size	Mean Particle Size	Particle Size Range
LHS-1	50 μm	60 μm	$< 0.04 - 400\ \mu m$
LHS-1D	5 μm	7 μm	$0 - 30\ \mu m$
LMS-1	45 μm	50 μm	$< 0.04 - 300\ \mu m$

For generating LHS-1, LHS-1D, and LMS-1 various minerals are mixed. It needs to be noted that the mineralogy of LHS-1 and LHS-1D is the same as they only differ in particle size. The mineralogy of the simulants according to their data sheets can be seen in table 4.2 in $Wt.\%$.

Table 4.2: *Mineralogy of LHS-1, LHS-1D and LMS-1 ([55]; [56]; [57])*

Component	Unit	LHS-1	LHS-1D	LMS-1
Anorthosite	$Wt.\%$	74.4	74.4	32.8
Glass-rich Basalt	$Wt.\%$	24.7	24.7	32.0
Ilmenite	$Wt.\%$	0.4	0.4	19.8
Olivine	$Wt.\%$	0.3	0.3	11.1
Pyroxene	$Wt.\%$	0.2	0.2	4.3
Σ	$Wt.\%$	100.0	100.0	100.0

The bulk composition of lunar regolith simulant LHS-1 and LMS-1, and real lunar regolith samples from Apollo 16 and Apollo 15 can be seen in table 4.3 and is determined via X-Ray Fluorescence (XRF). The Apollo 16 sample is sample 60501.13, which is taken from a highland region [58]. The Apollo 15 sample 15021.24 is taken from a mare region ([59]; [60]). The bulk composition of the Apollo 16 should therefore be represented by LHS-1 and the Apollo 15 sample by LMS-1. The bulk composition consists of the following oxides: silicon dioxide (SiO_2), titanium dioxide (TiO_2), aluminium oxide (Al_2O_3), iron (III) oxide (Fe_2O_3), iron oxide (FeO), calcium oxide (CaO), sodium oxide (Na_2O), potassium oxide (K_2O), magnesium oxide (MgO), manganese oxide (MnO), phosphorus pentoxide (P_2O_5), sulfur trioxide (SO_3), chloride (Cl), oxalic anhydride (C_2O_3), nickel oxide (NiO), sulfur (S) and strontium oxide (SrO). All of the named elements are given in percentage by weight ($Wt.\%$).

Table 4.3: *Bulk Chemistry of Lunar Simulants LHS-1, LMS-1 and Apollo 16 Sample 60501.13 and Apollo 15 Sample 15021.24 ([55]; [57]; [58]; [59]; [60]) in Wt.%*

Elements	Unit	LHS-1	Apollo 16	LMS-1	Apollo 15
SiO_2	$Wt.\%$	48.1	45.22	40.2	46.56
TiO_2	$Wt.\%$	1.1	0.59	7.3	1.75
Al_2O_3	$Wt.\%$	25.8	26.84	14	13.75
Fe_2O_3	$Wt.\%$	3.7	-	13.9	-
FeO	$Wt.\%$	-	5.51	-	15.21
CaO	$Wt.\%$	18.4	15.32	9.8	10.45
Na_2O	$Wt.\%$	-	0.4	-	0.41
K_2O	$Wt.\%$	0.7	0.114	0.6	0.2
MgO	$Wt.\%$	0.3	5.52	12	10.37
MnO	$Wt.\%$	0.1	0.072	0.3	0.2
P_2O_5	$Wt.\%$	1	0.137	1	0.18
SO_3	$Wt.\%$	0.3	-	-	-
Cl	$Wt.\%$	0.4	-	0.4	-
C_2O_3	$Wt.\%$	-	-	0.3	-
NiO	$Wt.\%$	-	-	0.2	-
S	$Wt.\%$	-	0.065	-	0.06
SrO	$Wt.\%$	0.1	-	0.1	-
Σ	$Wt.\%$	100	99.788	100.1	99.12

The amount of SiO_2, TiO, Al_2O_3, CaO, MnO, and P_2O_5 of the Apollo 16 sample is best matched with the LHS-1 simulant. The amount of K_2O is better represented with LMS-1, rather than LHS-1, and MgO is equally bad represented with LHS-1 or LMS-1. The amount of SiO_2, Al_2O_3, CaO, K_2O, MgO, MnO, P_2O_5 present in the Apollo 15 sample matches best with LMS-1. The amount of TiO of the Apollo 15 sample does not match LMS-1 but matches LHS-1. Fe_2O_3, Na_2O, SO_3, Cl, C_2O_3, NiO, S, and SrO can not be directly compared, since the content is unclear for the Apollo 16 and Apollo 15 sample or the simulants.

To simplify the comparison of the lunar dust simulants and the Apollo 16 and Apollo 15 sample the composition of each sample is displayed in a pie chart. These can be

seen for LHS-1 and Apollo 16 in figure 4.1 and and LMS-1 and Apollo 15 in figure 4.2. The percentages by weight from table 4.3 are used. It can be seen that there are main similarities between LHS-1 and the Apollo 16 sample and between LMS-1 and the Apollo 15 sample. Really noticeable is the visual match of SiO_2, Al_2O_3 and CaO. Additionally it needs to be noted, that a visual match in regards to quantity of FeO, which is present in the simulants, and Fe_2O_3, which is present in the Apollo samples, exist. However, since they are different compounds they cannot be directly compared.
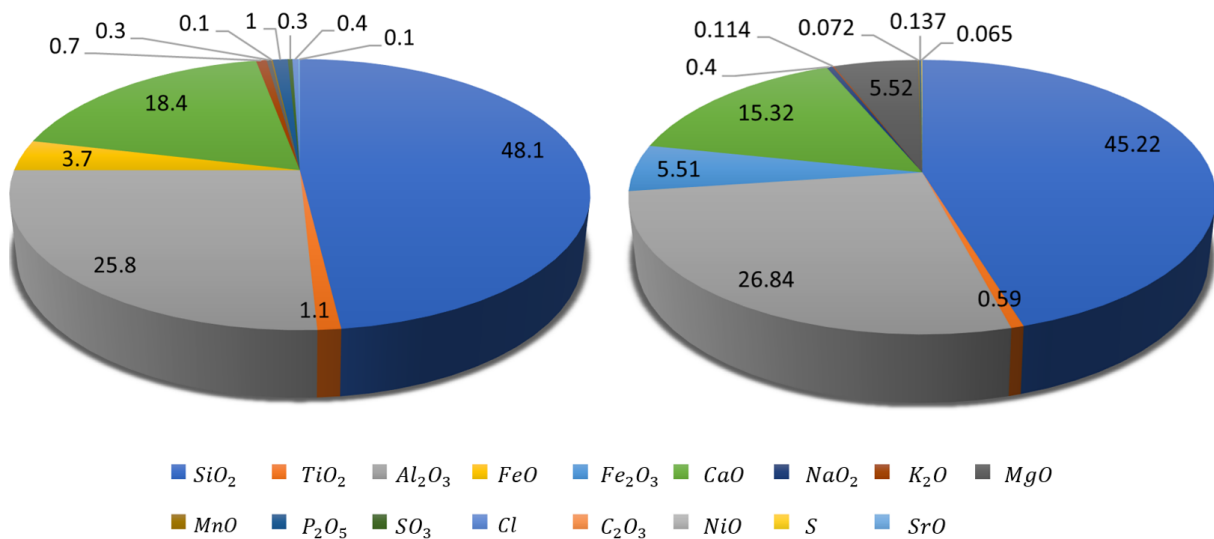
Figure 4.1: *Pie Chart of the Composition of LHS-1 (left) [55] and Apollo 16 Sample 60501.13 (right) [58] in [Wt.%]*
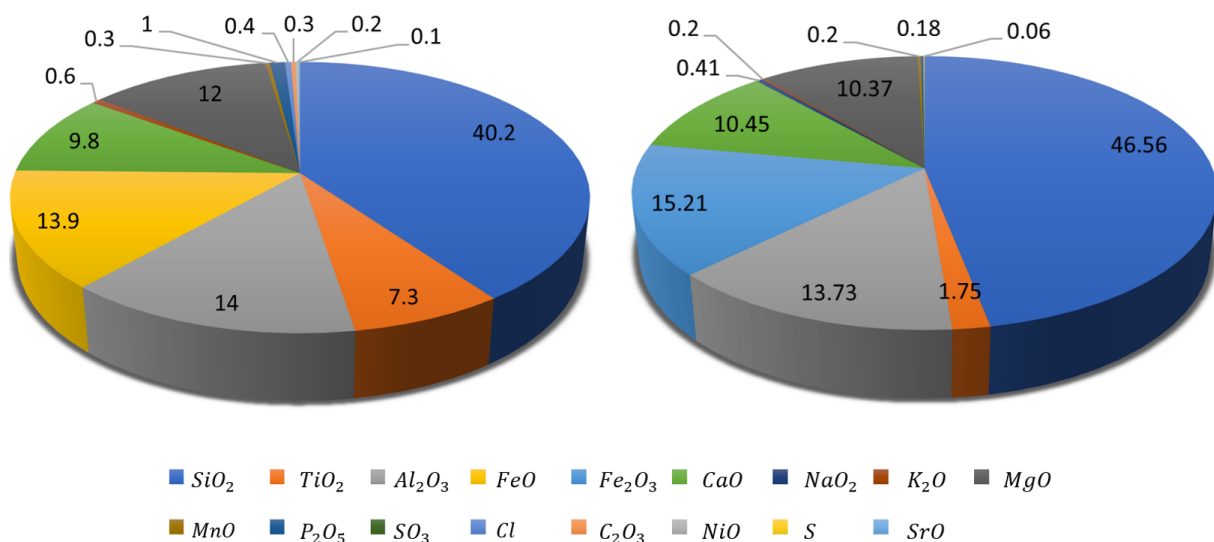
Figure 4.2: *Pie Chart of the Composition of LMS-1 (left) [57] and Apollo 15 Sample 15021.24 (right) [60] in [Wt.%]*

To sum it up, LHS-1 is an acceptable simulant for a highland region on the Moon as comparing its composition to Apollo 16 sample 60501.13 shows. LMS-1 is proven to be a simulant for the lunar mare region with reference to the Apollo 15 sample 15021.24. This supports the statement made by the *John Hopkins Applied Physics Laboratory* that the *Exolith Lab* simulants are a good match [15] and they are selected for the dissolution experiments.

4.1.2 Experimental Procedure

Dissolution experiments evaluate which elements are dissolving from solids into an aqueous solution over time. The solids are regolith simulants and the aqueous solution is ultrapure water or a buffer solution. For the dissolution experiments, two lunar regolith simulants are taken into account - LHS-1 and LMS-1. LHS-1 and LMS-1 from *Exolith Lab* are simulating the regolith from the highland region (LHS-1) and the mare region of the Moon (LMS-1). In this subsection, the preparation of the dissolution experiments, the experimental procedure, and the post-processing of the data are described. The experimental procedure is set by Freer, a member of the SMU research group at DLR, and the experiments are done according to her previous conducted dissolution experiments described in subsection 3.3.3. The experimental procedure can be found in the form of a check list in the appendix H.1.

In order to prepare the experiments, a clean and organised environment is desired. The distance between equipment and all technical devices has to be short to reduce possible unwanted contamination of samples. Measuring cups, pipettes and measuring cylinders are cleaned with ultrapure water to exclude pollution of samples by minerals dissolved in tap water. The data sheet of the used ultrapure water can be seen in the appendix B.1. A measuring cup for wastewater is labelled, to preclude mixing up measuring cups. For the dissolution experiments ultrapure water and a buffer solution with a pH of 5.6 are needed as aqueous solution. The ultrapure water is characterised by a conductivity of $\leq 0.056 \frac{\mu \cdot S}{cm}$.

A magnetic stirrer mixes ultrapure water with air to enrichen it with CO_2 resulting in a drop of the pH from 8 to 5.6.

The buffer solution's pH can be generated selectively due to added amounts of acids and bases. Buffer solutions are aqueous solutions in which a weak acid or base is dissolved in its corresponding base or acid. The buffer solution is relatively insensitive to further addition of base or acid due to an existing protolysis equilibrium. This means that the solution is relatively insensitive to a change of its pH value. The buffer capacity is describing how insensitive the solution is to a change of pH, in other words, how much base or acid can be added before the pH changes. Wearing nitrile gloves and safety goggles are mandatory

while preparing the buffer solution. For mixing the buffer solution, 26.978 g (Precision Balance PCB 350-3 by *KERN*) of ammonium acetate are measured and dissolved into ultrapure water inside a glass bottle. The ultrapure water is filled up, until the mixture has a volume of 0.5 l and filled into a 2.5 l glass bottle. In a second measuring cup, 50 ml of ultrapure water is filled into. 2.86 ml of acetic acid is added to the second measuring cup with a pipette. For handling acetic acid, chemical protection gloves need to be worn as it is highly corrosive. The ultrapure water and acetic acid mixture are filled up with ultrapure water until a volume of 0.5 l is reached. The mixture is then added to the 2.5 l measuring cup to the ammonium acetate solution. 2 l of ultrapure water are added to the buffer solution and 2 l of buffer solution with pH 5.6 is made.

Next, the sample tubes are labelled with the experiment variables:

- Mixture Ratio (1:100 or 1:500 (Simulant to Aqueous Solution))

- Simulant Name (LHS-1 or LMS-1)

- Extraction Time (2 min, 15 min, 30 min, 1 h, 12 h, 24 h, 72 h)

- With or Without Buffer Solution

- First or Second Experiment Batch

First and second experiment batches are done with the same experiment parameters. This is to show the reliability of the experiments as having - in the best case - the same results from two series of experiments. The sample tubes need to be labelled and since a water extraction and a filtration is done, double the amount of sample tubes are needed. For the ultrapure water experiments an extra third set of sample tubes is needed for acidifying each sample. Acidification results in correct concentration measurements after a long time period, because it prevents the molecules inside the sample from chemical precipitation. The pH meter (pH 7 vio by *XS Instruments*) and the oximeter (oxy 7 by *XS Instruments*) are calibrated before their first use during a series of experiments. The turbidity meter can be calibrated with samples from the turbidity meter manufacturing company *Tintometer*. The pH meter is calibrated with a pH 7 solution and a pH 4.01 solution. The oximeter is calibrated in a downwards direction for 2 minutes in ambient air. The datasheets and calibration sheets of the measuring instruments can be seen in the appendix (D.1; D.2; D.3; D.4; D.5; D.6).

For conducting the dissolution experiments, 250 ml of one of the aqueous solutions is measured using a measuring cylinder and filled into a plastic container. Using a pH meter the pH and the temperature of the aqueous solution are measured. Furthermore, the

oxygen content of the ultrapure water is measured with the oximeter before mixing in the simulant. It should be noted that the experiments are performed at approximately 20 $°C$ with a deviation of one degree.

Depending on the mixture ratio 2.5 g (mixture ratio: 1:100) or 0.5 g (mixture ratio: 1:500) of the lunar regolith simulant are weighed and added to an aqueous solution. As long as handling the regolith simulant directly, a lab coat, safety goggles, gloves, a FFP3 mask, and working under a laboratory fan is mandatory. For the ongoing process, only a lab coat, safety goggles and nitrile gloves are needed, because as the simulant is in contact with the water it does not dust anymore. Next, the mixture is permanently mixed with 20 Rotations Per Minute (RPM) with an overhead shaker (Hei-MIX Reax 2 by *heidolph*). The start time of the mixing process is the start time of the time measurements for the extraction time. A water extraction of each container is taken after 2 min, 15 min, 30 min, 60 min, 720 min (12 h), 1440 min (24 h) and 4320 min (72 h). The mixing process is stopped for these times and using a syringe approximately 10 ml are extracted into the first sample tube. It is important to mention that primarily the water from the water surface is taken. This is done to lower the risk of extracting regolith simulant particles as it as it makes the filtration by hand difficult. The solution is assumed as well homogenised due to mixing. Since this assumption is made the risk of having different ion concentrations over the filling level of the water inside the sample tube can be neglected.

Simplifying filtration of the extracted water is implemented by a sedimentation process. To force sedimentation, the extracted water is centrifuged at 6000 RPM (Eba 20 *Hettich*) for 10 minutes. 5 to 6 ml of the extracted water are filled into a measuring cup, letting the sediment sit in the sample tube which is disposed. The extracted water is drawn up with a new syringe (Inject Luer Lock syringe by *B.Braun*). The water sample is then filtered by hand using a PTFE 0.45 μm syringe filter (by *Membrane Solutions*), which is screwed onto the syringe. The extracted water is directly filtered into the second prepared sample tube.

For the acidification of the water samples nitric acid (HNO_3) is used. For analysing the extracted water, the laboratory needs 5 ml of a water sample and a molarity of 0.56 $\frac{mol}{l}$. Therefore, 4.8 ml of extracted, filtered water are filled into the third sample tube and 0.2 ml acid are added. The amount of required acid can be calculated with equation 4.1. The procedure is done for every water sample.

$$c_1 \cdot V_1 = c_2 \cdot V_2$$

$$\Leftrightarrow V_1 = \frac{c_2}{c_1} \cdot V_2$$

$$V_1 = \frac{0.56\frac{mol}{l}}{14\frac{mol}{l}} \cdot 0.005ml \tag{4.1}$$

$$V_1 = 0.2ml$$

Using a turbidity meter the turbidity of every ratio and simulant is measured (TB 211 IR by *Tintometer*) after the time period of 72 *h* to determine an average turbidity value. Therefore, the simulant aqueous solution mixture is prepared accordingly to the dissolution experiments but without water extractions. The measuring range of the turbidity meter is 0.01 to 1100 *NTU*. If the turbidity value is too high to be measured, the sample is diluted 1:10 and multiplied by ten. For measuring the turbidity 11 *ml* of each container are filled into a small glass tube which is inserted into the turbidity meter. A picture of the dissolution experiment setup can be seen in figure 4.3. The post-processing is done using *Excel* and *Tecplot.*
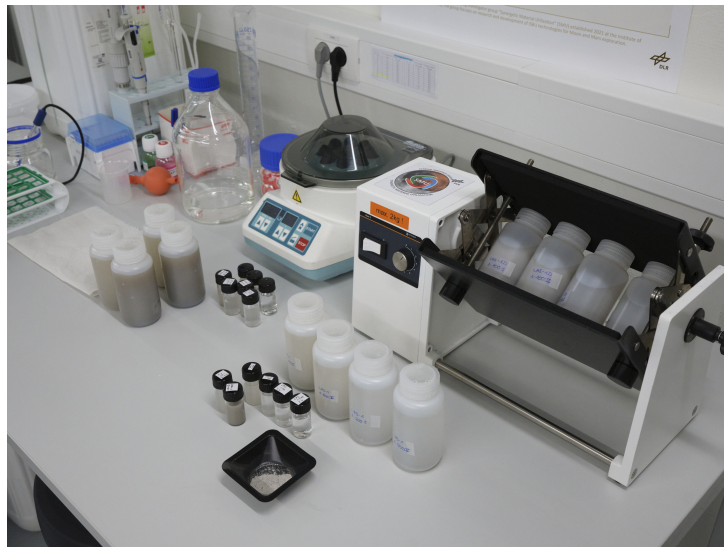
Figure 4.3: *Setup of Dissolution Experiment*

The water samples are sent to an external laboratory, the *Central Laboratory of the Technical University of Hamburg*, where the samples are analysed via ICP-OES, which is an advanced analytical technique for detecting chemical elements. It diffuses the sample into argon, where the chemical elements are atomised by high temperatures. The resulting emissions are analysed to determine measured elements.

4.2 Results of Dissolution Experiments

In this section the results of the dissolution experiments regarding its turbidity, pH and released ions into aqueous solution are presented. Ultrapure water and buffer solution are used as aqueous solution. The data gained through the results of the experiments are the basis for the selection of the lunar water simulant.

The presented diagrams in the subsequent sections follow the same form of presentation. LHS-1 and LMS-1 are represented with a ratio of 1:100 and 1:500. A legend in the diagram shows the following: LHS-1 can be seen in red shades, LHS-1 1:100 in red with a square symbol and LHS-1 1:500 in pink with a triangle symbol for each measuring point. LMS-1 can be seen in blue shades, LMS-1 1:100 in dark blue with a gradient symbol and LMS-1 1:500 in light blue with a diamond symbol for each measuring point. Furthermore, the results from the experiments with water use filled symbols and for buffer solutions outlined symbols are used. Because two batches are done the average values for the released ions are shown with a standard deviation in the form of error bars. The standard deviation δs is calculated using formula 4.2 in $\frac{mg}{g_{solid}}/\frac{mg}{l_{aqueous}}$. x is the sample value, $\overline{x}$ the sample mean average, both in the unit $\frac{mg}{g_{solid}}/\frac{mg}{l_{aqueous}}$, and n is the sample size without a unit.

$$\Delta s = \sqrt{\frac{\sum(x - \overline{x})}{(n - 1)}} \qquad (4.2)$$

The initial values of the dissolution experiments are shown in table 4.4, displaying the pH of the aqueous solution, the dissolved oxygen (O_2) in aqueous solution (Aq. S.), and the temperature of the aqueous solution. All measuring results used for the figures and texts can be seen in the appendix C.1, C.2, C.3, and C.4.

Table 4.4: *Initial Values of Dissolution Experiments*

Measured Value	Unit	1:100	1:500	1:100 Buffer	1:500 Buffer
Initial pH	[-]	5.6	5.6	5.6	5.6
Initial dissolved O_2 in Aq. S.	$[\frac{mg_{O_2}}{L}]$	8.7	8.7	8	8
Initial Temperature	[°C]	19.8	19.8	19.8	19.8

The initial pH is as required with a value of 5.6. The dissolved oxygen in the aqueous solution is the same for each buffer within the aqueous solution. The temperature for the conducted experiments is the same. Since the initial values of the first and second batch of experiments are congruent, the batches are considered comparable.

4.2.1 Turbidity Measurements

The average measured turbidity values can be seen in table 4.5. The results are always given for the first (I) and second (II) batch and a resulting median, all in the Nephelometric Turbidity Unit (NTU).

The tested lunar regolith simulants in ascending order of turbidity are: LMS-1, LHS-1 and LHS-1D. Regarding the regolith simulant ratio, the ratio 1:100 causes a higher turbidity than the ratio 1:500, a higher simulant mass causes a higher turbidity due to a higher amount of particles. Furthermore, it can be noted that the turbidity is not linear proportional to the mass of lunar regolith simulant.

Table 4.5: *Turbidity of LHS-1, LMS-1, and LHS-1D in the Ratio of 1:100 and 1:500*

Simulant	LHS-1		LMS-1		LHS-1D	
Ratio	1:100	1:500	1:100	1:500	1:100	1:500
I	999.7	222.3	594.3	422.7	9790	1054
II	1030.7	258.3	639.0	425.0	9933	1086
Average Value	1015.2	240.3	616.65	423.85	9861.5	1070

A picture of the turbidity samples of LHS-1, LMS-1 and of LHS-1D can be seen in figure 4.4.
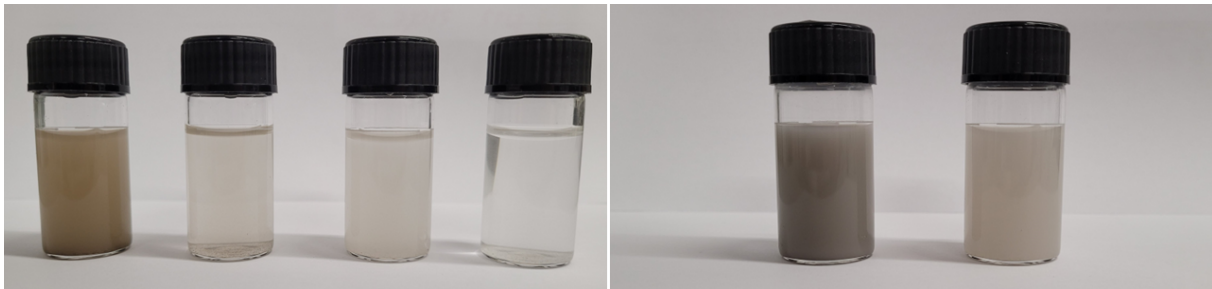
Figure 4.4: *Turbidity Samples, from left to right: LMS-1 1:100, LMS-1 1:500, LHS-1 1:100, LHS-1 1:500, LHS-1D 1:100, LHS-1D 1:500*

4.2.2 pH Level over Time

In figure 4.5 the pH level of LHS-1 and LMS-1 in ultrapure water are shown over time in h.

The pH level is displayed on the y-axis with a range of 5.0 to 9.5. The time can be read on the x-axis in h, it ranges from 0 to 72 h. The pH of LHS-1 1:500 starts at 5.6 and rises steeply within one h to 7.8. Then the pH settles at about 8. The same applies to LMS-1 1:500. The pH rises rapidly from 5.6 to 8.05 within one h. After that, the pH settles at

8. For LHS-1 1:100, the pH rises from an initial 5.6 to 9.35 after 12 h. It then decreases to 9 after 72 h. LMS-1 1:100 can show an increase in pH from 5.6 to 9.15 after 12 h. Afterwards, there is a decrease to a pH of 8.95 after 72 h.
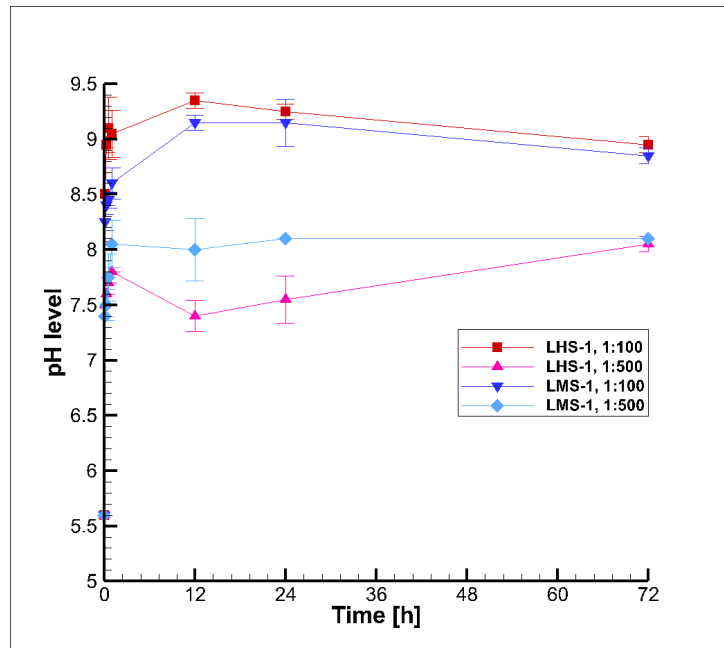
Figure 4.5: *pH Level of LHS-1 and LMS-1 in Ultrapure Water*

The results of the pH measurements in buffer solution can be seen in figure 4.6. For both simulants and both ratios the pH oscillates around 5.6 over 72 h.
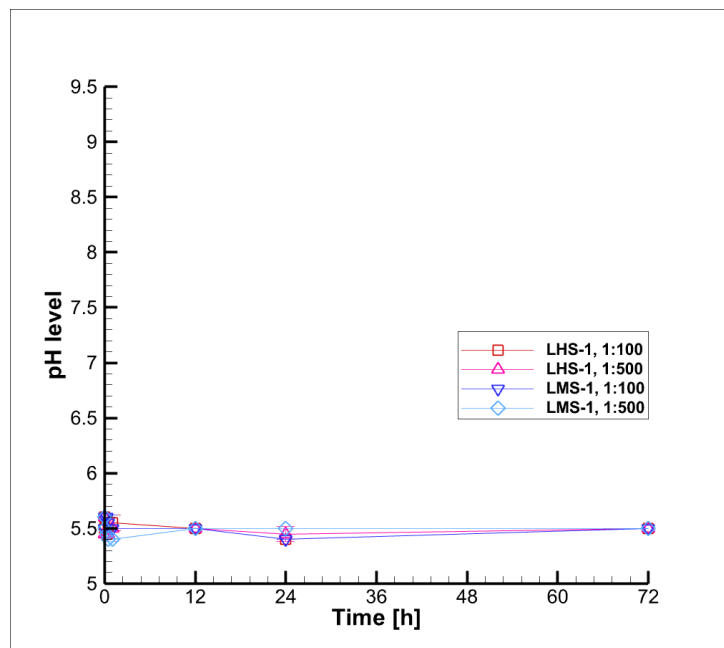
Figure 4.6: *pH Level of LHS-1 and LMS-1 in Buffer Solution*

4.2.3 Released Ions over Time

The unit of the released ions is $\frac{mg}{g_{solid}}$ with released ions in mg per simulant mass in g_{solid} or $\frac{mg}{l_{aqueous}}$ with released ions in mg per litre of aqueous solution ($l_{aqueous}$). A density of $1\ \frac{kg}{l}$ is assumed for a litre of aqueous solution. The unit $\frac{mg}{l_{aqueous}}$ is used as it is more common regarding contamination within aqueous solutions. For the figures in the following subsections, the released ions into aqueous solution from simulant in $\frac{mg}{g_{solid}}$ are presented on the y-axis. The range of released ions on the y-axis is always the same for an ion using ultrapure water and buffer solution to enable the comparison between the different aqueous solutions if needed. The time in h can be read on the x-axis, it ranges from 0 to 72 h. The buffer solution is corrosive to the ICP-OES. Therefore, it has to be diluted before calibration and analysing. This results in a different detection limit of the buffer solution and ultrapure water. For example, if the buffer solution is diluted five times compared to the ultrapure water the detection limit of the ICP-OES of the buffer solution is five times higher than of the ultrapure water.

The ion concentration is analysed at the *Central Laboratory of the Technical University of Hamburg* via ICP-OES. The tested ions are: aluminium (Al), calcium (Ca), iron (Fe), potassium (K), magnesium (Mg), manganese (Mn), sulfur (S), silicon (Si), titanium (Ti).

4.2.4 Released Ions into Ultrapure Water over Time

Regarding the released ions experimenting with ultrapure water the shape of the graphs of the dissoluted ions over time can be divided into four categories:

1. Linear increase

    The released aluminium ions using LHS-1 1:100, LMS-1 1:100 have a linear curve shape.

2. Parabolic increase within 12 hours and then a constant value

    The amount of released calcium ions and sulfur show a parabolic behaviour within 12 hours. After 12 hours the value stays constant.

3. Parabolic increase over 72 hours

    The amount of released magnesium using LMS-1, released potassium using LHS-1, and LMS-1 1:100 and released silicon ions have a parabolic behaviour over the test time of 72 hours. Except for silicon LMS-1 1:00 which has a big standard deviation towards the end and fits this behaviour until an extraction time of 24 hours.

4. No measured ions

No statement can be made regarding the behaviour of the released ions of aluminium using LHS-1 1:500 and LMS-1 1:500, iron, potassium using LMS-1 1:500, magnesium using LHS-1, manganese and titanium, because the detection limit using the ICP-OES is not reached.

A detailed description on the amount of released ions over time is presented for each element in the following subsections.

Released Aluminium Ions in Ultrapure Water

The released aluminium ions into ultrapure water over 72 h can be seen in figure 4.7. The released ions of LHS-1 with the ratio 1:100 increase from less than 0.005 $\frac{mg}{g_{solid}}$ after one h to 0.0471 $\frac{mg}{g_{solid}}$ after 72 h in a linear curve. For LMS-1 with the ratio 1:100 the released ions increase slightly from less than 0.005 to 0.0056 $\frac{mg}{g_{solid}}$ after 12 h. It then linearly increases to 0.0147 $\frac{mg}{g_{solid}}$ after 72 h. The amounts of the released aluminium ions by LHS-1 1:500 and LMS-1 1:500 do not exceed the detection limit.
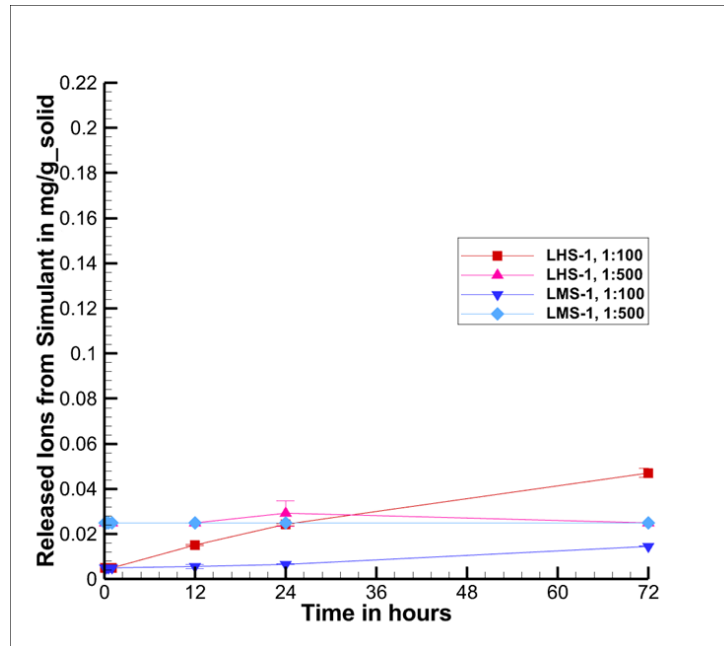
Figure 4.7: *Released Aluminium Ions into Ultrapure Water from Simulant over Time*

Released Calcium Ions in Ultrapure Water

The released calcium ions over 72 h can be seen in figure 4.8. The amount of released calcium ions of LHS-1 1:100 increases steeply within the first 12 h from 0.285 to 0.61 $\frac{mg}{g_{solid}}$, where it settles. The curve of LHS-1 1:500 is similar. The amount of released ions increases very steeply within the first 12 h from 0.731 and settles at approximately 1.4 $\frac{mg}{g_{solid}}$. LMS-1 with the ratio of 1:100 displays a steep curve within the first 12 h with a rise from 0.1412 $\frac{mg}{g_{solid}}$ to a constant value of 0.35 $\frac{mg}{g_{solid}}$. LMS-1 1:500 rises steeply from 0.5118 to a constant value of 0.8589 $\frac{mg}{g_{solid}}$ within the first 12 h.
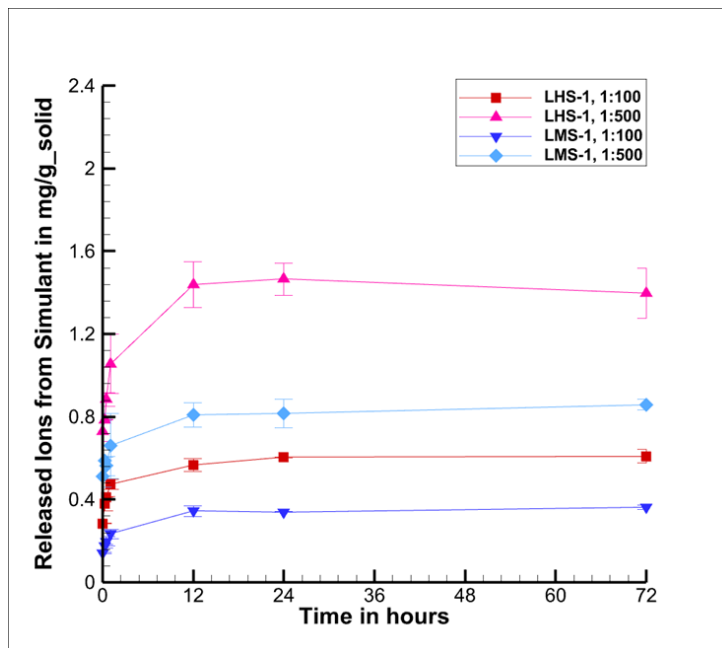
Figure 4.8: *Released Calcium Ions into Ultrapure Water from Simulant over Time*

Released Potassium Ions in Ultrapure Water

The released potassium ions into ultrapure water are displayed in figure 4.9. The amount of released potassium ions of LHS-1, 1:100 is less than 0.05 $\frac{mg}{g_{solid}}$ during the first h. It rises to 0.067 $\frac{mg}{g_{solid}}$ after 72 h in total. LHS-1 with the ratio of 1:500 rises steeply from 0.583 $\frac{mg}{g_{solid}}$ to 1.214$\frac{mg}{g_{solid}}$ within the first h. Afterwards it increases further but with a reduced slope. After 72 h an amount of released potassium ions of 1.539 $\frac{mg}{g_{solid}}$ is reached. For LMS-1, 1:100 the amount slowly rises from 0.0619 to a constant 0.1155 $\frac{mg}{g_{solid}}$ within the first h. The amount of the released potassium ions by LMS-1 1:500 does not exceed the detection limit.
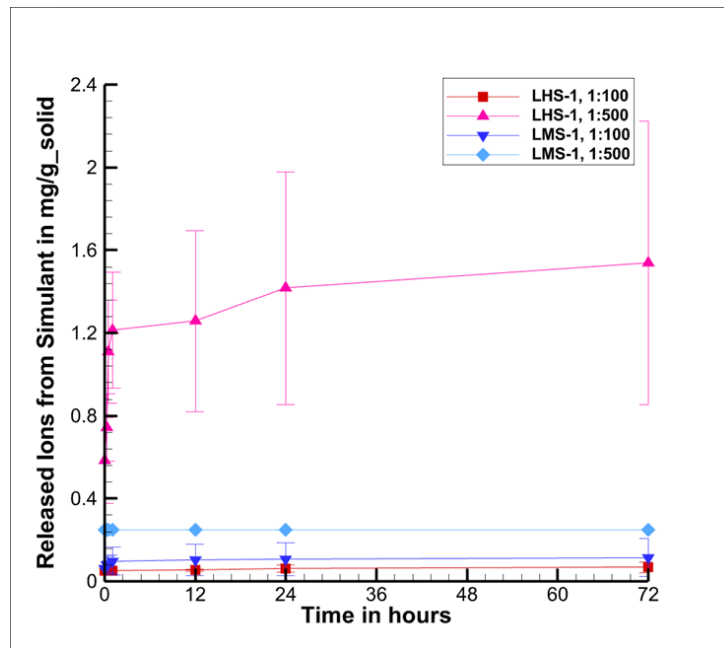
Figure 4.9: *Released Potassium Ions into Ultrapure Water from Simulant over Time*

Released Magnesium Ions in Ultrapure Water

Figure 4.10 shows the released magnesium ions over time. The released ions of LMS-1 in the ratio 1:100 and 1:500 rise parabolically, whereby the 1:500 curve is steeper. LMS-1 in the ratio of 1:100 rises over 72 h from 0.0356 to 0.0623 $\frac{mg}{g_{solid}}$ within the first h and with a decreased slope to 0.1388 $\frac{mg}{g_{solid}}$ after 72 h. With the ratio of 1:500, the amount of released magnesium ions rises from 0.0827 to 0.1472 $\frac{mg}{g_{solid}}$ within the first h and with a decreased slope to 0.3454 $\frac{mg}{g_{solid}}$ after 72 h. The amounts of the released magnesium ions by LHS-1 1:100 and 1:500 do not exceed the detection limit.
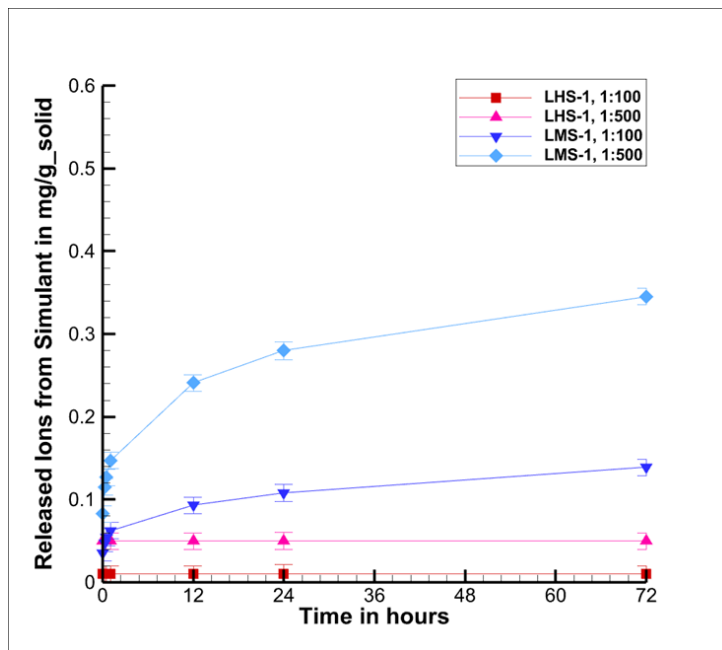
Figure 4.10: *Released Magnesium Ions into Ultrapure Water from Simulant over Time*

Released Sulfur Ions in Ultrapure Water

In figure 4.11, where the released sulfur ions over time are shown, the amount of released ions of LHS-1, 1:100 rises parabolically from 0.0073 $\frac{mg}{g_{solid}}$ to 0.0125 $\frac{mg}{g_{solid}}$ within 12 h. After 12 h, the amount of released ions stays constant at approximately 0.0125 $\frac{mg}{g_{solid}}$. LHS-1, 1:500 has a similar curve. The amount of released sulfur ions rises parabolically within 12 h from 0.016 $\frac{mg}{g_{solid}}$ to approximately 0.03 $\frac{mg}{g_{solid}}$. Afterwards, the value of released ions stays constant. For the simulant LMS-1, 1:100 the amount of released sulfur ions rises parabolically from 0.0056 $\frac{mg}{g_{solid}}$ within the first 12 h to 0.012 $\frac{mg}{g_{solid}}$. The same behaviour is shown by the released ions of LMS-1, 1:500. The amount of released sulfur ions is 0.015 and increases to constant 0.023 $\frac{mg}{g_{solid}}$.
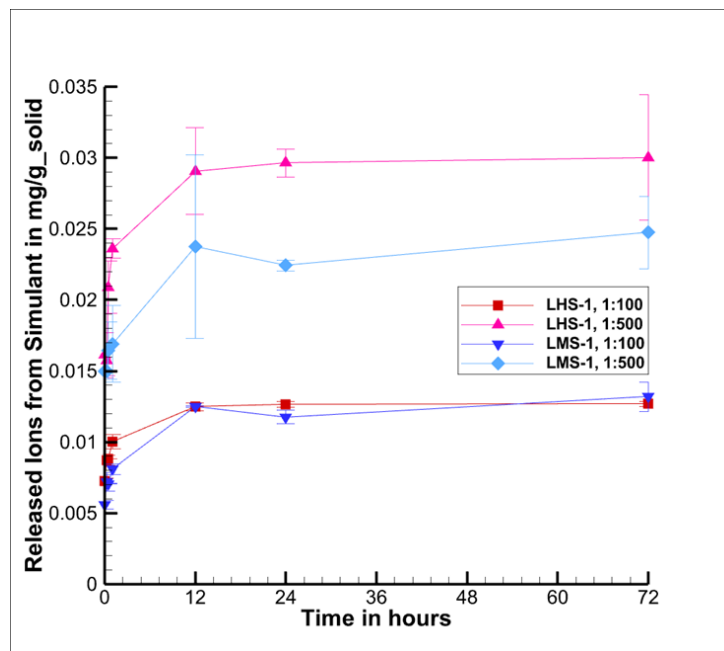
Figure 4.11: *Released Sulfur Ions into Ultrapure Water from Simulant over Time*

Released Silicon Ions in Ultrapure Water

In figure 4.12 the amount of released silicon ions can be seen. The amount of released ions of LHS-1, 1:100 rises parabolically from 0.0269 to 0.1097 $\frac{mg}{g_{solid}}$ within the first 72 h. The curve of LHS-1 with a ratio of 1:500 rises from 0.131 $\frac{mg}{g_{solid}}$ to 0.1996 within 24 h. The amount of released ions after 72 h is smaller than the amount of released ions after 24 h with 0.168 $\frac{mg}{g_{solid}}$. LMS-1, 1:100 rises parabolically from 0.0322 $\frac{mg}{g_{solid}}$ to 0.2303 $\frac{mg}{g_{solid}}$ within 72 h. With a ratio of 1:500 the amount of released silicon ions of LMS-1 decreases from 0.1523 to 0.1435 $\frac{mg}{g_{solid}}$ within one h. After the first h the curve rises parabolically and steeply to a value of 0.3845 $\frac{mg}{g_{solid}}$ after 72 h.
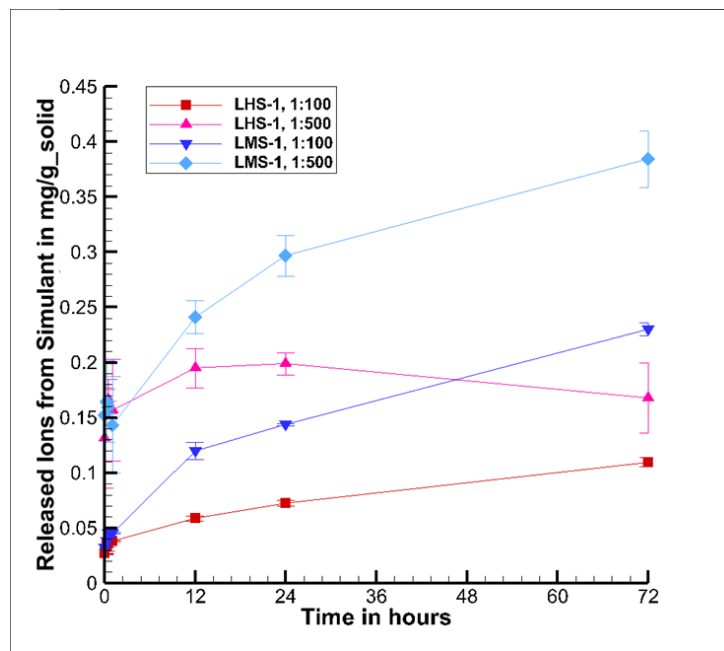
Figure 4.12: *Released Silicon Ions into Ultrapure Water from Simulant over Time*

4.2.5 Released Ions into Buffer Solution

Regarding the released ions experimenting with buffer solution the results can be divided into four categories:

1. Constant value

   The iron amount of released ions of LHS-1 1:500 and sulfur of LMS-1 1:100, manganese of LHS-1 1:100 and titanium LMS-1 1:100 present a constant value.

2. Parabolic behaviour within 12 hours and then a constant value

   The released calcium ions show a parabolic behaviour within 12 hours and then a constant value.

3. Parabolic behaviour over 72 hours

   The released aluminium, magnesium LMS-1 and silicon ions have a parabolic behaviour over 72 hours.

4. No measured ions

   No statement can be made regarding the released ions of iron using LHS-1 1:100, iron LMS-1, potassium, magnesium using LHS-1, manganese LMS-1, manganese LHS-1 1:500, sulfur LHS-1, sulfur LMS-1 1:500, titanium LHS-1, titanium LMS-1 1:500, because the detection limit using the ICP-OES is not reached.

For further detail and description of the released ions over time can be seen in the following subsections.

Released Aluminium Ions in Buffer Solution

The released aluminium ions into buffer solution over time can be seen in figure 4.13. The amount of released aluminium ions of LHS-1, 1:100 is approximately constant at 0.013 $\frac{mg}{g_{solid}}$. The amount of released ions of LHS-1, 1:500 cannot be described, except for the last value with 0.053 $\frac{mg}{g_{solid}}$ after 72 h. The released ions of LMS-1, 1:100 increase parabolically within the first 12 h from 0.01 to 0.102 $\frac{mg}{g_{solid}}$. After the first 12 h, the released ions decrease to 0.069 $\frac{mg}{g_{solid}}$. The amount of released ions of LMS-1, 1:500 rises parabolically within 12 h from 0.05 to 0.189 $\frac{mg}{g_{solid}}$. Afterwards, the amount of released ions decreases to 0.175 $\frac{mg}{g_{solid}}$ after 72 h.
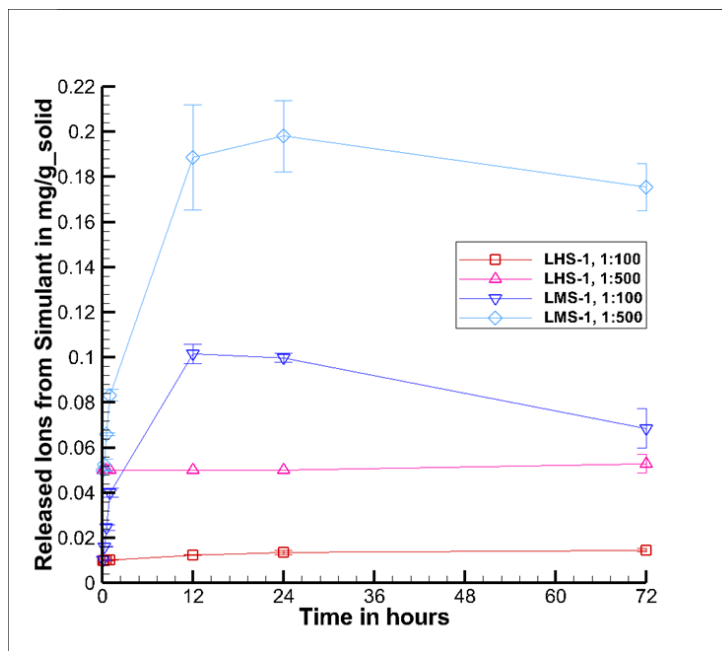
Figure 4.13: *Released Aluminium Ions into Buffer Solution from Simulant over Time*

Released Calcium Ions in Buffer Solution

Figure 4.14 displays the released calcium ions into buffer solution over 72 h. The curve shape is similar for both simulants and both ratios. The amount of released ions increases strongly in the first h and after 12 h it levels off. The amount of released calcium ions of LHS-1 1:100 increases from 1.242 to 1.411 $\frac{mg}{g_{solid}}$ within the first h and up to an approximate value of 1.5 $\frac{mg}{g_{solid}}$ after 12 h. With a ratio of 1:500, the released ions increase from 1.823 $\frac{mg}{g_{solid}}$ to approximately 20 $\frac{mg}{g_{solid}}$ after one h. The curve levels off with a value of 20.5 $\frac{mg}{g_{solid}}$. The second simulant, LMS-1, shows an increase from 0.546 to 0.671 $\frac{mg}{g_{solid}}$ in the first h and the released ions level off at 0.85 $\frac{mg}{g_{solid}}$ after 12 h. The curve of LMS-1, 1:500 rises steeply from 1.105 $\frac{mg}{g_{solid}}$ to 1.269 within one h. The curve levels off at 1.45 $\frac{mg}{g_{solid}}$ after 12 h.
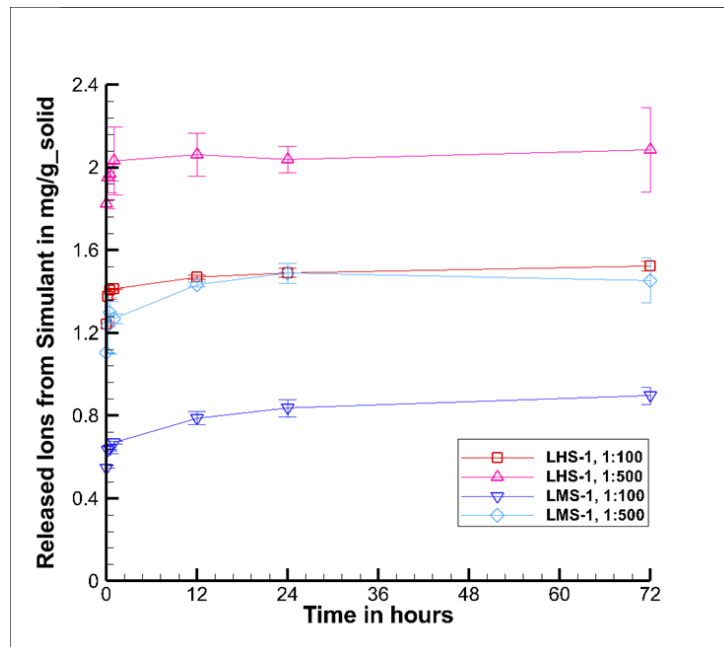
Figure 4.14: *Released Calcium Ions into Buffer Solution from Simulant over Time*

Released Iron Ions in Buffer Solution

In figure 4.15 the released ions of iron into buffer solution over time can be seen. LMS-1 with a ratio of 1:500 has a constant value of 0.21 $\frac{mg}{g_{solid}}$. The amounts of the released iron ions by LHS 1:100, LMS-1 1:100, and LMS-1 1:500 do not exceed the detection limit.
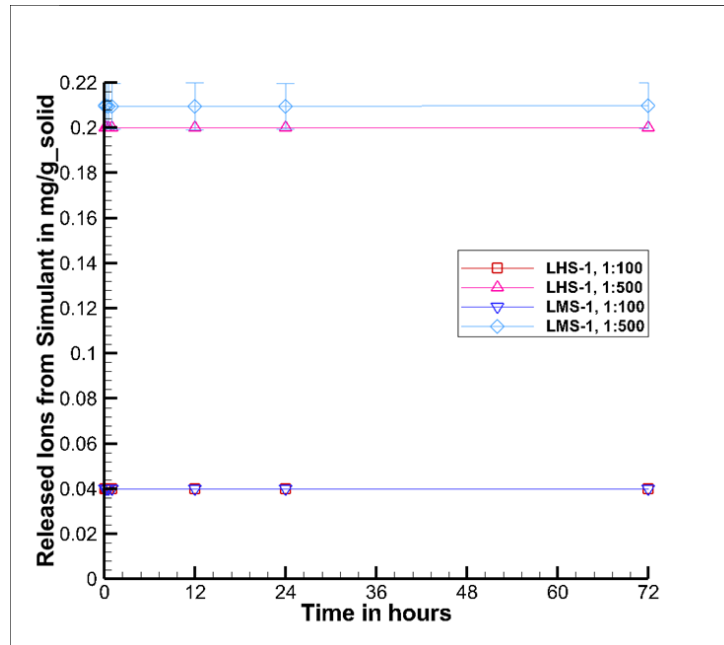
Figure 4.15: *Released Iron Ions into Buffer Solution from Simulant over Time*

Released Magnesium Ions in Buffer Solution

The released magnesium ions can be seen in figure 4.16. LMS-1, 1:100 shows a parabolic rise over the 72 h, the amount of released ions increases from 0.124 to 0.485 $\frac{mg}{g_{solid}}$. LMS-1, 1:500 has a parabolic curve as well. The released ions increase from 0.2 to 0.557 $\frac{mg}{g_{solid}}$. The amounts of the released magnesium ions by LHS-1 1:100 and 1:500 do not exceed the detection limit.
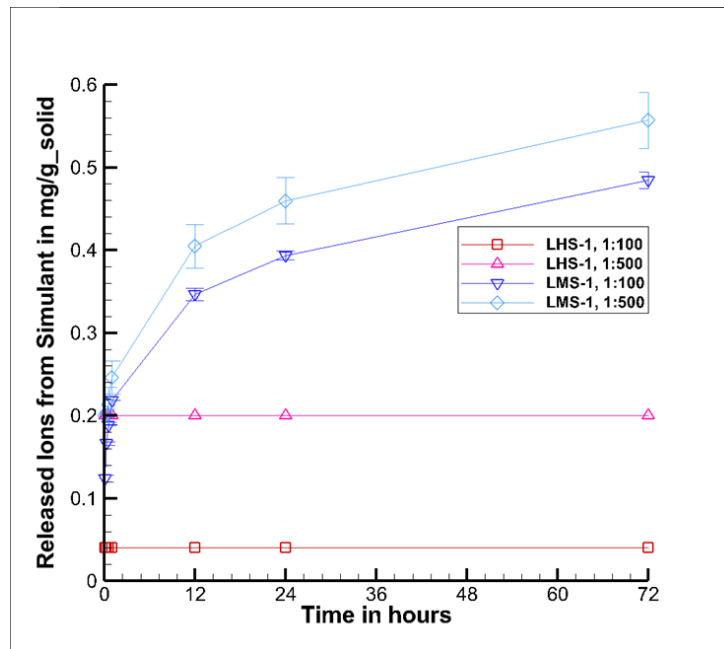
Figure 4.16: *Released Magnesium Ions into Buffer Solution from Simulant over Time*

Released Manganese Ions in Buffer Solution

The amount of manganese ions can be seen in figure 4.17. LHS-1 1:100 is the only experiment resulting in a measured value above the detection limit with $0.047 \frac{mg}{g_{solid}}$ after $72\ h$. The amounts of the released manganese ions by LHS-1 1:500, LMS-1 1:100, and LMS-1 1:500 do not exceed the detection limit.
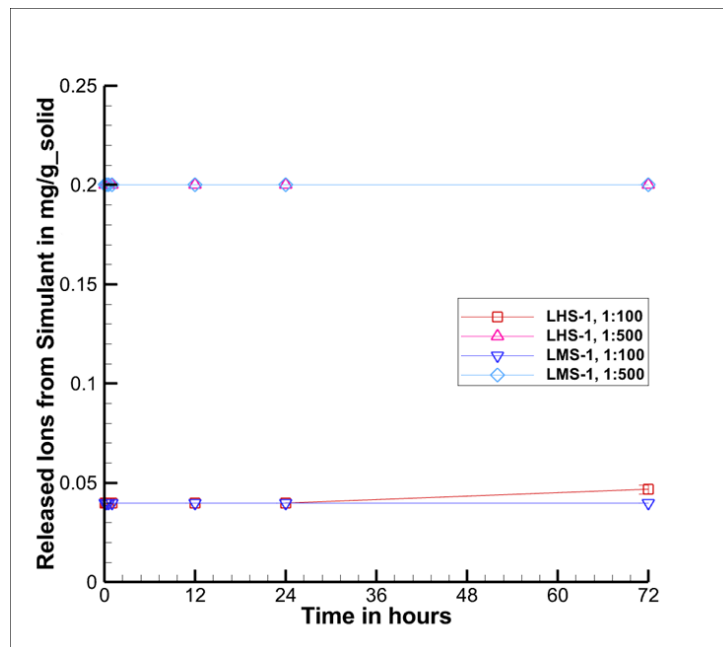
Figure 4.17: *Released Manganese Ions into Buffer Solution from Simulant over Time*

Released Sulfur Ions in Buffer Solution

Figure 4.18 displays the released ions of sulfur over time. Using LMS-1 1:100 released ions can be measured. After one h, the released sulfur ions can be first measured with 0.0074 $\frac{mg}{g_{solid}}$. At 12 h the amount of released ions is less than the detection limit. Afterwards it is constantly 0.0074 $\frac{mg}{g_{solid}}$. The amounts of the released sulfur ions by LHS-1 1:100, LHS-1 1:500, and LMS-1 1:500 do not exceed the detection limit.
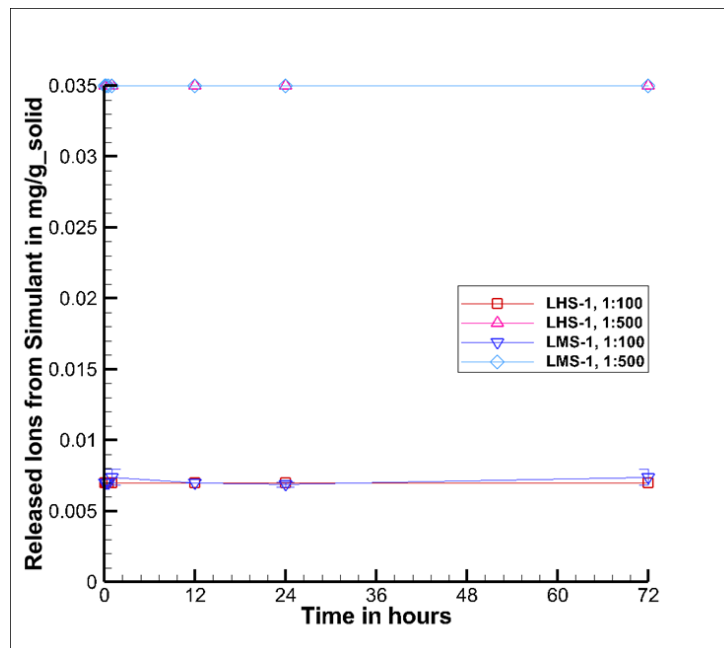
Figure 4.18: *Released Sulfur Ions into Buffer Solution from Simulant over Time*

Released Silicon Ions in Buffer Solution

The released amount of silicon ions is displayed in figure 4.19. LHS-1, 1:100 has a measurable amount of released ions after 12 h with 0.047 $\frac{mg}{g_{solid}}$. The amount of released ions rises to 0.089 $\frac{mg}{g_{solid}}$ after 72 h. The released ions of LHS-1, 1:500 are less than the detection limit with less than 0.2 $\frac{mg}{g_{solid}}$ until a time of 24 h. It then rises to a constant 0.2 $\frac{mg}{g_{solid}}$. The curve of LMS-1, 1:100 rises from less than 0.04 $\frac{mg}{g_{solid}}$ to 0.189 $\frac{mg}{g_{solid}}$ within the first h. The amount of released ions of LMS-1, 1:500 rises from less than 0.2 $\frac{mg}{g_{solid}}$ within the first 12 h to 0.281 $\frac{mg}{g_{solid}}$ after 72 h.
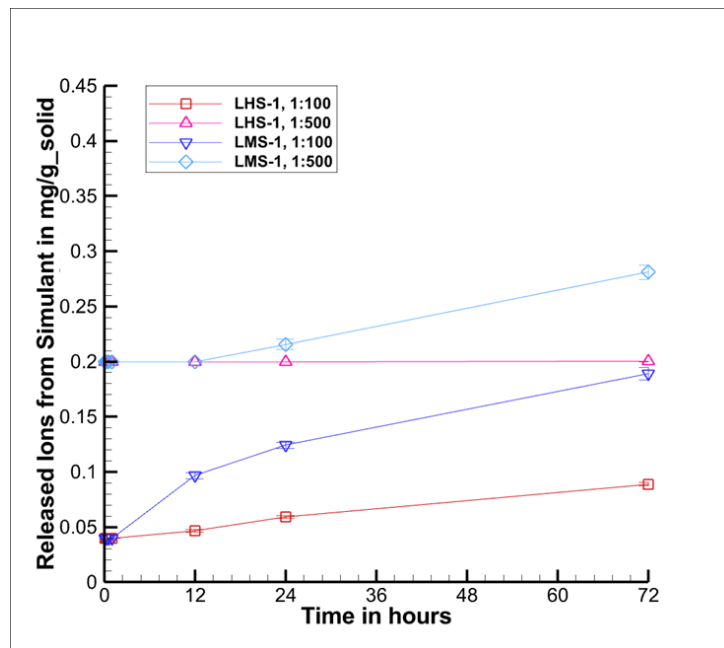
Figure 4.19: *Released Silicon Ions into Buffer Solution from Simulant over Time*

Released Titanium Ions in Buffer Solution

Figure 4.20 presents the released titanium ions into buffer solution. The amount of released ions exceeding the detection limit is caused by LMS-1, 1:100. The amount of released ions increases to 0.042 $\frac{mg}{g_{solid}}$ after 24 h and 0.048 $\frac{mg}{g_{solid}}$ after 72 h. The amounts of the released titanium ions by LHS-1 1:100, LHS-1 1:500, and LMS-1 1:500 do not exceed the detection limit.
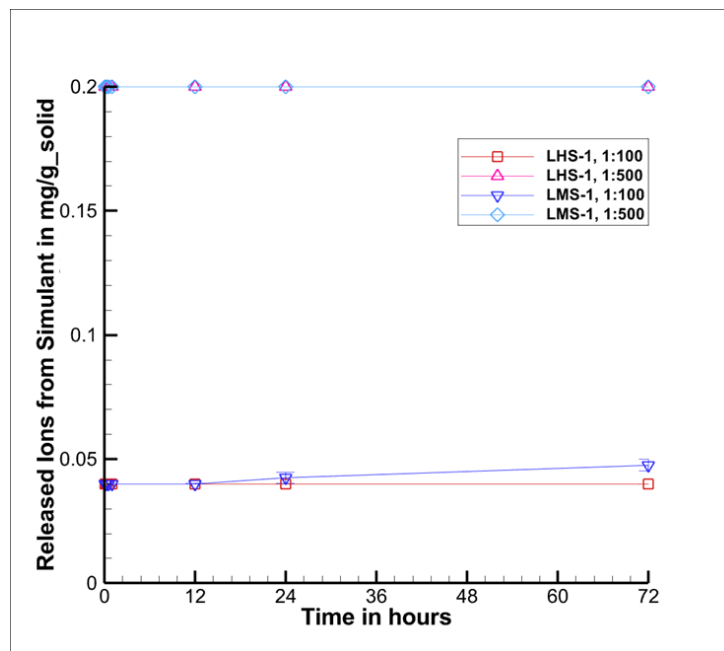
Figure 4.20: *Released Titanium Ions into Buffer Solution from Simulant over Time*

4.3 Discussion of Dissolution Experiments

In this section the results in regards to the influences of the aqueous solution, the simulant water ratio, the bulk chemistry, and the particle size are discussed, to determine a lunar water simulant with set values for these four factors. The theoretical background of the dissolution experiments, which is explained in section 3.3, forms the rationale for the discussion. The important key statements from the theoretical background are summed up for the discussion in the following.

Eick et al. concluded a direct proportional relationship between dissolved ions and bulk composition of dry simulant [48]. Eick et al. characterised the results of the dissolution experiments using simulant as surface-controlled reactions due to its parabolic increase over time [49], as well as Karl et al. [51] and Freer et al. Most importantly, Eick et al. stated that the quantity of released ions increased with a decreasing pH [49], which was also observed by Freer et al. Furthermore, Karl et al. stated accordingly to Whitney an inversely proportional relation between the particle size and the dissoluted ions and

explained it with the increased particle surface area for smaller particles ([46]; [51]). Following the square-cube law, small particles have an increased surface per volume ratio than bigger particles. Freer et al. stated that using the ratio 1:500 rather than 1:100 caused a higher amount of released ions in $\frac{mg}{g_{solid}}$ using LHS-1D as simulant. It was noted that the most ions were released within the first two minutes.

Following the results from Eick et al., Karl et al. and Freer et al. the discussion of the conducted dissolution experiments is categorised into four parts according to observations:

1. More ions are released into the buffer solution in $\frac{mg}{g_{solid}}$, due to the lower pH.

2. More ions are released in $\frac{mg}{l_{aqueous}}$ using the ratio 1:100.

3. The bulk composition of the simulant is directly connected to the amount of released ions in $\frac{mg}{g_{solid}}$.

4. More ions in $\frac{mg}{g_{solid}}$ are released by a simulant with a small particle size rather than with a bigger particle size.

4.3.1 Influence of pH

The pH increases approximately parabolically for the measured period of time for all experiments in ultrapure water. This can be seen in figure 4.5. The constant pH of the buffer solution over time, which can be seen in figure 4.6 in subsection 4.2.2, is a confirmation of the buffer capacity. The behaviour of the pH over time can be assumed to be the same for LHS-1 and LMS-1 since the measured results differ only slightly from each other. This proves the comparability of LHS-1 and LMS-1 as the pH is the same and therefore the ion dissolution caused by the pH is the same.
Comparing the results of Eick et al. and Freer et al. to the dissolution results, it can be said that their statements are consistent with the results. This can be seen as a verification of correctly reproduced dissolution experiments.

For the first observation it can be said that buffer solution results in a higher amount of released ions in $\frac{mg}{g_{solid}}$. This is due to its lower pH than ultrapure water and consequently higher ion solubility. This can be seen testing for aluminium, calcium, iron, magnesium, manganese and titanium. The tested elements that do not fit the observation are potassium, silicon and sulfur. For dissolved sulfur ions it needs to be noted, that no released sulfur ions into buffer solution are measured, except for one value. But released sulfur ions into ultrapure water are measured. However, the detection limit using buffer solution is higher than the measured released sulfur ions into water. Therefore, no statement can

be made if the amount of released sulfur ions into ultrapure water is higher or lower than into buffer solution.

4.3.2 Influence of Simulant to Water Ratio

For the second observation is can be said that using the ratio 1:100 results in a higher amount of released ions in $\frac{mg}{l_{aquous}}$ but the amount of released ions over time in $\frac{mg}{g_{solid}}$ is higher using 1:500. It is assumed that the higher amount of released ions in $\frac{mg}{l_{aquous}}$ using a 1:100 ratio is because a higher mass of simulant contaminates the aqueous solution. 1:500 results in a higher amount of released ions over time in $\frac{mg}{g_{solid}}$ than 1:100 for the following tested elements. Aluminium with an exception where LHS-1 1:100 exceeds LHS-1 1:500 after 24 h. In calcium 1:500 showed a higher release of ions, as well as in potassium, magnesium, sulfur and silicon. In iron, the amount of released ions exceeding the detection limit is caused by 1:500 ratio of LMS-1. For the released ions of manganese and titanium it is the opposite. The amount of released ions is exceeding the detection limit using LHS-1 1:100 for manganese and LMS-1 1:100 for titanium.

4.3.3 Influence of Bulk Chemistry

The bulk composition of LHS-1 and LMS-1 is described in subsection 4.1.1 and on the data sheets of the regolith simulants in appendix A.2 and A.3. The third observation, the connection between the bulk composition of the simulant and the amount of dissoluted ions in $\frac{mg}{g_{solid}}$, can be divided into 4 cases:

- No oxide containing one of the tested elements is tested in the simulant.

- A higher amount of an oxide is present in LMS-1 but LHS-1 releases more ions.

- A higher amount of an oxide is present in LHS-1 and LHS-1 releases more ions or a higher amount of an oxide is present in LMS-1 and LMS-1 releases more ions.

- A higher amount of an oxide is present in LHS-1 but LMS-1 releases more ions.

Regarding the first case it can be mentioned that it is not tested for SO_3 or another oxide including sulfur in LMS-1. 0.3 $Wt.\%$ of SO_3 is present in the bulk chemistry of LHS-1 and the only measurable released sulfur ions are caused using LMS-1. No statement can be made regarding the connection of the bulk chemistry and the released sulfur ions.

The second case can be seen looking at the released manganese ions. In the bulk chemistry LHS-1 has 0.3 $Wt.\%$ MnO and LMS-1 0.1 $Wt.\%$ MnO. Only LHS-1 released manganese ions, even though it has less MnO in its bulk chemistry. It needs to be noted, that only one value of released manganese ions is measured during the conducted experiments. Therefore, the second case is not further discussed.

The third case is presented in detail in the following. 18.4 $Wt.\%$ CaO are present in the bulk chemistry of LHS-1 and 9.8 $Wt.\%$ CaO in the bulk chemistry of LMS-1. LHS-1 has a higher content of CaO and using LHS-1 more calcium ions are released. In the chemical bulk composition LHS-1 has 3.7 $Wt.\%$ Fe_2O_3 and LMS-1 13.9 $Wt.\%$ Fe_2O_3. The dissolution of iron ions is only measurable using LMS-1. 0.3 $Wt.\%$ MgO is present in LHS-1 and 12.0 $Wt.\%$ MgO in LMS-1. LMS-1 causes a higher amount of released magnesium ions in $\frac{mg}{g_{solid}}$. 1.1 $Wt.\%$ TiO_2 is measured in LHS-1's bulk chemistry and 7.3 $Wt.\%$ TiO_2 in LMS-1's. The only released titanium ions in the dissolution experiments are measured using LMS-1.

The fourth case is described in the following. In the bulk composition Al_2O_3 exists with 25.8 $Wt.\%$ in LHS-1 and in LMS-1 with 14.0 $Wt.\%$. LHS-1 has a higher amount of Al_2O_3, but has fewer released aluminium ions in $\frac{mg}{g_{solid}}$. K_2O is present with an amount of 0.7 $Wt.\%$ in LHS-1 and 0.6 $Wt.\%$ in LMS-1. From one comparison of the measured values of LHS-1 and LMS-1 it leads to the conclusion that using LMS-1 shows an higher amount of released potassium ions even if it has less K_2O in its bulk composition. 48.1 $Wt.\%$ SiO_2 are measured in LHS-1 and 40.2 $Wt.\%$ SiO_2 in LMS-1. LMS-1 results in higher amounts of released silicon ions even if a higher SiO_2 content is present in the LHS-1 simulant. It needs to be noted, that the corresponding standard deviation is relatively big and accordingly the error bar.

The results of the third case prove the third observation. It is striking that the proportions of the same oxides are far apart between the different simulants. Case four seems as evidence to the contrary for the observation but not with respect to the fourth observation mentioned in section 4.3. The fourth observation states that a smaller particle size results in a higher amount of released ions since a bigger surface per volume is exposed to the aqueous solution. The amount of the oxides K_2O and SiO_2 are close to each other and LMS-1 has a smaller particle size than LHS-1. LMS-1 releases more potassium or silicon ions possibly due to the larger particle surface relative to the particle volume than the particle surface area of LHS-1 at the same ratio. This could lead to LMS-1 releasing more ions than LHS-1 even if LHS-1 has a higher amount of the named oxides in it. Another assumption for the different solution behaviour of LHS-1 and LMS-1 in the forth case can be due to a phenomenon described by Eick et al. [48]. It was described that the

amount of released elements were related to the solubility of the minerals in which they are contained [49]. The higher a mineral's solubility was and the more oxides it contained with specific ions the more ions were released. For the simulants LHS-1 and LMS-1 is no information about the exact composition of the minerals in the form of an elemental analysis given but only the oxide and the mineral composition of the simulants.

To sum it up, it can be said that the third observation is proven with the dissolution experiments.

4.3.4 Influence of Simulant Particle Size

To prove the fourth observation the released ions into aqueous solution from simulant of LHS-1 and LHS-1D in $\frac{mg}{g_{solid}}$ are compared when contaminating buffer solution as the pH for LHS-1 and LHS-1D can be assumed as similar and consequently the ion solubility as similar as well. LHS-1 and LHS-1D have the same bulk composition, but a different mean particle size, median particle size and particle size range. For further details look at subsection 4.1.1 or the data sheets of the lunar regolith simulants in the appendix A.1 and A.2. These aspects are important when comparing the simulants as the only changing parameter can be assumed to be particle size, and different bulk chemistry or ion solubility can be excluded. The results using the 1:500 ratio are compared, because the amount of released ions in aqueous solution in $\frac{mg}{g_{solid}}$ is higher than in the ratio 1:100. Using LHS-1 in buffer solution results in no dissoluted magnesium, potassium, titanium, iron or sulfur ions while using LHS-1D every tested for element is present in the buffer solution from the first extraction time. Released ions of manganese using LHS-1 is only measurable at the last extraction time and barely higher than the detection limit. Therefore, it is not considered in this section. The comparison regarding the released calcium, silicon and aluminium ions from LHS-1 and LHS-1D in $\frac{mg}{g_{solid}}$ over time can be seen in figure 4.21. The x-axis represents the time in hours and the y-axis represents the released ions into buffer solution from simulant in $\frac{mg}{g_{solid}}$. Released calcium ions are shown in pink, the released silicon ions in light blue, the released aluminium ions in dark blue. The results using LHS-1 are displayed with empty squares and the results using LHS-1D are displayed using colour filled delta symbols. It is noticeable that using LHS-1D results in more calcium, silicon and aluminium ions.
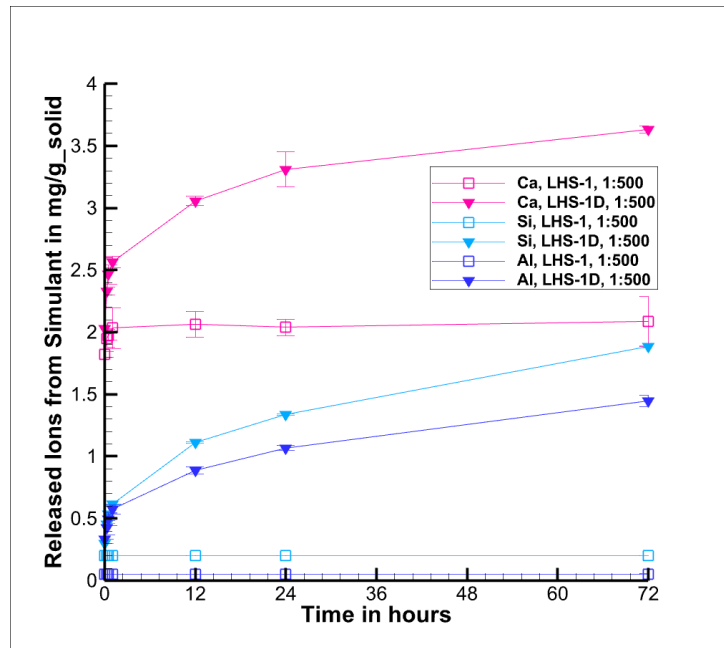
Figure 4.21: *Released Calcium, Potassium, Silicon Ions into Ultrapure Water over Time*

Comparing the amount of released calcium, silicon and aluminium ions of 1:500 of LHS-1 and LHS-1D prove to the hypothesis that the particle size and the released ions are connected. Since a bigger surface area is exposed to the aqueous solution using smaller particle sizes, more ions are released from the lunar regolith particles into the aqueous solution over time.

4.3.5 Selection of Lunar Water Simulant

After determining the released ions from simulant into aqueous solution, a water simulant shall be determined with reference to all experiments conducted by the SMU research group. The ratio - 1:100 or 1:500 - , the aqueous solution - ultrapure water or buffer solution with a pH of 5.6 -, and a lunar regolith simulant - LHS-1, LMS-1 or LHS-1D - shall be selected. The lunar water simulant with a known amount of released ions enables testing parts of the process chain without developing the prior processes. An example for this scenario is testing the lunar water purification system without completing the design of a lunar water extraction process.
Based on the findings of subsection 4.2.4 and section 4.3, a lunar water simulant with the parameters shown in table 4.6 is selected.

Table 4.6: *Parameters of the Lunar Water Simulant*

Parameter	Lunar Water Simulant
Lunar Regolith Simulant	LHS-1D
Simulant to Water Ratio	1:100
Aqueous Solution	Ultrapure Water

For the lunar water simulant, the parameters are selected to develop a worst-case simulant. The simulant LHS-1D leads to the greatest contamination out of the three tested *Exolith Lab* simulants by the SMU research group. LHS-1D has the smallest particle size of the presented *Exolith Lab* simulants. With the smallest particle size it also represents an important case for space applications - water pollution by small dust particles - which are more difficult to separate from water than bigger particles [5]. Furthermore, a ratio of 1:100 is selected, because the most ions are dissolved in $\frac{mg}{l}$ into ultrapure water. As aqueous solution the ultrapure water is chosen, because of its pH being approximately pH 9. The pH has a greater distance from the desired pH for electrolysis water with pH 7 than using buffer solution with pH 5.6 [61].

Consequently the water purification system is tested for the most polluted water derived from the conducted experiments. The procedure for preparing the lunar water simulant is congruent with the experiment procedure described in subsection 4.1.2 without water extractions. 10 *g* of the lunar regolith simulant LHS-1D is added into 1 *l* of ultrapure water with a pH of 5.6. Then it is mixed on the overhead shaker. After 72 *h*, the water simulant is ready for use.

For the lunar water simulant the released ions according to table 4.7 can be expected. These are the rounded results from the dissolution experiments by Freer et al. in the units $\frac{mg}{l}$ and $\frac{mg}{g_{solid}}$. The unit $\frac{mg}{l}$ is more applicable for the use of a lunar water purification system.

Table 4.7: *Released Ions within the Lunar Water Simulant*

Ions	Unit	Released Ion	Standard Deviation	Unit	Released Ion	Standard Deviation
Al	$\frac{mg}{g_{solid}}$	0.3114	0.0375	$\frac{mg}{l}$	3.1137	0.3748
Ca	$\frac{mg}{g_{solid}}$	0.6368	0.0461	$\frac{mg}{l}$	6.3676	0.4614
Fe	$\frac{mg}{g_{solid}}$	0.0034	0.0020	$\frac{mg}{l}$	0.0342	0.0197
K	$\frac{mg}{g_{solid}}$	0.1712	0.0000	$\frac{mg}{l}$	1.7120	0.0000
Mg	$\frac{mg}{g_{solid}}$	0.0932	0.0052	$\frac{mg}{l}$	0.9323	0.0525
Mn	$\frac{mg}{g_{solid}}$	0.0003	0.0000	$\frac{mg}{l}$	0.0026	0.0000
S	$\frac{mg}{g_{solid}}$	0.0157	0.0007	$\frac{mg}{l}$	0.1571	0.0075
Si	$\frac{mg}{g_{solid}}$	0.2431	0.0134	$\frac{mg}{l}$	2.4311	0.1338
Ti	$\frac{mg}{g_{solid}}$	0.0005	0.0003	$\frac{mg}{l}$	0.0052	0.0031

5 Lunar Water Purification System

While the water required for water electrolysis has to be ultrapure [4] it can be easily contaminated on the Moon with lunar regolith. Firstly, lunar regolith may block and clog instruments for water quality monitoring in the life support system. Secondly, the regolith may contaminate drinking water in pipes and storage tanks. Thirdly, the lunar regolith dust can contaminate extracted water regarding the water extraction from the lunar surface. Based on the information gained in subsection 3.2.3, it can be assumed that further purification measures are required for lunar water treatment rather than using a cold trap to reach the electrolysis water requirements explained in subsection 3.2.6. Therefore, a filtration of the extracted lunar water is required before any conversion as salts and metals can dissolve from the regolith into water due to contamination making a lunar water purification a necessary contribution to the ISRU effort. [5]

In this chapter the methodology, the results, and the discussion of the water purification system is given. The goal of the ongoing design of the water purification system is that it shall fully automatically purify lunar water.

5.1 Methodology of Water Purification System

In the following the methodology of the SMU research group's lunar water purification system is given, including existing control technology and selection the of measurement instruments within the framework of the master thesis. Afterwards, the sedimentation experiments are described. Lastly, the *LabVIEW* program for controlling the lunar water purification system using the existing control technology is presented.

5.1.1 Control Technology

The aim of the control technology is to set parameters reliably and to keep a parameter constant, e.g. temperature of the heating bath. Generally, a control's task is to keep a parameter at a constant value while compensating for the influence of disturbance parameters. A schematic of the first approach of the lunar water purification system existing at the beginning of the thesis can be seen in figure 5.1. As it is not decided between two approaches both are shown. The valves are numbered and the measuring points are marked with letters. The process of the first approach is not explained but the final schematic in figure 5.2.
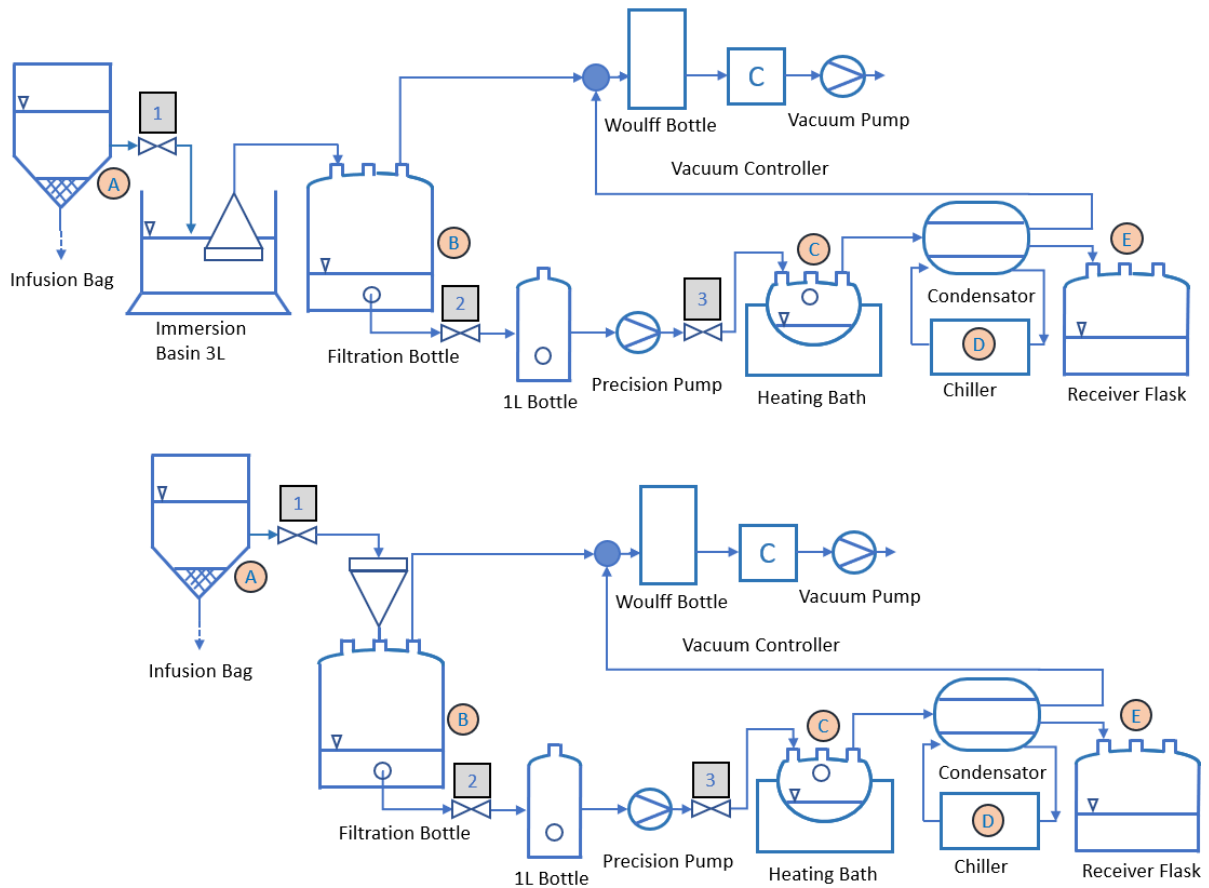
Figure 5.1: *Schematic of the First Approach of the Lunar Water Purification System*

The first approach of the lunar water purification system is modified for the following reasons. To protect the membrane precision pump from damage due to vacuum, additional valves are added so that the vacuum is not interacting with the membrane from either flow direction of the precision pump. The 1 l glass bottle between the filtration bottle and the precision pump is removed from the concept. It was intended to ensure enough water for the conveyance of the precision pump but is not necessary when a level sensor shall be used inside the filtration bottle confirming the minimum fluid level. Furthermore, valves are added to selectively guide the vacuum to the filtration bottle of the receiver flask. Following sedimentation tests it is decided to use a sedimentation bottle instead of an infusion bag to simplify the installation of the measuring instruments and drain the water from top to bottom. The schematic of the final lunar water purification system can be seen in figure 5.2 and its process is explained in the following.

The process of the lunar water purification system can be divided into three steps: sedimentation, filtration, distillation. For the sedimentation, the lunar water simulant is filled into the sedimentation bottle. A flexible hose is located in the bottom outlet of the sedimentation bottle. The hose's height can be adjusted so that only the upper layer

of the water of the sedimentation bottle, seen as clear water after the sedimentation, is selectively drained. The lunar water simulant is transported into the filtration bottle with less regolith simulant particles compared to prior the sedimentation. For the filtration, the first valve opens and with the aid of the vacuum pump (VACSTAR digital by *IKA*) producing a pressure of 700 $mBar$ the lunar water simulant is filtered and conveyed into the filtration bottle. It is filtered using filter paper with a pore size of $\leq 2\ \mu m$ (1507 by *Hahnemühle*). As the filtration is completed the ambient pressure is restored and the first valve closes. For the distillation, the second and third valve open and the lunar water simulant is conveyed with a precision pump (SIMDOS FEM 1.10 TT1.18RCP2 by *KNF*) to the evapouration flask. Since the evapouration flask inside the heating bath (HBR4 control by *IKA*) shall only be filled two thirds of its maximum volume, 660 ml be filled into the flask by the precision pump. As the filling process is finished, the second and third valve close and the fourth opens. The water in the heating bath is heated to 50 °C resulting in the lunar water simulant being heated to the same temperature. The pressure caused by the vacuum pump, which is lower than ambient pressure, results in a lower boiling temperature of water than 100 °C. The condenser is a Liebig condenser, which consists of two pipes with one pipe inside the other. The outer pipe has cooling fluid flowing through it in countercurrent to the water vapour. This causes the vapour of the evapouration flask, which is transported through the inner pipe by the vacuum pump - to condensate. The cooling fluid temperature is controlled by a chiller (RC 2 lite by *IKA*) and shall not be below 0 °C , because icing of the cooling fluid could potentially damage the Liebig condenser and the chiller. The cooling fluid temperature is set to a conservative 5 °C as lower and 10 °C as upper limit. As cooling fluid 2 l of ultra-pure water mixed with 0.2 g of sodium carbonate are used according to the chiller's manual. The condensate of the distillation process, the distillate, runs into a final glass bottle – the receiver flask. As the evapouration flask is empty the distillation is finished and the heating bath is stopped. When the evapouration flask reaches room temperature the vacuum pump shall restore the ambient pressure. This is necessary to prevent stress cracks in the evapouration bottle. Lastly, the fourth valve can be closed.
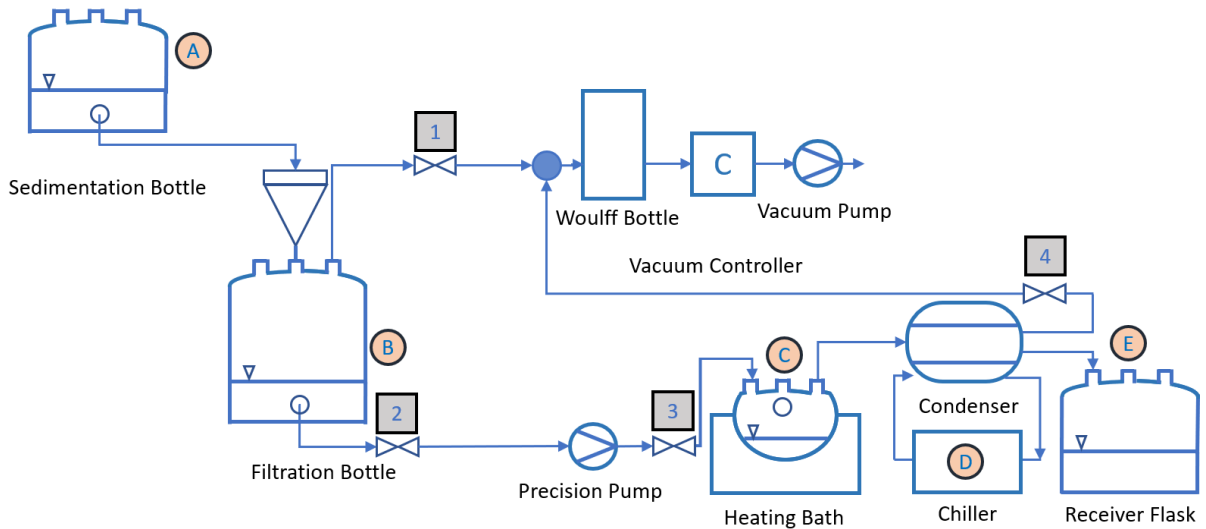
Figure 5.2: *Schematic of the Final Lunar Water Purification System*

There are six aspects of the purification system that can be controlled. Four of which shall be additionally controlled by a *LabVIEW* program, the third to sixth aspect.

1. Input to the System   via   Lunar Water Simulant Selection

2. Filtration Grade   via   Filter Selection

3. Temperature in Heating Bath   via   Heating Bath

4. Temperature of Cooling Fluid   via   Chiller

5. Fluid Mass Flow   via   Valves

6. Vacuum   via   Vacuum Pump

For contacting the control technology a connection between the control technology and the computer has to be made. Therefore, depending on hardware of the control device, a RS232 to USB-A (lines 1:1 or lines crossed) or alternatively a USB-A to USB-A can be used. Moreover, since the USB ports on a laptop are limited a USB multiport is purchased as well. The 2/2-way solenoid valves are normally closed (by Company *Bürkert*) and are wired and connected to a power supply. For controlling the valves, the valves need to have a permanent supply of power by an *NI*-module. Figure 5.3 shows the state before connecting to the water purification system, which is done in the context of this thesis. The switch for the valves is connected to a coloured cable (upper left of the picture) and this cable is connected to the *NI*-module inside the *DAQ*-chassis. The *NI*-module is then controlled via the *LabVIEW* program and powered by the basic voltage supply.
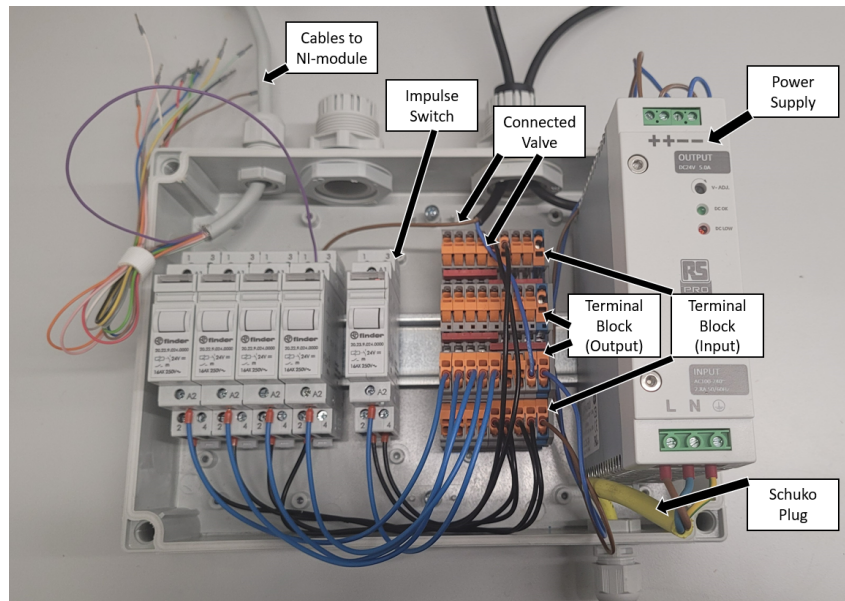
Figure 5.3: *Electrical Assembly of Basic Voltage Supply for Valves*

In order to have a safe environment for the experimenter an item box planned by the SMU research group is built. This box is covered with acrylic glass panes to keep the impact on the environment minimal in case of a bursting glass bottle etc. The heating bath is placed on a lifting platform to remove the evapouration flask from the influence of the heating bath and enable faster cooling. This is used as, e.g. the distillation is completed. All devices are plugged and connected further according to their handbooks. For data transport the vacuum controller (VC 10 lite by *IKA*) is connected to the vacuum pump and all control devices are connected to the USB-A multiport. All bottles, the Liebig cooler and the valves are attached to laboratory stands by means of stand clamps. This ensures that all components maintain their position, especially the solenoid valves, which move slightly as they are toggled. In figure 5.4 the setup of the lunar water purification system can be seen.
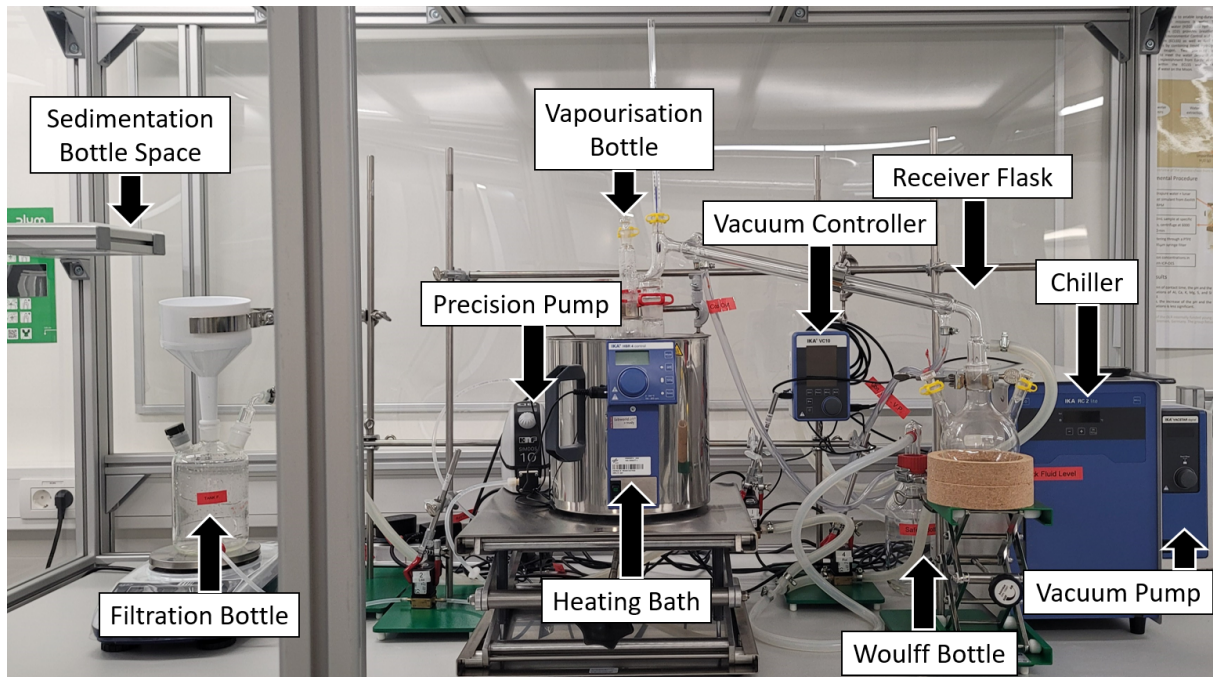
Figure 5.4: *Setup of the Lunar Water Purification System*

5.1.2 Measuring Instruments

The selection of the measuring instruments for the lunar water purification system is done as part of the thesis whereas the implementation into the purification system and *LabVIEW* program are not. For selecting the measuring instruments for the lunar water purification system the measuring points need to be determined first. The set measuring points can be seen in figure 5.2 as marked with letters and in table 5.1 the required measured parameters in the measuring points can be seen. The first measuring point is inside the sedimentation bottle where the pH and Electric Conductivity (EC) shall be measured. The second measuring point is inside the filtration bottle measuring the fluid level. As the level sensor gets in contact with water the sensor changes its signal. Like mentioned in subsection 5.1.1, 660 *ml* shall be filled into the heating bath. Therefore, the level sensor shall ensure 800 *ml* are inside the filtration bottle to protect the precision pump from sucking air. Inside the evapouration flask, pH, EC, and temperature shall be measured. Lastly, the pH, EC, and the temperature shall be measured in the receiver flask.

Table 5.1: *Required Parameters in Measuring Points of Lunar Purification System*

Measuring Point	Position	Parameter
1	Sedimentation Bottle	pH
1	Sedimentation Bottle	EC
2	Filtratration Bottle	Fluid Level
3	Evapouration Flask	pH
3	Evapouration Flask	EC
3	Evapouration Flask	Temperature
4	Receiver Flask	pH
4	Receiver Flask	EC
4	Receiver Flask	Temperature

For selecting the measuring instruments different requirements are set which can be seen in table 5.2. The highlighted color indicates how well a certain requirement is met. Green means the requirement is fulfilled to complete satisfaction. Orange means that the requirement is not fulfilled but a basic function is given. Red means that the requirement is not fulfilled.

Requirement 1.1 and 1.2 are in regards to the dimensions of the measuring instruments and sensors. They are set due to the dimensions of the present glass bottles of the lunar water purification system, where the instruments shall be installed. The smallest bottle neck is 29 mm wide and the smallest bottle is 170 mm high. Requirement 1.3 states that the measuring instruments and sensors shall be robust and endure 20 $mBar$ according to the minimal pressure produced by the vacuum pump.

The measuring instruments need to able to be connected to an *NI*-chassis with *NI*-modules for powering and for reading the results. Since present *NI*-modules shall be used, the measuring instruments shall be suited for the *NI*-modules regarding range and type of signal. This is set as requirement 2. An overview of the *NI*-modules is given in table 5.4.

Requirement 3.1 states that the temperature measuring instruments shall have a range of 0 to 150°C. Requirement 3.2 is that the temperature measuring sensor shall function with a PT 100 or PT 1000 since these are reliable and mature technologies.

According to requirement 4.1 the pH measuring instrument shall cover the entire pH range, which is 0 to 14. This requirement is set to make the lunar water purification system flexible for further experiments. Future experiments may include fluids with a wider range of pH values and would otherwise require the purchase a new pH measuring

instrument. Requirement 4.2 is regarding the function of the pH measuring instrument in fluids with low EC. It is aimed for the characteristics of ultra pure water, which has a low EC of $0.056\frac{\mu s}{cm}$. Therefore, a very sensitive measuring instrument is required since pH measuring instruments require EC to measure a pH value. The EC measuring instrument shall have a lower limit of $0.05\frac{\mu s}{cm}$ according to requirement 5. This is to determine whether the purified water meet the required EC of ultra pure water with $0.056\frac{\mu s}{cm}$, the required EC value for electrolysis water according to table 3.3 and [4].

Requirement 6 is that the level sensor shall change its signal as it gets in contact to water.

The last requirement is that a turbidity sensor shall be installed in the sedimentation bottle. Determining the turbidity in the sedimentation bottle gives a reference about the state of the sedimentation in the sedimentation bottle.

With the selected sensors requirement 1.2 is not met to complete satisfaction. The temperature sensor, the pH sensor, and the EC sensor are too short to reach the bottom of the bottles. Due to the insufficient length of the otherwise optimally fitting sensors it is decided to purchase smaller glass bottles and flasks, in which the sensors can already measure at the beginning of a filling process. The level sensor is short as well, but since it has a M10 thread it can be screwed onto a threaded rod to extend the shaft for attachment. Requirement 7 is highlighted red since no turbidity sensor is purchased. It is rather thought of determining a time period when a desired sedimentation can be ensured as alternative solution via sedimentation experiments.

Table 5.2: *Requirements for Measuring Instruments of Lunar Water Purification System*

Req Number	Parameter	Requirement
Req 1.1	Dimensions	All Measuring Instruments Shall Have a Diameter Smaller Than 29 mm
Req 1.2	Dimensions	All Measuring Instruments Shall Have a Length Bigger Than 170 mm
Req 1.3	Dimensions	All Measuring Instruments Shall Be Robust Enough to Endure Pressure of $20m$ Bar by Vacuum Pump
Req 2	Modules	All Measuring Instruments Shall Be Powered and Read by *NI*-Modules
Req 3.1	Temperature	All Temperature Measuring Instruments Shall Have a Range of $0°$ C to $120°$ C
Req 3.2	Temperature	All Temperature Measuring Instruments shall Have a PT100 or Better
Req 4.1	pH	All pH Measuring Instruments Shall Cover the Entire pH Range, $0 - 14$
Req 4.2	pH	All pH Measuring Instruments Shall Function in Fluids With a Low EC
Req 5	EC	All EC Measuring Instruments Shall Have a Lower Limit of 0.05 $\frac{\mu s}{cm}$
Req 6	Level Sensor	The Level sensor Shall Change its Signal as Gets in Contact with Water
Req 7	Turbidity	The Turbidity in the Sedimentation Bottle Shall Be Determined

The selected EC sensor is the "Optisens Cond 7200" by the company *Krohne*, which also functions as temperature sensor using an integrated PT100. As a pH sensor the "Optisens pH 8100" by the company *Krohne* is selected. As level sensor "OLS7" by the company *Cynergy3* is chosen. The parameters of the selected measuring instruments can be seen in table 5.3. The data sheets of the selected measuring instruments can be seen in the appendix D.7, D.8 and D.9.

Table 5.3: *Parameters of Selected Measuring Instruments (D.7, D.8, D.9)*

Parameter	EC Sensor (D.7)	Temperature Sensor (D.7)	pH Sensor (D.8)	Level Sensor (D.9)
Range	$0.0\ 5 - 10\frac{\mu S}{cm}$	$0 - 135\ °C$ (PT 100)	$0 - 14$	On, Off
Accuracy	$\pm\ 10\%$	$\pm\ 10\%$	$\pm\ 0.1$	not given
Resolution	$0.01\ \frac{\mu S}{cm}$	$0.1\ °C$	0.1	not given
Length	$115\ mm$	$115\ mm$	$110\ mm$	30mm
Diameter	$16\ mm$	$16\ mm$	$12\ mm$	$10.4\ mm$
Pressure	$0 - 16\ Bar$	$0 - 16\ Bar$	$0 - 10\ Bar$	$0 - 7\ Bar$
Temperature	$0 - 135\ °C$	$0 - 135\ °C$	$0 - 130\ °C$	$-25 - 80\ °C$

Requirement 2 is to use the already present *NI*-modules. An overview of the *NI*-modules is given in table 5.4. The *NI*-module number, the module type, the signal type, the number of channels, and the range, can be seen.

Table 5.4: *Overview of NI-Modules*

Module Number	Module Type	Signal Type	Number of Channels	Range	Amount
NI 9203	Analog Input	Current	8	$\pm\ 20\ mA$	1
NI 9226	Analog Input	Thermocouple	8	0 - 4000 Ω	2
NI 9220	Analog Input	Voltage	16	$\pm\ 10\ V$	1
NI 9264	Analog Output	Voltage	16	$\pm\ 10\ V$	1
NI 9264	Digital Output	Voltage	16	$\pm\ 10\ V$	1

5.1.3 Sedimentation Experiments

For measuring the sedimentation different sensors are considered but none is found to fulfill the requirements. A first approach is using a sensor, e.g. colour sensor, particle counter, laser sensor, or turbidity sensor. A sensor to measure the colour of milk to detect water leakage is unsuited for tracking changes caused by sedimentation. Additional difficulties are that the sensor shall function under low pressure and that the particles may clog sensors, like with a particle counter, or are depending on consistent lightning, like with

laser sensors or turbidity sensors. Moreover, the latter sensors cannot measure though glass but may not endure vacuum.

As finding an alternative solution for requirement 7 according to subsection 5.1.2 it is thought of determining a time period when a desired sedimentation can be ensured via sedimentation experiments. For the sedimentation experiments two methods are done: using an infusion bag and using a glass bottle further called sedimentation bottle. The parameters of all sedimentation experiments can be seen in table 5.5.

Table 5.5: *Parameters of Sedimentation Experiments*

Number	Container	Ultrapure Water Volume in l	Lunar Regolith Simulant Mass in g	Simulant to Aqueous Solution Ratio
1	Infusion Bag	1	10	1:100
2	Sedimentation Bottle	0.5	1	1:500
3	Sedimentation Bottle	1	10	1:100

Firstly, 1 l ultrapure water and 10 g LHS-1D are mixed. LHS-1D is selected as it has the smallest mean and median particles comparing the three simulants and it it the simulant that is likely to be selected for the lunar water simulant. The mixture is then directly poured into a sedimentation bag. The sedimentation bag is hung up in a 30° angle. The structure for the sedimentation experiment can be seen in figure 5.5. Approximately 15 ml water are extracted from the outlet after 1 h, 2 h, 3 h, 4 h, 24 h.

Figure 5.5: *Structure of Sedimentation Experiment Using Infusion Bag*

The second sedimentation method is mixing 1 l ultrapure water and 10 g LHS-1D and filling it into a bottle with a bottom outlet with a flexible hose. For this method two requirements are set. The volume of extracted clear water shall be minimum two thirds of the input water volume. The turbidity shall be lower than 100 NTU. The structure can be seen in figure 5.6 and is done accordingly for the third experiment.

Figure 5.6: *Structure of Second Sedimentation Experiment*

5.1.4 *LabVIEW* Program for Water Purification System

LabVIEW is a graphical programming system by *National Instruments (NI)*. Using *NI*-hardware, like the *Data Acquisition System (DAQ)*-chassis with *NI*-modules, e.g. analog and digital outputs and inputs of voltage, current, temperature can be applied or be read of connected lines.

This *LabVIEW* program is written to control the devices of the lunar water purification system via the front panel, the *LabVIEW* graphical user interface. In table 5.6 the program steps that are realised can be seen. The valve positions are indicated with the number of the valve and "O" for open or "X" for closed.

Table 5.6: *LabVIEW Program Steps*

Step	Funtion	Commands
	Start Filtration	**Via Button 1**
1	Toggle Valve to Required Position	1O 2X 3X 4X
2	Set Vacuum Pump to 700 $mBar$	Out_SP_66 700
3	Wait 2ms	Wait
4	Start Vacuum Pump	START_66
	Stop Filtration	**Via Button 2**
5	Stop Vacuum Pump	STOP_66
6	Wait 6000 ms	Wait
7	Toggle Valve to Required Position	1X 2O 3O 4X
	Precision Pump	**Via Switch 1**
8	Track Status of Precision Pump	
	Start Distillation	**Via Button 3**
9	Toggle Valve to Required Position	1X 2X 3X 4O
10	Set Vacuum Controller to 60 $mBar$	OUT_SP_66 60
11	Wait 2 ms	Wait
12	Start Vacuum Pump	START_66
13	Set Chiller Temperature to 6 $°C$	OUT_SP_1 6
14	Wait 2 ms	Wait
15	Start Chiller	START_1
	Heating Bath	**Via Switch 2**
16	Track Status of Heating Bath	Switch
	Stop Distillation	**Via Button 4**
17	Stop Vacuum Pump	STOP_66
18	Stop Chiller	STOP_1
19	Wait 12000 ms	Wait
20	Toggle Valve to Required Position	1X 2X 3X 4X

Every *LabVIEW* program is composed of two parts: the block diagram contains the functions displayed as boxes of the program and the front panel is the graphical user interface. For explaining the block diagram it is split into 3 parts: the control of the devices, the control of the valves, the non-controllable devices.

The basis of the program is a while loop, which can be seen as grey border around the functions. It ensures a permanent execution of the program for an unlimited time until the loop is stopped by pressing a button on the front panel. It is always recommended to stop the program with the stop button of the while loop since it can otherwise cause a database corruption. The input data of the while loop are the addresses of the vacuum controller, the chiller and the lines of the used *NI*-module. The output data of the while loop are the functions "Error Handler"s and "DAQmx Stop Task", "DAQmx Clear Task". *LabVIEW* functions are written in quotes in the context of the program explanation. The program can be seen in figure 5.7, 5.8 and 5.9. It is split into three parts to enable readability.
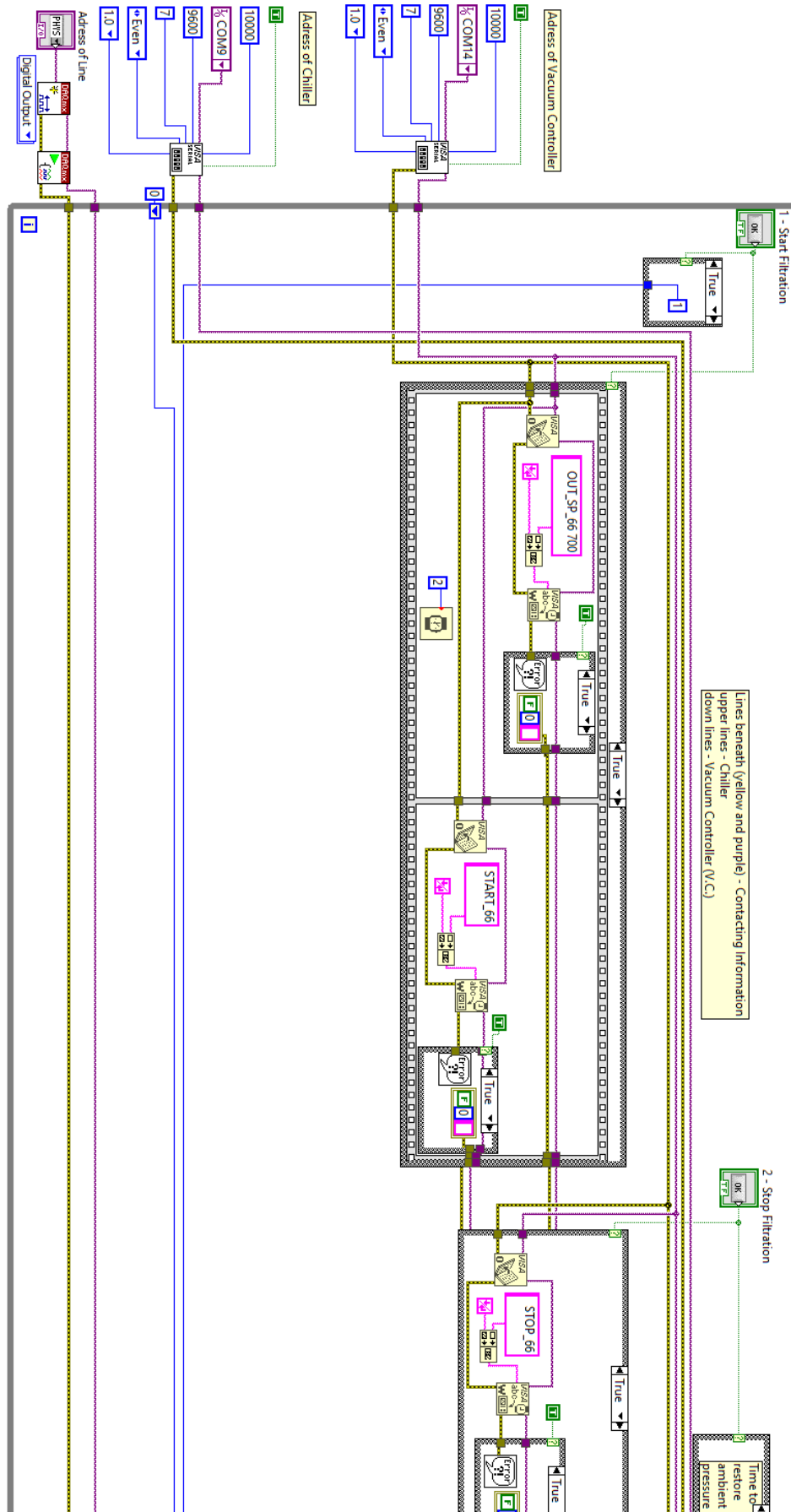
Figure 5.7: *Block Diagram of LabVIEW Program for Controlling Lunar Water Purification System - Part 1*
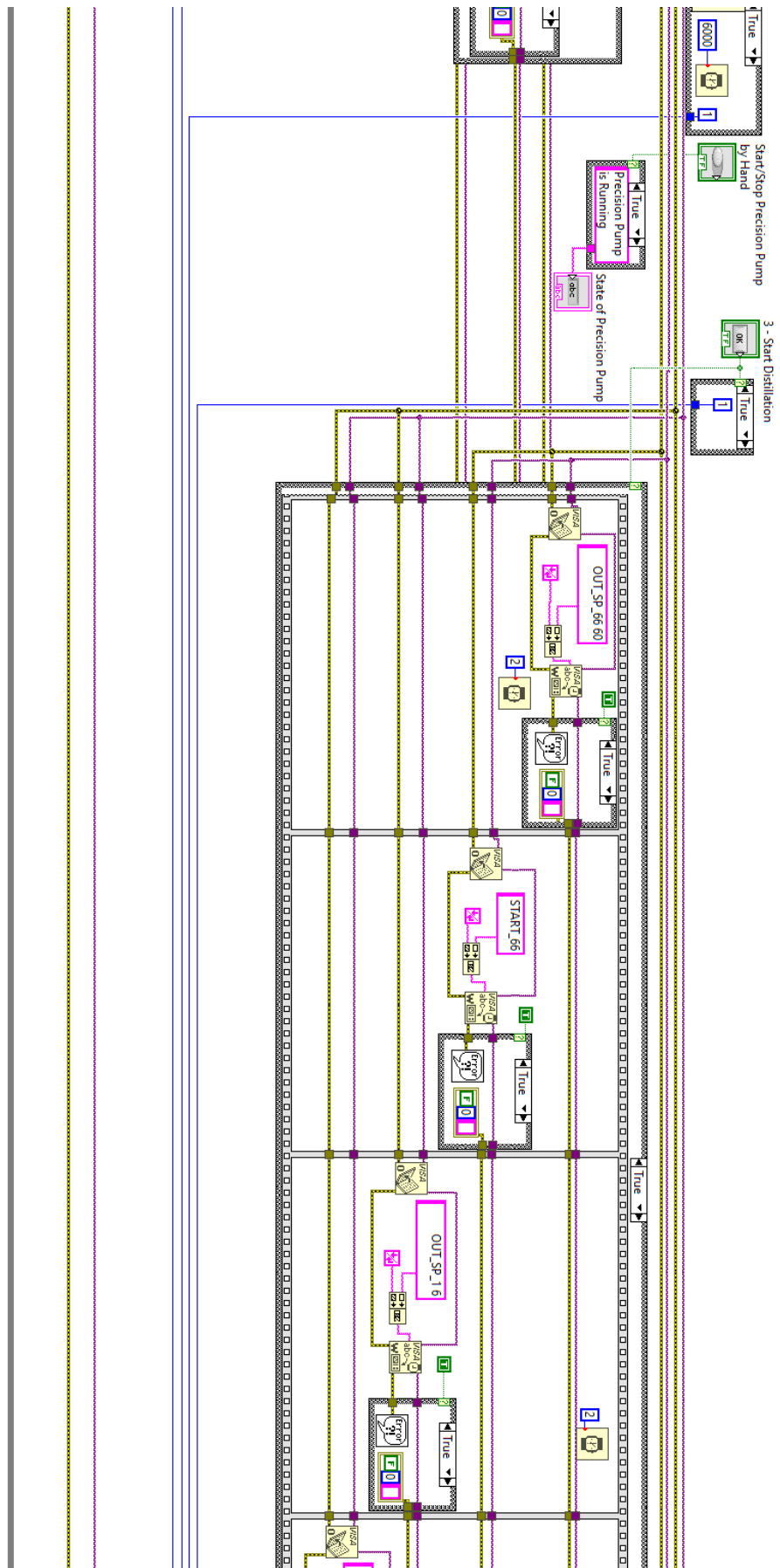
Figure 5.8: *Block Diagram of LabVIEW Program for Controlling Lunar Water Purification System - Part 2*
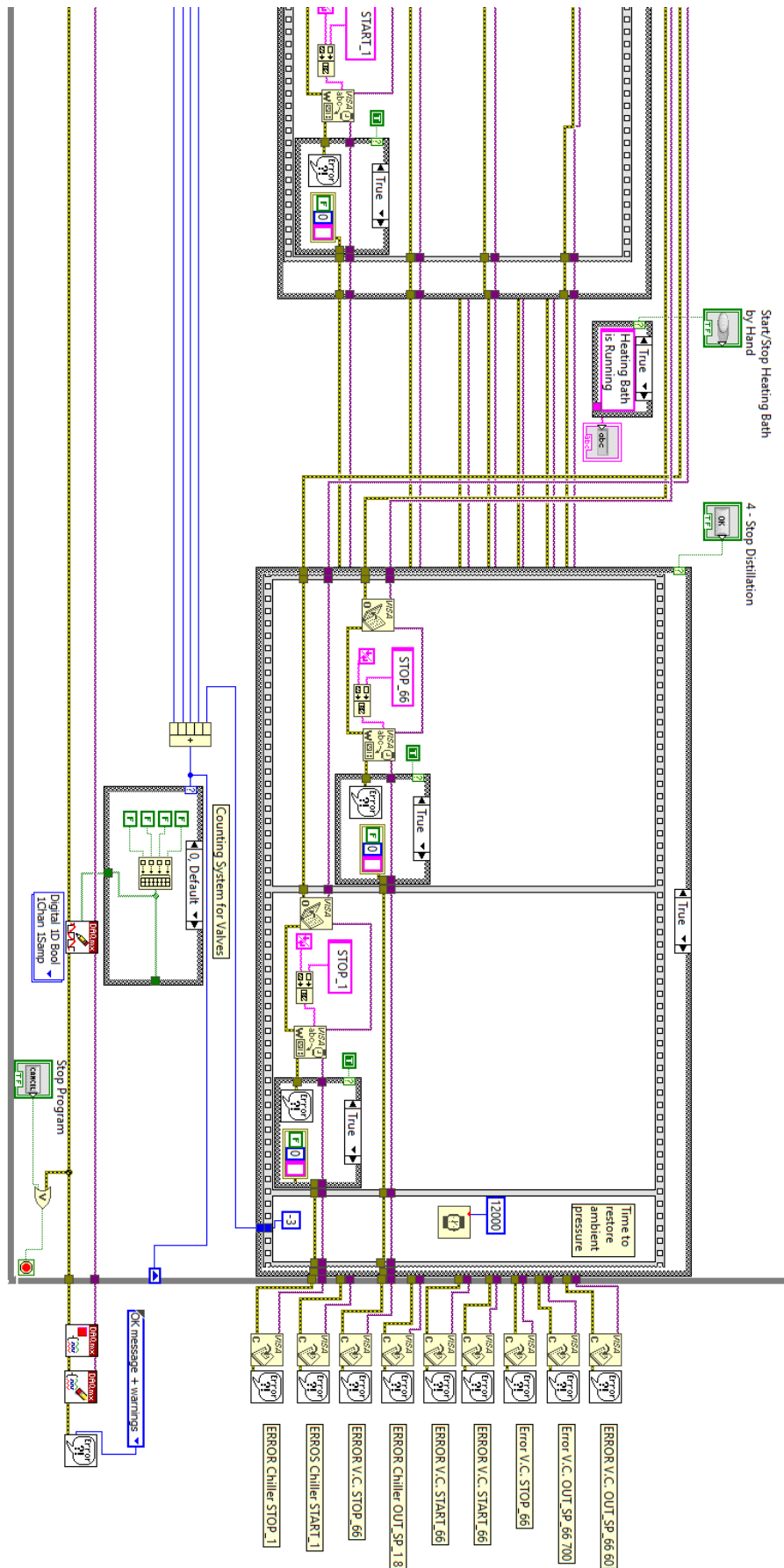
Figure 5.9: *Block Diagram of LabVIEW Program for Controlling Lunar Water Purification System - Part 3*

Since the vacuum controller and the chiller are connected via a serial port they can be contacted using the Virtual Instrument Software Architecture (VISA) functions by *LabVIEW*. Therefore, a "VISA Configure Serial Port" initialises the serial port. The input data for the "VISA Configure Serial Port" function are explained from top to lowest parameter according to the figure 5.10 in table 5.7.

Table 5.7: *Input Parameter for "VISA Configure Serial Port" Function*

Input Parameter	Set Value
Enable Termination Char	Boolean true
Timeout	10000 Milliseconds
VISA Resource Name	Com-Port Number
Baud Rate	9600
Data Bits	7
Parity	Even
Stop Bit	1

The recommended settings from the manual of the devices are used which are mostly the default settings of *LabVIEW*. For the chiller the same parameters are selected except for the "VISA resource name" since it is connected to a different serial port. The following functions are located in a flat sequence structure within a case structure. A case structure can be seen as grey frame with the case name top in the middle. It contains multiple structures which are executed if the case occurs. The condition for the case structure can be Boolean true and false, a string, or numeric. When a button on the front panel is pressed a Boolean true is triggered and the functions inside the "True" case structure are executed. The button latches when released. The flat sequence structure is displayed as a film frame. The flat sequence structure has multiple frames with functions that are executed sequentially. The use of the flat sequence structure together with a "Wait" block is necessary when sending more than one command to a device, because otherwise the device only executes the first sent command. The "Wait" block is given a time of 2 milliseconds resulting in the first sequence to wait before the second sequence is executed. The time of 2 milliseconds results from testing and the observation that using 1 millisecond only one command, the first one, is transmitted. Inside the flat sequence structure the "VISA Open" opens a session to the desired serial port with the connected device. It is given the VISA resource name and the error information from the previous function and hands same parameters to the next function. The "VISA Write" writes the command to the device is not only given the VISA resource name and the error information but

a write buffer that shall be transmitted. The commands for the write buffer are found in the device's handbooks. As stop bit, a bit to let the device know that the command ends, an "End of Line Constant" is used. Using the "Concatenate Strings" the command, e.g. "OUT_SP_66 700" is appended by an "End of Line Constant" which is written "\\r \\n". The VISA resource name and error information are given as input into the inner case structure. Using a "Simple Error Handler" the error information is read and a new error is created consisting of a Boolean false, a zero and an empty string. This is done to determine whether an error occurs at this position of the program. In case of an error anywhere in the program one error messages would be given at the end of one execution, because of the "Simple Error Handler" at the end of the program. Using the "Simple Error Handler" inside this described flat sequence structure inside the case structure the program would give two rather than one error message at the end of one execution. This is helpful when determining the cause of an error. The VISA resource name and the new error information are passed from the inner case structure inside the flat sequence structure inside the outer case structure to the "VISA Close" which is outside of the while loop and closes the session with the device. It gives an error information to the "Simple Error Handler", which indicates whether an error occurred. The functions for contacting a serial port can be seen in figure 5.10. It is done accordingly for further commands.
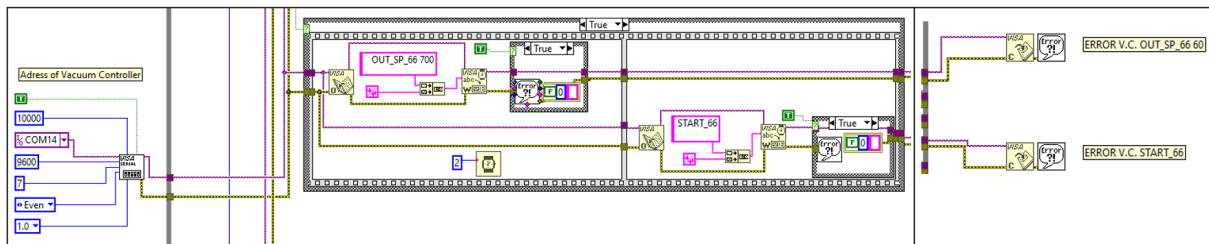
Figure 5.10: *Contacting a Serial Port via LabVIEW Program*

The "False" case structure, which is triggered by not pressing a specific button, the error and the task are given from "VISA Write" to "VISA Close" without writing a buffer. This leads to no change in the state of the device. The "False" cases can be seen in figure 5.11 with on the left side a false inner case structure and on the right a false outer case structure. This can be seen for the whole *LabVIEW* program in appendix F.1 and F.2.
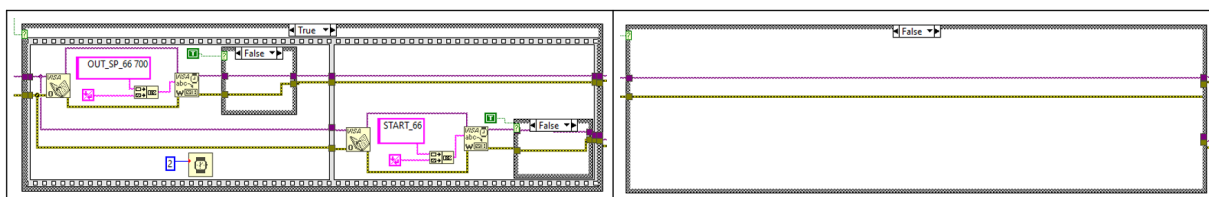
Figure 5.11: *"False" Cases for Contacting a Serial Port via LabVIEW Program*

For contacting the *DAQ*-chassis and the *NI*-module in which the cables for controlling the valves are located the *DAQmx* functions are used. The "DAQmx Create Channel (DO-Digital Output)" is used to create a channel where *LabVIEW* can generate digital signals. The lines of valves are handed as input to this function while a task out and error information are given as output. This output is taken as input for the "DAQmx Start Task" to start the task to supply the selected lines with voltage. The "DAQmx Write (Digital 1D Bool 1Chan 1Samp)" writes given data in the form of Boolean values to the task. The task is given as input in the form of a task in and the error information is given and hands it to "DAQmx Stop Task" as input as task and error information. The "DAQmx Stop Task" stops the task and hands task and error to the "DAQmx Clear Task". The task is cleared to release the task's resources. These functions can be seen in figure 5.12.
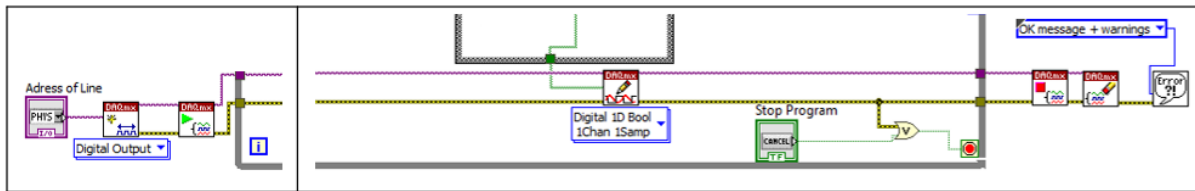
Figure 5.12: *DAQ Functions Used in LabVIEW Program*

The positions of the valves during the process steps of the lunar water purification system are given as array with Boolean values inside a case structure. For creating the array a "Build Array" function concatenates Boolean values with the first value being for the first line in the *NI*-module where the first valve is controlled with. This case structure has the numeric cases 0, 1, 2, 3 with 0 as default case. In the default case all valves are closed. The cases can be seen in figure 5.13 and are according to 5.6.
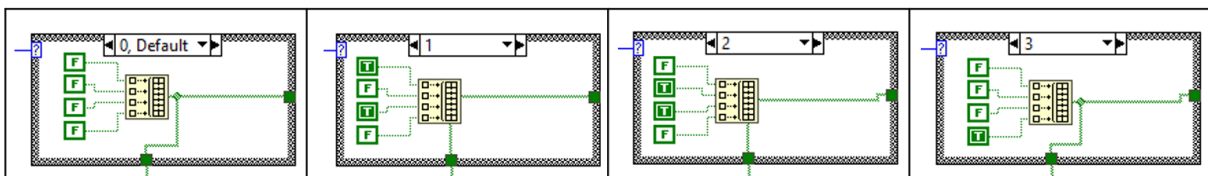
Figure 5.13: *Cases of Valve Positions via LabVIEW Program*

To reset the counter variable to zero as the program is started a zero is initialised outside the while loop. The zero is connected to an "Compound Arithmetic" function which adds data and gives an output. The "Compound Arithmetic" is also connected to the case structure of step: 1 - Start Filtration, 2 - Stop Filtration, 3 - Start Distillation, 4 - Stop Distillation. Pressing the buttons of the first, second, third step adds one to the numeric value and for the fourth step it subtracts three. This results in four cases for the valve positions. When the buttons are not pressed a zero is added to not change the counter

variable. To save the counter variable in between the loop execution a shift register is implemented which can be seen as blue bordered boxes with an upwards or downwards arrow. The "Compound Arithmetic", "Shift Register" and case structure can be seen in figure 5.14. In the left the true case and in the right the false case is displayed.
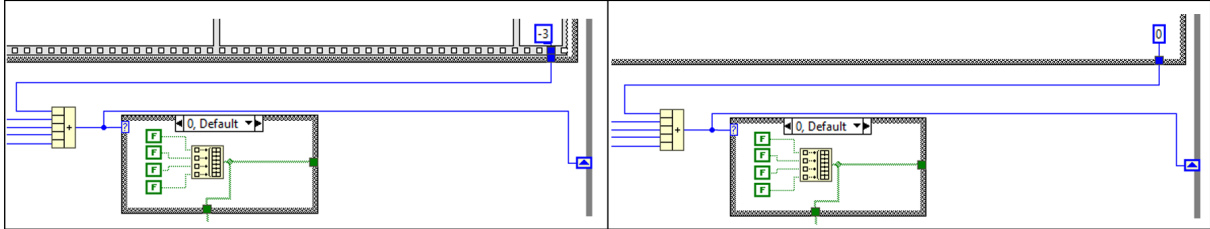
Figure 5.14: *System for Changing Valve Case Structure via LabVIEW Program (Left - True Case, Right - False Case)*
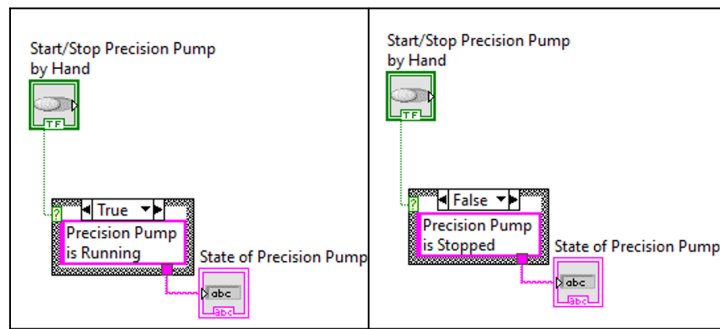
Figure 5.15: *Functions for Non-Controllable Devices via LabVIEW Program*

The user interface, or accordingly to *LabVIEW* named the front panel, can be seen in figure 5.16.
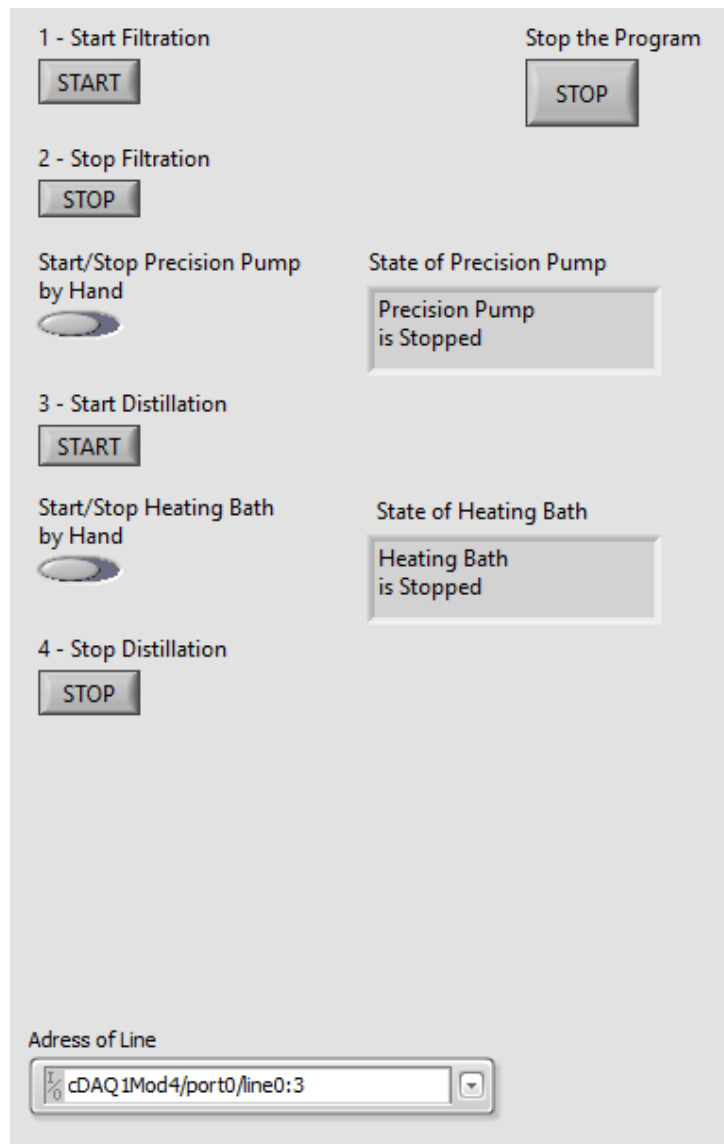
Figure 5.16: *User Interface of LabVIEW Program*

5.2 Results of Purification System

The results of the sedimentation experiments and the results of the lunar water purification system with the lunar water simulant are explained in the following.

5.2.1 Results of Sedimentation Experiments

The method of the first sedimentation experiment, explained in subsection 5.1.3, shows a heavy fluctuation in the measured turbidity values. These turbidity values can be seen in the following table 5.8. There is a possibility that the regolith simulant sediments into the infusion bag bottom outlet. Moreover, the extraction process might swirl the simulant up again. It can be noted that this method does not produce reproducible data. As using a

sedimentation bottle simplifies implementation of measuring instruments a sedimentation bottle is used for further sedimentation experiments.

Table 5.8: *Turbidity Values of First Sedimentation Experiments with Infusion Bag*

Time in h	I	II	Average Value	Unit
1	9702	9295	9498.5	NTU
2	376	390	383	NTU
3	471	510	490.5	NTU
4	848	728	788	NTU
24	883	829	856	NTU

After 24 h, the lunar regolith simulant is sedimented and has a visible clear water layer, as seen in detail in figure 5.17. The flexible hose is in the bottom outlet of the sedimentation bottle and adjusting the hose's height only the clear layer of the water is selectively drained. The turbidity value decreases from 993 NTU before sedimentation to 7.27 NTU after 24 h of sedimentation. From a mass of approximately 0.5 kg water regolith simulant mixture 0.335 kg are extracted.

Figure 5.17: *Visible Layer of Lunar Regolith Simulant after 24 Hours during Sedimentation Experiment*

The sedimentation time period of 24 h is selected for the tests with the lunar water pu-

rification system.

It is observed that the time period of 24 h do not fulfill required sedimentation using 1 l and 1:100 rather than 0.5 l and the ratio 1:500. Because of the false assumption another sedimentation experiment is conducted to determine the required sedimentation time period.

Therefore, 1 l ultrapure water and 10 g regolith simulant are tested according to the lunar water simulant. The sedimentation after zero days, one day, two days, three days and six days can be seen in figure 5.18. Due to the slow sedimentation 24 h intervals are measured. After six days 0.676 kg are extracted, which fulfills the requirements that two-thirds of the initial water volume shall be extracted. The turbidity decreased from 9516 NTU to 56 NTU making it the optimised period of time for the sedimentation process of the lunar water purification system.
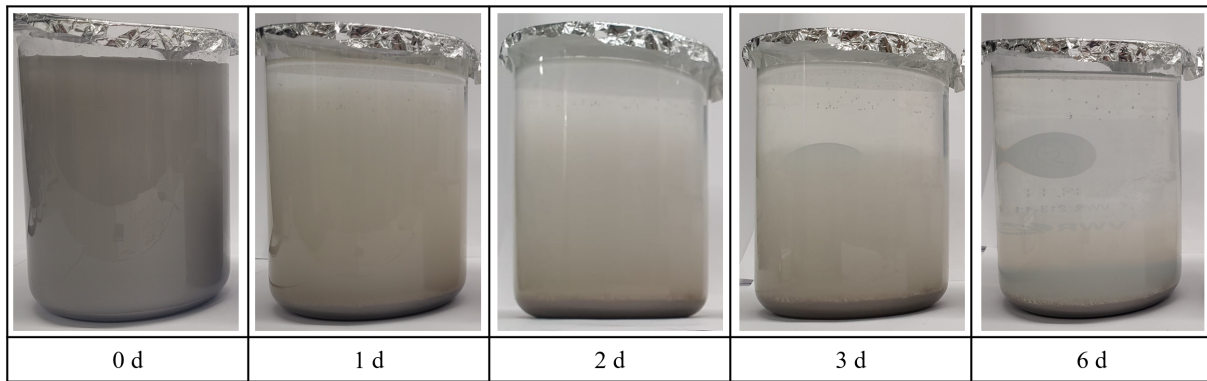
Figure 5.18: *Results of Third Sedimentation Experiment in Days*

5.2.2 Results of Water Purification System

For evaluating the purification abilities of the lunar water purification system the lunar water simulant is purified and the input and the distillate are analysed via ICP-OES. The lunar water simulant is described in subsection 4.3.5. It needs to be noted that the testing procedure described in this subsection deviates from the process described in subsection 5.1.1. The sedimentation and filtration malfunctioned, the sedimentation was not as expected from the second sedimentation result and after three attempts of filtering through the filtration bottle the lunar water simulant was given into the evapouration flask. The filtration process malfunctioned since the filtration paper started to lift off as the lunar water simulant was filled into the filtration bottle. Since two batches were supposed to be done the process was tested twice as described here. The analysed ions via ICP-OES are the same as for the dissolution experiments: aluminium (Al), calcium (Ca), iron (Fe), potassium (K), magnesium (Mg), manganese (Mn), sulfur (S), silicon (Si), and titanium (Ti). The results can be seen in table 5.9. No amount of released

iron, manganese, and titanium ions are measured at t_{start} and t_{end}. Released aluminium, potassium, magnesium, sulfur, and silicon ions are above the detection limit at t_{start} but below the limit at t_{end}. The values under the detection limit can be seen in orange. The value of potassium of batch one is highlighted in red as it is deviating from the second batch and from the value measured before, displayed in table 4.7. Released calcium ions are measured at t_{start} and t_{end}.

Table 5.9: *Elemental Analysis of Distillate of Lunar Water Purification System*

Element	Batch	Unit	t_{start}	t_{end}	Unit	t_{start}	t_{end}
Al	I		0.289	<0.005		2.890	<0.050
	II	$\frac{mg}{g_{solid}}$	0.287	<0.005	$\frac{mg}{l}$	2.870	<0.050
Ca	I		0.675	0.073		6.750	0.728
	II	$\frac{mg}{g_{solid}}$	0.661	0.081	$\frac{mg}{l}$	6.610	0.807
Fe	I		<0.005	<0.005		<0.050	<0.050
	II	$\frac{mg}{g_{solid}}$	<0.005	<0.005	$\frac{mg}{l}$	<0.050	<0.050
K	I		0.613	<0.010		6.130	<0.100
	II	$\frac{mg}{g_{solid}}$	0.153	<0.010	$\frac{mg}{l}$	1.530	<0.100
Mg	I		0.086	<0.005		0.863	<0.050
	II	$\frac{mg}{g_{solid}}$	0.087	<0.005	$\frac{mg}{l}$	0.865	<0.050
Mn	I		<0.005	<0.005		<0.050	<0.050
	II	$\frac{mg}{g_{solid}}$	<0.005	<0.005	$\frac{mg}{l}$	<0.050	<0.050
S	I		0.017	<0.003		0.169	<0.030
	II	$\frac{mg}{g_{solid}}$	0.016	<0.003	$\frac{mg}{l}$	0.156	<0.030
Si	I		0.297	<0.010		2.970	<0.100
	II	$\frac{mg}{g_{solid}}$	0.287	<0.010	$\frac{mg}{l}$	2.870	<0.100
Ti	I		<0.005	<0.005		<0.050	<0.050
	II	$\frac{mg}{g_{solid}}$	<0.005	<0.005	$\frac{mg}{l}$	<0.050	<0.050

Additionally, the EC of the distillate is measured as it is a requirement for the electrolysis input water according to table 3.3. The EC is measured with the selected EC measuring instrument, described in subsection 5.1.2 (Optisens Cond 7200 with MAC 100 by *Krohne*). The EC and turbidity are measured for the lunar water simulant before the sedimentation

and purification as well as after purification and can be seen in table 5.10.

Table 5.10: *EC and Turbidity Before Sedimentation and After Distillation*

Time	Unit	EC		Unit	Turbidity	
		I	II		I	II
Before Sedimentation	$\frac{\mu S}{cm}$	100	100	NTU	9765	9977
After Distillation, t_{end}	$\frac{\mu S}{cm}$	12.57	14.68	NTU	0.26	0.31

5.3 Discussion of Water Purification System

The results of the water purification system are discussed in the following. Additionally, the implemented and suggested optimisations of the lunar water purification system and the *LabVIEW* program are discussed.

5.3.1 Discussion of Water Purification Ability

The input water for the lunar water purification system is a lunar water simulant defined in subsection 4.3.5. To evaluate the purification ability of the lunar water purification system the results of the ICP-OES of the lunar water simulant at t_{start}, the beginning of the purification process, are compared to t_{end}, the distillate. These results can be seen in table 5.9. The measured released ions at t_{start} are compared to the lunar water simulant defined in table 4.7 as control. Slight deviations from the defined water simulant may be expected due to the manufacturing process and potential fluctuations of the homogeneity of the lunar regolith simulant.

It can be stated that the amount of released ions at t_{start} match within $\pm\,0.5\,\frac{mg}{l}/\pm\,0.05\,\frac{mg}{g_{solid}}$ except for potassium ions of $6.13\,\frac{mg}{l}/0.613\,\frac{mg}{g_{solid}}$ inside the first batch rather than expected $1.7\,\frac{mg}{l}/0.17\,\frac{mg}{g_{solid}}$. For the second batch the amount of released potassium ions coincides within acceptable small deviation for t_{start} with the defined composition of the lunar water simulant. The amount of released potassium ions in the first batch is atypical and a contamination of unknown cause is suspected as the reason. Inside the distillate at t_{end} the only measured released ions are calcium ions.

Whether the distillate meets the electrolysis input water requirements according to table 3.3 cannot be evaluated regarding the compounds and tested ions. The EC decreased from $100\,\frac{\mu S}{cm}$ to $12.57\,\frac{\mu S}{cm}$ for the first and $14.68\,\frac{\mu S}{cm}$ for the second batch. It can be stated, that the measured EC values at t_{end} do not fulfill the requirement of the electrolysis input water with an EC of $<\ 0.056\,\frac{\mu S}{cm}$. The turbidity of the lunar water simulant is reduced from approximately 9800 NTU to approximately 0.285 NTU by the purification process.

The measured EC and turbidity values can be seen in table 5.10.

An overlap compared to the requirements of potable water on the ISS according to table 3.4 is regarding the manganese content. Manganese shall be below 0.3 $\frac{mg}{l}$. The ICP-OES measures an amount of manganese ions of under 0.050 $\frac{mg}{l}$. Therefore, the NASA requirement for amount of manganese ions is fulfilled. Regarding the WHO requirements for drinking water, the amount of released aluminium, calcium, iron, magnesium, and manganese ions can be evaluated. These requirements can be found in table 3.5. Iron has an upper limit of 0.02 $\frac{mg}{l}$. Since the analysis method ICP-OES is only able to provide the information that the measured amount of released iron ions is $< 0.05 \frac{mg}{l}$ no statement can be made whether the requirement is fulfilled. The requirements for aluminium, calcium, magnesium, and manganese are fulfilled.

To sum it up, additional measures to the lunar water purification system have to take place to produce water without measurable aluminium, calcium, iron, potassium, magnesium, manganese, sulfur, silicon, titanium ion content via ICP-OES, which would result in a lower EC as required for the electrolysis input water.

5.3.2 Optimisation of Water Purification System

The explained optimisations consist of carried out optimisations and further optimisation suggestions.

With the first tests of the lunar water purification system using only ultrapure water without lunar regolith simulant, six points of interests are identified for possible optimisation. The most important parameter that shall be optimised is the mass flow of the distillate to provide a rapid water purification process.

The first point of interest for optimisation is the pressure during the distillation process. For a first test an initial vacuum of 70 $mBar$ is set. However, the vacuum pump is only able to provide a stable vacuum of $79 - 80$ $mBar$ for the set value. The boiling temperature for water decreases with pressure. A lower pressure consequently results in a faster and more efficient distillation, as the required energy that has to be put into the evapouration flask via the heating bath is lower. The lowest and therefore optimised set pressure value, where the vacuum pump can still provide a stable pressure, is 60 $mBar$. With this set value $69 - 70$ $mBar$ are stably provided and the water boiling temperature changes from 41.5 °C to 38.7 °C [62].

The second point of interest is the upper temperature limit of the cooling fluid, being the only adjusted parameter of the chiller. To determine the optimised temperature the mass flow is determined by measuring the time it takes to produce 40 drops of distillate, which equals approximately 2 g. The measuring process starts as the cooler displays that the set temperature is reached. The properties for the best mass flow shall be selected as set

values for the controlling devices. For distillation in general the only requirement of the cooling fluid temperature is that it shall be lower than the boiling temperature so that the vapour will condensate. But at the same time it shall be above $0\,^\circ C$ with a safety margin to prevent icing of the cooling fluid. The lower the temperature of the cooling fluid the faster condensation is forced. The initial set fluid temperature is $5\,^\circ C$ as lower limit and $10\,^\circ C$ as upper limit with a mass flow of $0.0029\,\frac{g}{s}/10.58\,\frac{g}{h}$. The chiller generally provides cooling fluid with the set upper limit temperature with slight fluctuations to the lower temperature limit in the magnitude of up to $0.5\,^\circ C$. As lowest upper limit temperature $6\,^\circ C$ is tested as this ensures a relatively small buffer to the $5\,^\circ C$ lower limit. $6\,^\circ C$ results in a mass flow of $0.003\,\frac{g}{s}/12\,\frac{g}{h}$ and is the optimised temperature for the cooling fluid. It is set for further tests.

The third point of interest is the temperature of the heating bath. The initial temperature is set to $50\,^\circ C$ with a set pressure of $60\,mBar$ and reaches $69\,mBar$ and a cooling fluid temperature of $6\,^\circ C$. To optimise the temperature of the heating bath, the set temperature is increased in $5\,^\circ C$ steps and the mass flow is measured until the mass flow does not increase significantly. It is waited 15 minutes for the evapouration flask to be heated to the set temperature before measuring the time it takes to produce 40 drops of distillate. The temperature and achieved mass flow can be seen in table 5.11. The chosen optimised temperature is $95\,^\circ C$, because with a higher heating bath temperature - $100\,^\circ C$ and $105\,^\circ C$ - , the mass flow increases less significantly. Increasing the heating bath temperature has reached a point of diminishing return.

Table 5.11: *Mass Flow depending on Temperature of the Heating Bath*

Temperature in $°C$	Mass Flow in $\frac{g}{s}$	Mass Flow in $\frac{g}{h}$
50	0.0033	12.000
55	0.0050	18.000
60	0.0083	30.000
65	0.0104	37.500
70	0.0125	45.000
75	0.0148	53.500
80	0.0208	75.000
85	0.022	80.000
90	0.025	90.000
95	0.031	110.000
100	0.031	112.500
105	0.032	113.760

A homogenised mixture inside the evapouration flask is the fourth point of interest. A homogenised temperature can help vapourise fluids faster. Homogenising the fluid is achieved by adding a magnetic stirring bar into the flask and using the heating bath's additional function of a magnetic mixer with set 170 RPM.

The last point of interest is that the pipes shall touch none of the glasses or other pipes. This minimises the thermal losses through conduction and unwanted condensation.

Table 5.12: *Initial and Optimised Parameters of the Lunar Water Purification System*

Point of Interest	Initial Value	Optimised Value
Pressure during Distillation	$79mBar$	$69mBar$
Temperature of Heating Bath	$50°C$	$95°C$
Temperature of Cooling Fluid	$10°C$	$6°C$
Magnetic Mixer	0 RPM	170 RPM
Pipes are not in Contact	No	Yes

Suggested optimisations are explained in the following.

The time period for the sedimentation of the lunar water simulant shall be longer, as one day is not resulting in a satisfactory sedimentation. From subsection 5.2.1 a sedimentation time period of six days is recommended using $1 \ l$ of lunar water simulant.

During the first lunar water purification test the filtration process malfunctioned as addressed in subsection 5.2.2. As water is filled into the filtration bottle the filtration paper lifts off slightly and does not seal the inlet - a proper filtration is not provided. To solve this problem a metal ring can be placed on top of the filtration paper to weigh it down. Significant problems with calcium filtration using the lunar water purification system are apparent. To further purify the distillate, it can be distilled again using the purification system. Multiple distillations are often used to obtain a purer end product. With the lunar purification system, however, there are currently no results from multiple distillation. Possible post-processing methods to remove calcium if required are membrane distillation, reverse osmosis and ion exchange technology [63]. Membrane distillation uses a microporous hydrophobic membrane to separate vapour from other molecules. It achieves a calcium removal of over 96% which would in case of the distillate of the water purification system result in $0.032 \ \frac{mg}{l}/0.0032 \ \frac{mg}{g_{solid}}$ remaining calcium ions. Reverse osmosis uses $20 - 70 \ Bar$ pressure to separate molecules, including calcium ions from water at a semipermeable membrane. It removes $95 - 99\%$ of calcium ions leading to $0.04 - 0.008 \ \frac{mg}{l}/0.004 - 0.0008 \ \frac{mg}{g_{solid}}$ remaining calcium ions in the distillate of the water purification system. [63] Ion exchange technology uses the interchange of ions between a liquid and a solid, undesirable ions within the liquid are replaced by ions of the solid. These solids may be organic resin.

5.3.3 Optimisation of *LabVIEW* Program

As first step of the optimisation of the *LabVIEW* program the front panel is optimised. The schematic of the lunar water purification system is implemented. Moreover the buttons for controlling are lined up at the bottom as well as the box for selecting the address of the lines inside the *NI*-module. The buttons are framed individually to visually separate them. The stop button to stop the program is made to stand out in red. This is done to make it easy to find if it is urgently needed. To depicture the valve positions, LEDs are added, one for every valve. The LEDs shine light green as the valve is open and are dark green as the valve is closed.
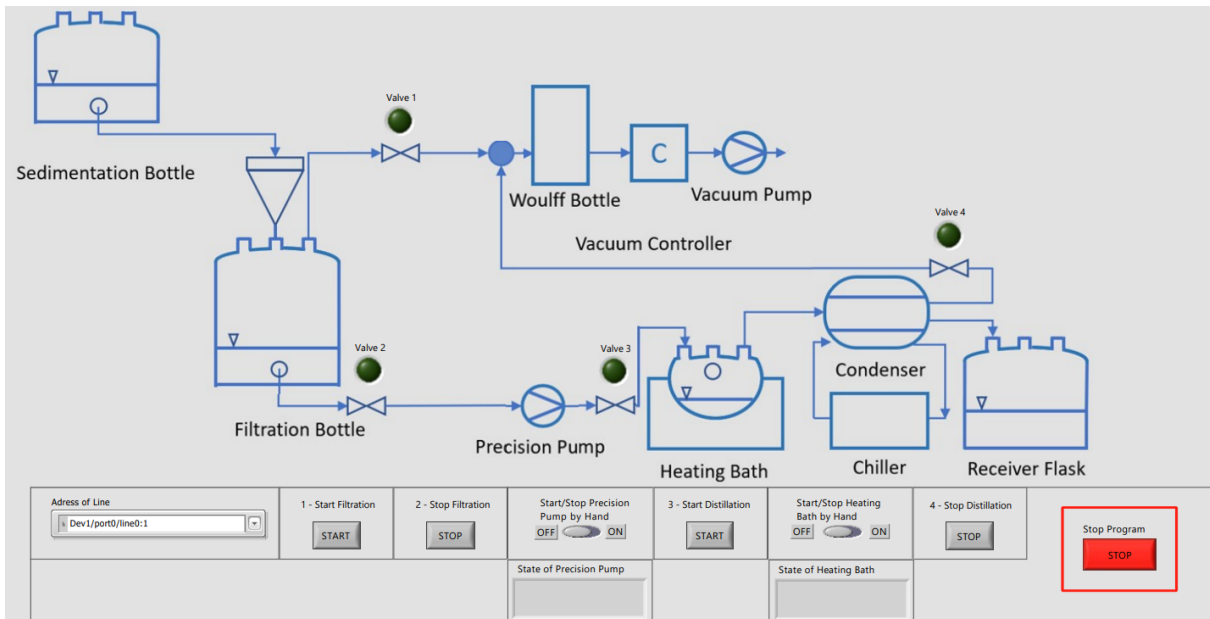
Figure 5.19: *Optimised Front Panel of LabVIEW Program*

The LEDs are implemented with a simple connection between the Boolean valve values inside the case structure and the LEDs outside the case structure. The implementation for case zero can be seen in figure 5.20 and the first, second, and third case are done accordingly. The whole *LabVIEW* program can be seen in the appendix G.1 and the "False" cases of the program in G.2 and G.3.
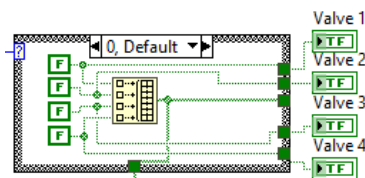
Figure 5.20: *Optimisation Using LEDs of LabVIEW Program*

A further optimisation step would be determining the reason for the contacting problem with the precision pump and the heating bath. Currently, this contacting problem results in the inconvenience to control the precision pump and the heating bath by hand. It needs to be noted that the computer indicates them as connected but contacting the devices via *LabVIEW* commands is not possible.

The connection cable between the precision pump and computer is included in its delivery scope. Consequently a wrong cable for the precision pump can be excluded as reason for the failing contact attempts. The connection cable between the computer and the heating bath is not included in the scope delivery. The heating bath requires a crossed RS232 to RS232 cable, unlike the other used *IKA* devices, which require a RS232 to RS232 cable with 1:1 lines. The first contacting attempt is made with a RS232 to USB-A cable, which does not provide the required crossed line wiring. The second contacting attempt is made

94

with a RS232 to RS232 cable with crossed lines and a RS232 to USB-A multiport by *IKA*. The third contacting attempt is made with a RS232 to RS232 cable with crossed lines by *IKA* and a RS232 to USB-A multiport by *IKA*. A possibility for the ongoing contacting problem of the heating bath may be the RS232 to USB-A multiport by *IKA* which was not specifically tested. To exclude this possibility an additional contacting attempt using, a computer with a RS232 port and *LabVIEW* license can be made. This is not tested because a computer with these properties is not available.

Through contact with the company *KNF* and *IKA* it can be stated that the correct input values, including baud rate, start or stop bit etc., which can be seen in table 4.4, are selected and consequently are not causing the connection problem. Using additionally provided *LabVIEW* programs by *KNF* for the precision pump still results in the same contacting problem.

The selected measuring instruments, described in subsection 5.1.2, shall be connected to the *DAQmx*-chassis and read. For then constantly tracking the pH, EC, level, and temperature, accordingly to the selected measuring instruments, a numeric indicator can be implemented on the front panel of the *LabVIEW* program.

6 Sources of Error

The sources of error can be divided into environmental, procedural, and instrumental error. The environmental error contains errors produced, because of missing data of lunar regolith and the incapability to reproduce lunar environment while experimenting. Additionally the procedural errors are highlighted within the dissolution experiments and the lunar water purification tests. The instrumental error consists of errors caused by measuring instruments, controlling devices, and elemental analysis technology.

6.1 Environmental Error

There are still open questions regarding basic information of the Moon, e.g. occurrence and abundance of water on the lunar surface and especially inside lunar regolith. The state-of-the-art is described in subsection 3.1.3. Various samples of regolith from the lunar polar regions will be collected in the future under, e.g. the Artemis missions and analysed to obtain more date of its properties and water content and state [29]. The lunar regolith from the polar regions is expected to be different from the lunar regolith samples from highland and mare regions taken during the Apollo missions [64]. Along with determining its chemical composition, the electrostatic and magnetic properties should be measured [64].
Experimenting on the Earth, lunar regolith behaves differently [15]. The different gravity, which is resulting in different forces between the regolith particles, is only one of the differences [15]. For example, the solar wind, cosmic rays and volatile constituents are further influences, as well as the electromagnetic and particle radiation [15]. These properties shall be taken into consideration for simulating lunar environment on Earth regarding lunar regolith simulant and the lunar water purification system. Other aspects that have to be taken into account is how the lunar environment would change the purification process. The sedimentation is an example. Because the Moon only has a sixth of Earth's gravitation, the gravitational based separation process of sedimentation, would take longer on the Moon to reach same results.

The simulation qualities of the lunar regolith simulant are limited by materials and minerals available on Earth. Therefore, differences between real lunar regolith and lunar regolith simulant are inevitable.

The lunar regolith simulant is more sodic than lunar regolith collected during Apollo missions. Generally, terrestrial plagioclase contains more sodium than plagioclase from the Moon. For simulating agglutinates or lunar pyroclastic glasses from the Moon, terrestrial balsatic glass is used. But balsatic glass is not a good substitute for agglutinates in terms of particle shape [15]. It needs to be noted that agglutinates only form on planets without atmosphere, as described in subsection 3.1.1. Basaltic glasses have many phases, this limits the diagnostic skills of the x-ray diffraction technology, e.g. XRF, with which the bulk composition of the lunar regolith simulant is determined. Furthermore, terrestrial rocks contain hydrated mineral species, which do not provide ideal matches to lunar regolith for some scientific applications, like for water or oxygen extraction.

In addition, the nanophase iron - particle size under 100 nm -, which is found in actual regolith, is not simulated in the simulant. The nanophase iron gives the regolith its magnetic properties. [15]

Furthermore, the simulant abilities of the *Exolith Lab* simulant are summed up and are explained in subsection 4.1.1. The simulant LMS-1 needs improvement matching the titanium dioxide content, LHS-1, LHS-1D, and LMS-1 regarding the potassium oxide content and LHS-1 and LHS-1D regarding the magnesium oxide content.

6.2 Procedural Error

A parameter that is not controlled during the dissolution experiments and the lunar water purification test is the ambient temperature. Inside the laboratory, the temperature is approximately 20 °C but may fluctuate. This can cause an error since a different temperature results in a different reactivity of elements.

For the dissolution experiments with LHS-1D exist two sources of error. For every second extraction time data of only one batch exists. Secondly, for magnesium and potassium data of only one batch is available for all extraction times. This means that no comparative data can be provided for some extraction times within the dissolution experiment with LHS-1D. However, the results after 72 h using LHS-1D 1:100 can be compared to the analysed inlet water of the lunar water purification test. The results of both tests are in accordance. To evaluate the different influences on the lunar water purification system, a sensitivity analysis of the purification system can be done. Influences on the system are determined by changing individual parameters like, e.g. changes in the purification process, pressure, and temperature, in the final purification system.

6.3 Instrumental Error

The pH meter and oximeter are calibrated before their first use. The pH meter is calibrated with a pH 7 solution and a pH 4.01 solution. For further tests the pH meter shall be calibrated with an additional pH 10.01 solution to establish more precise measurements. The oximeter is calibrated in a downwards direction for 2 minutes in air. The ambient air has different compositions depending on the location which leads to a slight deviation for different locations. The turbidimeter can only be calibrated with samples provided by the company *Lovibond*. Test samples have an *NTU* of < 0.1, 20, 200, and 800. This could potentially result in inaccuracies for measured turbidity values outside the calibrated range. The resolution, accuracy and measuring range of the measuring instruments and control devices can be seen in the following table and in the data sheets in the appendix.

Table 6.1: *Resolution, Accuracy and Measuring Range of used Devices*

Device	Resolution	Accuracy	Measuring Range
Dissolution Experiments			
pH Meter (D.1)	0.1	$\pm$ 0.02	$0 - 14$
Oxygen Meter (D.3)	0.1 $\frac{mg}{l}$	$\pm$ 0.5 %	$0.0 - 19.99$ $\frac{mg}{l}$ %
EC Meter (D.7)	0.01 $\frac{\mu S}{cm}$	$\pm$ 10 %	$0.05 - 10 \frac{\mu S}{cm}$
Temperature (D.1)	0.5 °C	0.1 °C	$0 - 50$ °C
Turbidity Meter (D.5)	0.01 NTU	2.50 %	$0.01 - 1100$ NTU
Balance (D.6)	0.001 g	$\pm$ 0.003 g	$0.002 - 350$ g
Water Purification System			
Vacuum Controller (E.1)	1 $mBar$	$\pm$ 1 $mBar$	$1 - 1100$ $mBar$
Vacuum Pump (E.2)	1 $mBar$	$\pm$ 1 $mBar$	$2 - 1030$ $mBar$
Precision Pump (E.3)	1 $\frac{ml}{min}$/1 ml	$\pm$ 2 %	$1 - 100$ $\frac{ml}{min}$/1 $- 999$ ml
Heating Bath (E.4)	1 °C	$\pm$ 2 °C	room temp.-200 °C
Chiller (E.5)	0.1 °C	$\pm$ 0.5 °C	$-10 - 70$ °C

For the element analysis of the extracted water samples ICP-OES is used. While the analysis method is precise it analyses only specific ions: aluminium , calcium, iron, potassium, magnesium, manganese, sulfur, silicon, and titanium. The calibration values are

set so that the measured values lie in the middle of these. Each sample is measured twice by the ICP-OES, the two measured values are within a deviation of less than 5%.

7 Summary

In this master thesis, a lunar water simulant was selected and a *LabVIEW* program was written to control a related lunar water purification system.

The dissolution experiments provide information about the amount of released aluminium, calcium, iron, potassium, magnesium, manganese, sulfur, silicon, and titanium ions using *Exolith Lab*'s lunar highland simulant LHS-1 and lunar mare simulant LMS-1. From the results of all dissolution experiments, a lunar water simulant was developed. The dissolution experiments are conducted using LHS-1 and LMS-1 and an aqueous solution - ultrapure water or buffer solution - with a pH of 5.6. During a time period of three days, water samples are extracted and analysed using ICP-OES. The released ions are measured in $\frac{mg}{l_{aqueous}}$ with released ions in mg per litre of the aqueous solution in $l_{aqueous}$ or $\frac{mg}{g_{solid}}$ as released ions in mg per simulant mass in g_{solid}. A density of 1 $\frac{kg}{l}$ is assumed for the litre of solution. Four observations can be made according to the results and are discussed:

1. More ions are released into the buffer solution in $\frac{mg}{g_{solid}}$ due to the lower pH.

2. More ions are released in $\frac{mg}{l_{aqueous}}$ using the ratio 1:100.

3. The bulk composition of the simulant is directly connected to the amount of released ions in $\frac{mg}{g_{solid}}$.

4. More ions in $\frac{mg}{g_{solid}}$ are released by a simulant with a small particle size rather than with a bigger particle size.

Using the data of all conducted dissolution experiments within the SMU research group a worst-case lunar water simulant is experimentally developed. The worst-case lunar water simulant is prepared using LHS-1D from *Exolith Lab* in a 1:100 ratio in ultrapure water answering the first research question. The released aluminium, calcium, iron, potassium, magnesium, manganese, sulfur, silicon, and titanium ions of the lunar water simulant are measured via ICP-OES.

The second part focusses on the lunar water purification system. The control technology and the process of the water purification are explained. In addition, the selection of the measuring instruments for the lunar water purification system is described, as well as sedimentation experiments, and the *LabVIEW* program to control the purification system. It is not possible to control all control devices via the program. The valves, the vacuum

pump, and the chiller can be controlled via *LabVIEW*, the precision pump and the heating bath cannot be contacted. After two tests of the lunar water purification system, tested with the lunar water simulant, the purification abilities of the system are evaluated. The released aluminium, iron, potassium, magnesium, manganese, sulfur, silicon, and titanium ions are removed while calcium remains in the distillate. Additionally, the required EC for electrolysis input water is not achieved. During the discussion of the purification system, optimisations - implemented and suggested ones - for the purification system and the *LabVIEW* program are described. Consequently, the research question of how the lunar water purification system can be controlled with the help of *LabVIEW* is answered with a detailed description.

Using the lunar water simulant, individual technologies of the ISRU process chain for water extraction on the Moon can be tested, e.g. the water purification. The *LabVIEW* program enables a partial control of the system and sets a basis to implement further measuring instruments into the program.

8 Outlook

For future dissolution experiments and the related lunar purification system open questions and suggestions are pointed out in the following regarding lunar regolith, lunar regolith simulant, analysing dissolution experiments, lunar water purification system, and related *LabVIEW* program.

"In general, basic research on the dissolution/precipitation of individual lunar minerals and glasses is a fundamental research need [46]. Such work would benefit all efforts which involve lunar dust/regolith in contact with water (water ice, astrobiology, habitat construction, greenhouses, dust inhalation etc.). All original Apollo samples have disintegration due to minuscule amounts of water vapor [65], illustrating the importance of such work" [51, p.11]. The best possibility to determine possible released ions of lunar regolith would be experimenting with actual lunar regolith. The Artemis mission may benefit the research by providing more samples and more data. The solubility and the released ions of lunar minerals from various lunar regions would be of interest as well. Generally, further analysis of the lunar regolith and the lunar regolith simulant are of interest. If the regolith simulant would be tested for the same oxides as the Apollo samples, it would enable a better comparison, as seen in table 4.3 (in subsection 4.1.1).

To further investigate the influences of particle sizes and bulk chemistry of *Exolith Lab*'s lunar simulants on released ions, LHS-1 and LMS-1 should be ground to the same mean, median, and particle size range. This enables the investigation of dissolution experiments with only one changing parameter - the bulk chemistry or the particle size. Different minerals or compounds of the regolith simulant, like e.g. olivine, could be milled to a specific particle size and their released ions could be determined for further investigation. Regarding various simulants it is recommended to test a simulant including nanophase iron oxides or include nanophase iron into regolith simulant to investigate their magnetic behaviour. Nanophase iron is present in the lunar regolith and gives it its magnetic properties [15].

For analysing the dissolution experiments, the water samples should be tested for a wider variety of ions and it shall be additionally tested for compounds. It is recommended to test for chloride, silica and sodium since those are requirements for the electrolysis input water set by ASTM as mentioned in table 3.3 (in subsection 3.2.5). Furthermore, the requirements for electrolysis input water shall be made more detailed to include further requirements for ions, especially the ions tested for within the dissolution experiments.

Another problem regarding analysing the water samples was that the ICP-OES's detection limit was not reached for specific ions. Therefore, it cannot be conclusively stated that these ions are not present. A more precise analysis can be done using Inductively Coupled Plasma Mass Spectronomy (ICP/MS). The detection limits are up to three orders of magnitude more precise [66].

Regarding the lunar water purification system, some aspects need to be optimised as explained in subsection 5.3.2 and 5.3.3. In order to provide a distillate with less ions than with the current purification, processes using, e.g. membrane distillation, reverse osmosis, ion exchange technology, or multiple distillation processes with the purification system, can be implemented before or after the current purification process. Additionally, the filtration process and the sedimentation require optimisation. For testing the lunar water purification system, the use of actual lunar regolith would be interesting as well. Considering especially its sharp edges in contact with filter paper, plastic pipes, etc., lunar regolith could present new challenges regarding the currently used materials and components. Regarding future plans for the lunar water purification system, LUWEX plans to investigate the extraction and the purification process with LCROSS contaminants in a lunar water simulant and in a lunar water ice simulant.

The *LabVIEW* program can now be used as a basis for controlling the purification system and be further expanded in the future. As optimisation for the lunar water purification system, the measuring instruments shall be installed into the purification system. When connected to the *DAQ*-chassis, the *LabVIEW* program is able to provide a real-time pH, EC, and temperature tracking. The contacting problem with the precision pump and the heating bath needs to be solved to control them via the *LabVIEW* program.

The results within this master thesis improve the understanding of dissolution experiments and the related lunar water purification system. The dissolution experiments, the first steps using the water purification system and the optimisations carried out and suggested bring the lunar water purification system closer to a fully automated system. The tested technology shall enable the purification of lunar water so that it can be used to produce oxygen and hydrogen through water electrolysis. These products can be used for generating propellant and sustaining life support. This lays the foundation for a technology that, adapted to the lunar environment, offers many possibilities for long-duration or deep space exploration.

Bibliography

[1] DLR. SOFIA Stratospheric Observatory For Infrared Astronomy. 2010.

[2] A. Colaprete et. al. Detection of Water in the LCROSS Ejecta Plume. *Science*, 330 (6003):463–468, 2010.

[3] NASA, L. Hall. April 2020. URL: https://www.nasa.gov/isru. last checked: 7.4. 2023.

[4] P. Cavaliere. Hydrogen Assisted Direct Reduction of Iron Oxides. 2022.

[5] R. Mugnuolo et al. International Agency Working Group. Dust Mitigation Gap Assessment Report. 2016.

[6] DLR. LUWEX Kick-Off Meeting. 2022.

[7] R. Freer et al. System Analysis of a shared Water-Hydrogen-Oxygen Infrastructure for future Space Habitats. Space resources Week 2020.

[8] D. Criswell. Horizon-glow and the motion of lunar dust. Photon and Particle Interactions With Surfaces in Space. 1973.

[9] R. Caston et. al. Assessing Toxicity and Nuclear and Mitochondrial DNA Damage Caused by Exposure of Mammalian Cells of Lunar Regolith Simulants. *GeoHealth*, 2 (4):139–148, 2018.

[10] G. Heiken et al. *Lunar sourcebook: a user's guide to the moon.* Press Syndicate of the University of Cambridge, 1st edition, 1991.

[11] M. Pickett et al. Regenerative water purification for space applications: Needs, challenges, and technologies towards 'closing the loop'. *Life Sciences in Space Reasearch*, 24:64–82, 2020.

[12] Deutsches Zentrum für Luft- und Raumfahrt. Die Oberfläche des Mondes. no date. URL: https://solarsystem.dlr.de/mond/61-die-oberflaeche-des-mondes. last checked: 7. March 2023.

[13] ESA, J. Josset. May 2016. URL: https://www.esa.int/Science_Exploration/Space_Science/SMART-1/Highlands_and_Mare_landscapes_on_the_Moon. last checked: 7. March 2023.

[14] S. Noble. The Lunar Regolith. 2019.

[15] D. Blewett et. al. 2021 lunar simulant assessment. 2021.

[16] K. Watson et. al. The behavior of volatiles on the lunar surface. *Journal of Geophysical Research (1896-1977)*, 66 (9):3033–3045, 1961.

[17] M. Anand. Lunar Water: A Brief Review. *Earth Moon Planets*, 107:65–73, 2010.

[18] S. Li et al. Direct evidence of surface exposed water ice in the lunar polar regions. *PNAS*, 115 (36):8907–8912, 2018.

[19] R. Clark. Detection of Adsorbed Water and Hydroxyl on the Moon. *Science*, 326 (5952):562–564, 2009.

[20] C. Pieters et. al. Character and spatial distribution of OH/H2O on the surface of the Moon seen by M3 on Chandrayaan-1. *Science*, 326 (5952):568–572, 2009.

[21] J. Sunshine et. al. Temporal and Spatial Variability of Lunar Hydration As Observed by the Deep Impact Spacecraft. *Science*, 326 (5952):565–568, 2009.

[22] E. Fischer et al. Evidence for surface water ice in the lunar polar regions using reflectance measurements from the Lunar Orbiter Laser Altimeter and temperature measurements from the Diviner Lunar Radiometer Experiment. *Isarus*, 292:74–85, 2017.

[23] P. Hayne et al. Evidence for exposed water ice in the Moon's south polar regions from Lunar Reconnaissance Orbiter ultraviolet albedo and temperature measurements. *Icarus*, 255:58–69, 2015.

[24] P. Spudis et. al. Initial results for the north pole of the Moon from Mini-SAR, Chandrayaan-1 mission. *Geophysical Research Letters*, 37 (6), 2010.

[25] J. Boyce et. al. Lunar apatite with terrestrial volatile abundances. *Nature*, 466 (7305):466–469, 2010.

[26] F. McCubbin et. al. Nominally hydrous magmatism on the Moon. *Proceedings of National Academy of Sciences*, 107 (25):11223–11228, 2010.

[27] A. Saal et. al. Volatile content og lunar volcanic glasses and the presence of water in the Moon's interior. *Nature*, 454:192–195, 2008.

[28] B. Keeter, NASA. NASA Radar Finds Ice Deposits at Moon's North Pole: Additional evidence of water activity on moon. March 2010. URL: https://www.nasa.gov/mission_pages/Mini-RF/multimedia/feature_ice_like_deposits.html. last checked: 17. February 2023.

[29] NASA. NASA Identifies Candidate Regions for Landing Next Americans on Moon. August 2022. URL: https://www.nasa.gov/press-release/nasa-identifies-candidate-regions-for-landing-next-americans-on-moon. last checked: 5. May 2023.

[30] A. Paige J. Zhang. Cold-trapped organic compounds at the poles of the Moon and Mercury: Implications for origins. *Geophysical Research Letters*, 36 (16):1–5, 2019.

[31] J. Arnold. Ice in the lunar polar regions. *Geophysical Research Letters*, 84:5659–5668, 1979.

[32] Y. Liu et al. Water extraction from icy lunar regolith by drilling-based thermal method in a pilot-scale unit. *Acta Astronautica*, 202:386–399, 2023.

[33] L. Kiewiet at al. Trade-off and optimization for thermal Lunar water extraction system. International Astronautical Congress 2022.

[34] N. Jurado. arified W Rarified Water Vapor Deposition F apor Deposition From Icy L om Icy Lunar Regolith On An unar Regolith On An Engineered Cold Plate. 2021.

[35] J. Holquist et al. Analysis of a Cold Trap as a Purification Step for Lunar Water Processing. International Conference on Environmental Systems 2020.

[36] J. Holquist et al. Experimental Proof of Concept of a Cold Trap as a Purification Step for Lunar Water Processing. 50th International Conference on Environmental Systems 2021.

[37] M. Carmo et. al. A comprehensive review on PEM water electrolysis. *International Journal of Hydrogen Energy*, 38:4901–4934, 2013.

[38] D. Zhang K. Zeng. Recent progress in alkaline water electrolysis for hydrogen production and applications. 2009.

[39] NASA. *Human Integration Design Handbook (HIDH)*. NASA, 2nd edition, 2014.

[40] World Health Organisation. Guidelines for drinking-water qualities. 2022.

[41] K. Brinkert et al. Efficient solar hydrogen generation in microgravity. *Nature Communications*, 9, 2018. 2019.

[42] G. Sanders et al. NASA Plans for In Situ Resource Utilization (ISRU) Development, Demonstration, and Implementation. Committee on Space Research (COSPAR). 2022.

[43] D. Kornuta et al. Commercial lunar propellant architecture: A collaborative study of lunar propellant production. 2019.

[44] J. Holquist et al. ISRU-derived water purification and Hydrogen Oxygen Production (IHOP) Component Development. 2020.

[45] J. Wang. AEM Water Electrolysis: How it Works. October 2020. URL: https://www.enapter.com/newsroom/aem-water-electrolysis-how-it-works. last checked: 25. February 2023.

[46] G. Whitney et al. Geochemistry of Soils for Lunar Base Agriculture: Future Research Needs. *Ming, D.W., Henninger, D.L. (Eds.), Lunar Base Agriculture: Soils for Plant Growth. American Society of Agronomy, Crop Science Society of America, Soil Science Society of America*, 1:213–235, 1989.

[47] N. Pal et al. Equilibrium and dynamic adsorption of gemini surfactants with different spacer lengths at oil/aqueous interfaces. *Colloids and Surfaces A: Physicochemical and Engineering*, 2017.

[48] M. Eick et. al. Dissolution kinetics of lunar glass simulant at 25°C: The effect of pH and organic acids. *Geochimca et Coamochimica Acta*, 60 (1):157–170, 1996.

[49] M. Eick et. al. Dissolution of a lunar basalt simulant as affected by pH and organic anions. *Geoderma*, 74:139–160, 1996.

[50] D. Karl et. al. Clay in situ resource utilization with Mars global simulant slurries for additive manufacturing and traditional shaping of unfired green bodies. *Acta Astronautica*, 174:241–253, 2020.

[51] D. Karl et. al. Synthetic H 2 O Weathering of Simple Feldspar Lunar Regolith Simulants Aiming to Build High Strength "Sandcastles" Using Fusion Drying. 2021.

[52] R. Kerschmann et. al. Testing of Lunar Dust Dissolution in Aqueous Environments. 2020.

[53] R. Kerschmann et. al. Profiling lunar dust dissolution in aqueous environments: The design concept. 2021.

[54] C. Stewart et. al. Protocol for analysis of volcanic ash samples for assessment of hazards from leachable elements. 2013.

[55] Exolith Lab. LHS-1 Simulant Fact Sheet. 01/2022.

[56] Exolith Lab. LHS-1D Dust Simulant Fact Sheet. 02/2022.

[57] Exolith Lab. LMS-1 Simulant Fact Sheet. 01/2022.

[58] A. Duncan et. al. Composition and inter-relationships of some Apollo 16 samples. 21973.

[59] J. Laul and R. Schmitt. Chemical composition of Apollo 15, 16, and 17 samples. *Proceedings of the Fourth Lunar Science Conference*, 2:1349–1367, 1973.

[60] J. Laul and R. Schmitt. The Apollo 15 Lunar Samples: A Preliminary Description. *Science*, 175 (4020):363–375, 1972.

[61] M. Peech. *Hydrogen Ion Activity. In: Norman, A., et al., Eds., Chemical and Microbiological Properties, Part 2.* American Society of Agronomy, 1965.

[62] E. Lemmon et al. *NIST Chemistry WebBook, NIST Standard Reference Database Number 69, Eds. P.J. Linstrom and W.G. Mallard: Thermophysical Properties of Fluid Systems.* National Institute of Standards and Technology, 2023.

[63] N. Qasem et al. Removal of heavy metal ions from wastewater: a comprehensive and critical review. *Nature Partner Journals Clean Water*, 36:1–15, 2021.

[64] S. Wagner NASA B. Johnson Space Center. An Assessment on Dust Effects on Planetary Surface Systems to Support Exploration Requirements. 2004.

[65] B. Cooper et al. Disintegration of Apollo lunar soil. *Nature Geoscience*, 8 (9):657–658, 2015.

[66] M. Eick et. al. Elemental Analysis using ICP-OES and ICP/MS. *Analytical Chemistry*, 63 (1):12A–21A, 1991.

Appendix

Appendix A.1: Lunar Highlands Dust Simulant

LHS-1D Dust Simulant| **Fact Sheet**

January, 2021

Simulant Name: LHS-1D Dust Simulant
Simulant Type: Extra-fine lunar highlands simulant for dust studies
Reference Material: Average lunar highlands
Uncompressed Bulk Density:
Mean Particle Size: 7 µm
Median Particle Size: 5 µm
Particle Size Range: <0.04 – 35 µm

Mineralogy

As mixed.

Component	Wt.%
Anorthosite	74.4
Glass-rich basalt	24.7
Ilmenite	0.4
Olivine	0.3
Pyroxene	0.2

Safety

See SDS for details. Primary hazard is dust inhalation; wear a respirator in dusty conditions.

Bulk Chemistry

Measured by XRF.

Oxide	Wt.%
SiO_2	48.1
Al_2O_3	25.8
CaO	18.4
Fe_2O_3	3.7
K_2O	0.7
MgO	0.3
MnO	0.1
P_2O_5	1.0
TiO_2	1.1
SO_3	0.3
Cl	0.4
SrO	0.1
Total	99.9

Particle Size Distribution

FTIR Spectrum

In progress.

Photo credit Matthew Villegas.

Appendix A.2: Lunar Highlands Simulant

LHS-1 Lunar Highlands Simulant | **Fact Sheet**
January, 2021

Simulant Name: LHS-1 Lunar Highlands Simulant
Simulant Type: General purpose
Reference Material: Average lunar highlands
Uncompressed Bulk Density: 1.30 g/cm³
Mean Particle Size: 60 µm
Median Particle Size: 50 µm
Particle Size Range: <0.04 µm – 400 µm

Mineralogy

As mixed.

Component	Wt.%
Anorthosite	74.4
Glass-rich basalt	24.7
Ilmenite	0.4
Olivine	0.3
Pyroxene	0.2

Safety

See SDS for details. Primary hazard is dust inhalation; wear a respirator in dusty conditions.

Bulk Chemistry

Measured by XRF.

Oxide	Wt.%
SiO_2	48.1
Al_2O_3	25.8
CaO	18.4
Fe_2O_3	3.7
K_2O	0.7
MgO	0.3
MnO	0.1
P_2O_5	1.0
TiO_2	1.1
SO_3	0.3
Cl	0.4
SrO	0.1
Total	99.9

Particle Size Distribution

FTIR Spectrum

Photo credit Matthew Villegas. FTIR spectrum courtesy of Katerina Slavicinska, Bennett Lab, UCF. Apollo particle size data adapted from the Lunar Soils Grain Size Catalog, Graf, 1993.

Appendix A.3: Lunar Mare Simulant

LMS-1 Lunar Mare Simulant | **Fact Sheet**
January, 2021

Simulant Name: LMS-1 Mare Highlands Simulant
Simulant Type: General purpose
Reference Material: Average lunar maria
Uncompressed Bulk Density: 1.56 g/cm^3
Mean Particle Size: 50 µm
Median Particle Size: 45 µm
Particle Size Range: <0.04 µm – 300 µm

Mineralogy

As mixed.

Component	Wt.%
Pyroxene	32.8
Glass-rich basalt	32.0
Anorthosite	19.8
Olivine	11.1
Ilmenite	4.3

Safety

See SDS for details. Primary hazard is dust inhalation; wear a respirator in dusty conditions.

Bulk Chemistry

Measured by XRF.

Oxide	Wt.%
SiO_2	40.2
Al_2O_3	14.0
CaO	9.8
Fe_2O_3	13.9
K_2O	0.6
MgO	12.0
MnO	0.3
P_2O_5	1.0
TiO_2	7.3
Cl	0.4
Cr_2O_3	0.3
NiO	0.2
SrO	0.1
Total	100.0

Particle Size Distribution
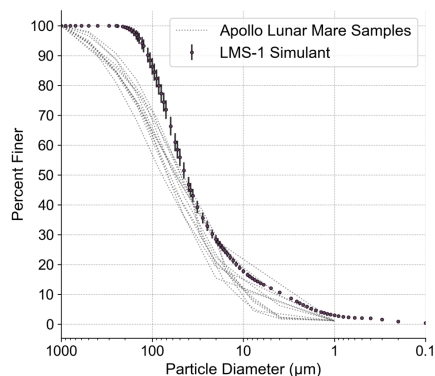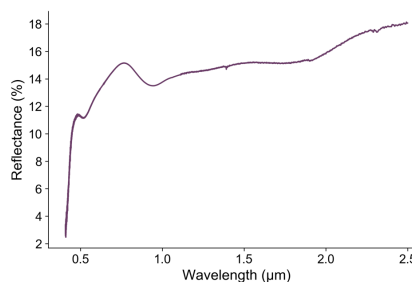
FTIR Spectrum

Photo credit Matthew Villegas. FTIR spectrum courtesy of Katerina Slavicinska, Bennett Lab, UCF. Apollo particle size data adapted from the Lunar Soils Grain Size Catalog, Graf, 1993.

Appendix B.1: Ultrapure Water Data Sheet

Spezifikation

Artikelnummer: A511

Wasser

ROTISOLV® HPLC Gradient Grade

CAS-Nummer: 7732-18-5   Druckdatum: 16.06.2023

Formel: H_2O

Dichte: 1

Molekulargewicht: 18,02 g/mol

Garantieanalyse

Spez. elektr. Widerstand (z. Zt. d. Herstellung)	≥18 MΩ*cm
Abdampfrückstand	≤0,0003 %
Freie Säure (als CH3COOH)	≤0,0002 %
Freies Alkali (als NH3)	≤0,0002 %

Fluoreszenz (als Chinin):

254 nm	≤1,0 ppb
365 nm	≤0,5 ppb

Gradiententest UV-Absorption des größten eluierten Peaks:

210 nm	≤5,0 mAU
254 nm	≤0,5 mAU

Unsere Produkte sind für Laborzwecke geprüft.
Die Angaben beziehen sich auf den aktuellen Stand der Produktqualität.
Wir behalten uns vor, notwendige Änderungen durchzuführen.

Dr. R. Niemand   **S. Lorsee**
Head of Quality Assurance   *Head of Quality Management*

Dieses Dokument wurde maschinell erstellt und ist ohne Unterschrift gültig.

Carl Roth GmbH + Co. KG   Telefon 0721/5606-0   Die Firma ist eine Kommanditgesellschaft mit Sitz in Karlsruhe, Reg.
Schoemperlenstraße 3-5   Telefax 0721/5606-149   Gericht Mannheim HRA 100055. Persönlich haftende Gesellschafterin ist
                                                            die Firma Roth Chemie GmbH mit Sitz in Karlsruhe, Reg. Gericht
76185 Karlsruhe   E-Mail: info@carlroth.de   Mannheim HRB 100428. Geschäftsführer: André Houdelet

Seite 1 von 1

Appendix C.1: pH over Time Using LHS-1 and LMS-1 in Ultrapure Water

Ultrapure Water

Time	Time in h	pH LMS-1, 1:100 I	pH LMS-1, 1:100 II	pH LHS-1, 1:100 I	pH LHS-1, 1:100 II	Time in h	pH LMS-1, 1:500 I	pH LMS-1, 1:500 II	pH LHS-1, 1:500 I	pH LHS-1, 1:500 II
t0	0.00	5.60	5.60	5.60	5.60	0.00	5.60	5.60	5.60	5.60
t1	0.03	8.30	8.20	8.20	8.80	0.03	7.40	7.40	7.60	7.40
t2	0.25	8.40	8.40	8.90	9.00	0.25	7.40	7.60	7.60	7.60
t3	0.50	8.50	8.40	8.90	9.30	0.50	7.60	7.90	7.70	7.70
t4	1.00	8.70	8.50	8.90	9.20	1.00	8.20	7.90	7.80	7.80
t5	12.00	9.20	9.10	9.30	9.40	12.00	8.20	7.80	7.50	7.30
t6	24.00	9.30	9.00	9.20	9.30	24.00	8.10	8.10	7.70	7.40
t7	72.00	8.80	8.90	9.00	8.90	72.00	8.10	8.10	8.00	8.10

Time	Time in h	Mean pH LMS-1, 1:100	Mean pH LHS-1, 1:100	Δx LMS-1, 1:100	Δx LHS-1, 1:100	Time in h	Mean pH LMS-1, 1:500	Mean pH LHS-1, 1:500	Δx LMS-1, 1:500	Δx LHS-1, 1:500
t0	0.00	5.60	5.60	0.00	0.00	0.00	5.60	5.60	0.00	0.00
t1	0.03	8.25	8.50	0.07	0.42	0.03	7.40	7.50	0.00	0.14
t2	0.25	8.40	8.95	0.00	0.07	0.25	7.50	7.60	0.14	0.00
t3	0.50	8.45	9.10	0.07	0.28	0.50	7.75	7.70	0.21	0.00
t4	1.00	8.60	9.05	0.14	0.21	1.00	8.05	7.80	0.21	0.00
t5	12.00	9.15	9.35	0.07	0.07	12.00	8.00	7.40	0.28	0.14
t6	24.00	9.15	9.25	0.21	0.07	24.00	8.10	7.55	0.00	0.21
t7	72.00	8.85	8.95	0.07	0.07	72.00	8.10	8.05	0.00	0.07

Appendix C.2: pH over Time Using LHS-1 and LMS-1 in Buffer Solution

Buffer Solution

Time	Time in h	LMS-1, 1:100 I (pH)	LMS-1, 1:100 II (pH)	LHS-1, 1:100 I (pH)	LHS-1, 1:100 II (pH)	Time in h	LMS-1, 1:500 I (pH)	LMS-1, 1:500 II (pH)	LHS-1, 1:500 I (pH)	LHS-1, 1:500 II (pH)
t0	0.00	5.60	5.60	5.60	5.60	0.00	5.60	5.60	5.60	5.60
t1	0.03	5.50	5.50	5.50	5.50	0.03	5.50	5.50	5.50	5.40
t2	0.25	5.60	5.60	5.50	5.40	0.25	5.40	5.50	5.50	5.40
t3	0.50	5.50	5.60	5.50	5.50	0.50	5.40	5.40	5.40	5.50
t4	1.00	5.50	5.50	5.60	5.50	1.00	5.50	5.40	5.50	5.50
t5	12.00	5.50	5.50	5.50	5.50	12.00	5.50	5.50	5.50	5.50
t6	24.00	5.40	5.40	5.40	5.40	24.00	5.50	5.50	5.40	5.50
t7	72.00	5.50	5.50	5.50	5.50	72.00	5.50	5.50	5.50	5.50

Time	Time in h	Mean pH LMS-1, 1:100	Mean pH LHS-1, 1:100	Δx LMS-1, 1:100	Δx LHS-1, 1:100	Time in h	Mean pH LMS-1, 1:500	Mean pH LHS-1, 1:500	Δx LMS-1, 1:500	Δx LHS-1, 1:500
t0	0.00	5.60	5.60	0.00	0.00	0.00	5.60	5.60	0.00	0.00
t1	0.03	5.50	5.50	0.00	0.00	0.03	5.50	5.45	0.00	0.07
t2	0.25	5.60	5.45	0.00	0.07	0.25	5.45	5.45	0.07	0.07
t3	0.50	5.55	5.50	0.07	0.00	0.50	5.40	5.45	0.00	0.07
t4	1.00	5.50	5.55	0.00	0.07	1.00	5.40	5.50	0.00	0.00
t5	12.00	5.50	5.50	0.00	0.00	12.00	5.50	5.50	0.00	0.00
t6	24.00	5.40	5.40	0.00	0.00	24.00	5.50	5.45	0.00	0.07
t7	72.00	5.50	5.50	0.00	0.00	72.00	5.50	5.50	0.00	0.00

Appendix C.3: Amount of Released Ions from LHS-1, LMS-1, LHS-1D into Ultrapure Water

Ca	Ca	Ca	Ca	Ca	Ca	Ca	Ca
Released Ions from Simulant into Ultrapure Water							
Time in hours	Unit	LHS-1, 1:100	LHS-1, 1:500	LMS-1, 1:100	LMS-1, 1:500	LHS-1D, 1:100	LHS-1D, 1:500
0.0333	mg/g_solid	0.285	0.731	0.141	0.512	0.479	0.835
0.25	mg/g_solid	0.379	0.786	0.174	0.587	0.530	1.114
0.5	mg/g_solid	0.410	0.884	0.198	0.562	0.546	1.175
1	mg/g_solid	0.473	1.056	0.233	0.659	0.570	1.226
12	mg/g_solid	0.566	1.439	0.344	0.809	0.622	1.520
24	mg/g_solid	0.604	1.466	0.340	0.816	0.623	1.631
72	mg/g_solid	0.610	1.398	0.363	0.859	0.637	1.729

Mg	Mg	Mg	Mg	Mg	Mg	Mg	Mg
Released Ions from Simulant into Ultrapure Water							
Time in hours	Unit	LHS-1, 1:100	LHS-1, 1:500	LMS-1, 1:100	LMS-1, 1:500	LHS-1D, 1:100	LHS-1D, 1:500
0.0333	mg/g_solid	0.010	0.050	0.036	0.083	0.039	0.061
0.25	mg/g_solid	0.010	0.050	0.047	0.115	0.049	0.080
0.5	mg/g_solid	0.010	0.050	0.054	0.127	0.054	0.088
1	mg/g_solid	0.010	0.050	0.062	0.147	0.061	0.105
12	mg/g_solid	0.010	0.050	0.093	0.241	0.084	0.214
24	mg/g_solid	0.011	0.050	0.108	0.280	0.088	0.243
72	mg/g_solid	0.010	0.050	0.139	0.345	0.093	0.272

K	K	K	K	K	K	K	K
Released Ions from Simulant into Ultrapure Water							
Time in hours	Unit	LHS-1, 1:100	LHS-1, 1:500	LMS-1, 1:100	LMS-1, 1:500	LHS-1D, 1:100	LHS-1D, 1:500
0.0333	mg/g_solid	0.050	0.583	0.062	0.250	0.076	0.243
0.25	mg/g_solid	0.050	0.744	0.080	0.250	0.080	0.207
0.5	mg/g_solid	0.050	1.109	0.083	0.250	0.087	0.221
1	mg/g_solid	0.050	1.214	0.097	0.250	0.236	0.234
12	mg/g_solid	0.054	1.258	0.103	0.250	0.141	0.369
24	mg/g_solid	0.061	1.417	0.107	0.250	0.151	0.388
72	mg/g_solid	0.067	1.539	0.115	0.250	0.171	0.497

Si	Si	Si	Si	Si	Si	Si	Si
Released Ions from Simulant into Ultrapure Water							
Time in hours	Unit	LHS-1, 1:100	LHS-1, 1:500	LMS-1, 1:100	LMS-1, 1:500	LHS-1D, 1:100	LHS-1D, 1:500
0.0333	mg/g_solid	0.027	0.131	0.032	0.152	0.049	0.055
0.25	mg/g_solid	0.034	0.165	0.038	0.165	0.076	0.095
0.5	mg/g_solid	0.036	0.167	0.045	0.159	0.096	0.123
1	mg/g_solid	0.038	0.157	0.046	0.143	0.135	0.173
12	mg/g_solid	0.059	0.195	0.120	0.241	0.238	0.798
24	mg/g_solid	0.073	0.199	0.144	0.297	0.209	0.926
72	mg/g_solid	0.110	0.168	0.230	0.385	0.243	1.138

Mn	Mn	Mn	Mn	Mn	Mn	Mn	Mn
Released Ions from Simulant into Ultrapure Water							
Time in hours	Unit	LHS-1, 1:100	LHS-1, 1:500	LMS-1, 1:100	LMS-1, 1:500	LHS-1D, 1:100	LHS-1D, 1:500
0.0333	mg/g_solid	0.005	0.025	0.005	0.025	0.000	0.002
0.25	mg/g_solid	0.005	0.025	0.005	0.025	0.000	0.002
0.5	mg/g_solid	0.005	0.025	0.005	0.025	0.000	0.002
1	mg/g_solid	0.005	0.025	0.005	0.025	0.000	0.002
12	mg/g_solid	0.005	0.025	0.005	0.025	0.000	0.002
24	mg/g_solid	0.005	0.025	0.005	0.025	0.000	0.002
72	mg/g_solid	0.005	0.025	0.005	0.025	0.000	0.002

Ti	Ti	Ti	Ti	Ti	Ti	Ti	Ti
Released Ions from Simulant into Ultrapure Water							
Time in hours	Unit	LHS-1, 1:100	LHS-1, 1:500	LMS-1, 1:100	LMS-1, 1:500	LHS-1D, 1:100	LHS-1D, 1:500
0.0333	mg/g_solid	0.005	0.025	0.005	0.025	0.001	0.001
0.25	mg/g_solid	0.005	0.025	0.005	0.025	0.000	0.001
0.5	mg/g_solid	0.005	0.025	0.005	0.025	0.000	0.002
1	mg/g_solid	0.005	0.025	0.005	0.025	0.000	0.001
12	mg/g_solid	0.005	0.025	0.005	0.025	0.000	0.001
24	mg/g_solid	0.005	0.025	0.005	0.025	0.000	0.001
72	mg/g_solid	0.005	0.025	0.005	0.025	0.001	0.001

Al	Al	Al	Al	Al	Al	Al	Al
Released Ions from Simulant into Ultrapure Water							
Time in hours	Unit	LHS-1, 1:100	LHS-1, 1:500	LMS-1, 1:100	LMS-1, 1:500	LHS-1D, 1:100	LHS-1D, 1:500
0.0333	mg/g_solid	0.005	0.025	0.005	0.025	0.077	0.042
0.25	mg/g_solid	0.005	0.025	0.005	0.025	0.106	0.087
0.5	mg/g_solid	0.005	0.025	0.005	0.025	0.097	0.108
1	mg/g_solid	0.005	0.025	0.005	0.025	0.157	0.118
12	mg/g_solid	0.015	0.025	0.006	0.025	0.272	0.589
24	mg/g_solid	0.024	0.029	0.007	0.025	0.211	0.690
72	mg/g_solid	0.047	0.025	0.015	0.025	0.311	0.980

Fe	Fe	Fe	Fe	Fe	Fe	Fe	Fe
Released Ions from Simulant into Ultrapure Water							
Time in hours	Unit	LHS-1, 1:100	LHS-1, 1:500	LMS-1, 1:100	LMS-1, 1:500	LHS-1D, 1:100	LHS-1D, 1:500
0.0333	mg/g_solid	0.005	0.025	0.005	0.025	0.004	0.005
0.25	mg/g_solid	0.005	0.025	0.005	0.025	0.000	0.006
0.5	mg/g_solid	0.005	0.025	0.005	0.025	0.003	0.008
1	mg/g_solid	0.005	0.025	0.005	0.025	0.002	0.005
12	mg/g_solid	0.005	0.025	0.005	0.025	0.002	0.005
24	mg/g_solid	0.005	0.025	0.005	0.025	0.002	0.006
72	mg/g_solid	0.005	0.025	0.010	0.025	0.003	0.006

S	S	S	S	S	S	S	S
Released Ions from Simulant into Ultrapure Water							
Time in hours	Unit	LHS-1, 1:100	LHS-1, 1:500	LMS-1, 1:100	LMS-1, 1:500	LHS-1D, 1:100	LHS-1D, 1:500
0.0333	mg/g_solid	0.007	0.016	0.006	0.015	0.012	0.027
0.25	mg/g_solid	0.009	0.016	0.007	0.015	0.011	0.028
0.5	mg/g_solid	0.009	0.021	0.007	0.016	0.015	0.034
1	mg/g_solid	0.010	0.024	0.008	0.017	0.012	0.030
12	mg/g_solid	0.012	0.029	0.013	0.024	0.016	0.035
24	mg/g_solid	0.013	0.030	0.012	0.022	0.015	0.038
72	mg/g_solid	0.013	0.030	0.013	0.025	0.016	0.043

Ca	Ca	Ca	Ca	Ca	Ca	Ca	Ca
		Δx	Δx	Δx	Δx	Δx	Δx
Time in hours	Unit	LHS-1, 1:100	LHS-1, 1:500	LMS-1, 1:100	LMS-1, 1:500	LHS-1D, 1:100	LHS-1D, 1:500
0.0333	mg/g_solid	0.003	0.052	0.002	0.054	0.068	0.021
0.25	mg/g_solid	0.034	0.001	0.009	0.019	0.000	0.030
0.5	mg/g_solid	0.006	0.033	0.022	0.047	0.040	0.014
1	mg/g_solid	0.025	0.143	0.022	0.157	0.042	0.044
12	mg/g_solid	0.031	0.111	0.026	0.059	0.035	0.007
24	mg/g_solid	0.001	0.078	0.002	0.070	0.034	0.069
72	mg/g_solid	0.034	0.122	0.011	0.026	0.046	0.044

Mg	Mg	Mg	Mg	Mg	Mg	Mg	Mg
		Δx	Δx	Δx	Δx	Δx	Δx
Time in hours	Unit	LHS-1, 1:100	LHS-1, 1:500	LMS-1, 1:100	LMS-1, 1:500	LHS-1D, 1:100	LHS-1D, 1:500
0.0333	mg/g_solid	0.000	0.000	0.002	0.008	0.007	0.013
0.25	mg/g_solid	0.000	0.000	0.002	0.008	0.000	0.012
0.5	mg/g_solid	0.000	0.000	0.003	0.005	0.003	0.018
1	mg/g_solid	0.000	0.000	0.006	0.021	0.003	0.022
12	mg/g_solid	0.000	0.000	0.005	0.007	0.004	0.007
24	mg/g_solid	0.001	0.000	0.000	0.001	0.005	0.006
72	mg/g_solid	0.000	0.000	0.010	0.011	0.005	0.009

K	K	K	K	K	K	K	K
		Δx	Δx	Δx	Δx	Δx	Δx
Time in hours	Unit	LHS-1, 1:100	LHS-1, 1:500	LMS-1, 1:100	LMS-1, 1:500	LHS-1D, 1:100	LHS-1D, 1:500
0.0333	mg/g_solid	0.000	0.208	0.017	0.000	0.000	0.001
0.25	mg/g_solid	0.000	0.162	0.042	0.000	0.000	0.060
0.5	mg/g_solid	0.000	0.250	0.046	0.000	0.000	0.049
1	mg/g_solid	0.000	0.280	0.067	0.000	0.000	0.048
12	mg/g_solid	0.005	0.437	0.075	0.000	0.000	0.064
24	mg/g_solid	0.016	0.562	0.080	0.000	0.000	0.089
72	mg/g_solid	0.025	0.686	0.092	0.000	0.000	0.223

Si	Si	Si	Si	Si	Si	Si	Si
		Δx	Δx	Δx	Δx	Δx	Δx
Time in hours	Unit	LHS-1, 1:100	LHS-1, 1:500	LMS-1, 1:100	LMS-1, 1:500	LHS-1D, 1:100	LHS-1D, 1:500
0.0333	mg/g_solid	0.000	0.046	0.006	0.002	0.005	0.008
0.25	mg/g_solid	0.005	0.011	0.006	0.037	0.000	0.047
0.5	mg/g_solid	0.001	0.018	0.002	0.006	0.006	0.041
1	mg/g_solid	0.001	0.046	0.001	0.044	0.011	0.037
12	mg/g_solid	0.002	0.018	0.008	0.015	0.001	0.074
24	mg/g_solid	0.003	0.010	0.001	0.019	0.034	0.126
72	mg/g_solid	0.004	0.032	0.006	0.026	0.013	0.158

Mn	Mn	Mn	Mn	Mn	Mn	Mn	Mn
		Δx	Δx	Δx	Δx	Δx	Δx
Time in hours	Unit	LHS-1, 1:100	LHS-1, 1:500	LMS-1, 1:100	LMS-1, 1:500	LHS-1D, 1:100	LHS-1D, 1:500
0.0333	mg/g_solid	0.000	0.000	0.000	0.000	0.000	0.001
0.25	mg/g_solid	0.000	0.000	0.000	0.000	0.000	0.001
0.5	mg/g_solid	0.000	0.000	0.000	0.000	0.000	0.001
1	mg/g_solid	0.000	0.000	0.000	0.000	0.000	0.001
12	mg/g_solid	0.000	0.000	0.000	0.000	0.000	0.001
24	mg/g_solid	0.000	0.000	0.000	0.000	0.000	0.001
72	mg/g_solid	0.000	0.000	0.000	0.000	0.000	0.001

Ti	Ti	Ti	Ti	Ti	Ti	Ti	Ti
		Δx	Δx	Δx	Δx	Δx	Δx
Time in hours	Unit	LHS-1, 1:100	LHS-1, 1:500	LMS-1, 1:100	LMS-1, 1:500	LHS-1D, 1:100	LHS-1D, 1:500
0.0333	mg/g_solid	0.000	0.000	0.000	0.000	0.000	0.002
0.25	mg/g_solid	0.000	0.000	0.000	0.000	0.000	0.002
0.5	mg/g_solid	0.000	0.000	0.000	0.000	0.000	0.001
1	mg/g_solid	0.000	0.000	0.000	0.000	0.000	0.002
12	mg/g_solid	0.000	0.000	0.000	0.000	0.000	0.002
24	mg/g_solid	0.000	0.000	0.000	0.000	0.000	0.002
72	mg/g_solid	0.000	0.000	0.000	0.000	0.000	0.002

Al	Al	Al	Al	Al	Al	Al	Al
		Δx	Δx	Δx	Δx	Δx	Δx
Time in hours	Unit	LHS-1, 1:100	LHS-1, 1:500	LMS-1, 1:100	LMS-1, 1:500	LHS-1D, 1:100	LHS-1D, 1:500
0.0333	mg/g_solid	0.000	0.000	0.000	0.000	0.009	0.012
0.25	mg/g_solid	0.000	0.000	0.000	0.000	0.000	0.006
0.5	mg/g_solid	0.000	0.000	0.000	0.000	0.048	0.004
1	mg/g_solid	0.000	0.000	0.000	0.000	0.000	0.005
12	mg/g_solid	0.000	0.000	0.001	0.000	0.024	0.020
24	mg/g_solid	0.000	0.006	0.000	0.000	0.117	0.063
72	mg/g_solid	0.002	0.000	0.000	0.000	0.037	0.043

Fe	Fe	Fe	Fe	Fe	Fe	Fe	Fe
		Δx	Δx	Δx	Δx	Δx	Δx
Time in hours	Unit	LHS-1, 1:100	LHS-1, 1:500	LMS-1, 1:100	LMS-1, 1:500	LHS-1D, 1:100	LHS-1D, 1:500
0.0333	mg/g_solid	0.000	0.000	0.000	0.000	0.001	0.007
0.25	mg/g_solid	0.000	0.000	0.000	0.000	0.000	0.006
0.5	mg/g_solid	0.000	0.000	0.000	0.000	0.002	0.003
1	mg/g_solid	0.000	0.000	0.000	0.000	0.003	0.007
12	mg/g_solid	0.000	0.000	0.000	0.000	0.003	0.006
24	mg/g_solid	0.000	0.000	0.000	0.000	0.003	0.006
72	mg/g_solid	0.000	0.000	0.002	0.000	0.002	0.006

S	S	S	S	S	S	S	S
		Δx	Δx	Δx	Δx	Δx	Δx
Time in hours	Unit	LHS-1, 1:100	LHS-1, 1:500	LMS-1, 1:100	LMS-1, 1:500	LHS-1D, 1:100	LHS-1D, 1:500
0.0333	mg/g_solid	0.000	0.002	0.000	0.000	0.001	0.009
0.25	mg/g_solid	0.000	0.001	0.001	0.000	0.000	0.010
0.5	mg/g_solid	0.000	0.002	0.000	0.002	0.005	0.004
1	mg/g_solid	0.000	0.001	0.000	0.003	0.000	0.005
12	mg/g_solid	0.000	0.003	0.000	0.006	0.000	0.018
24	mg/g_solid	0.000	0.001	0.000	0.000	0.001	0.014
72	mg/g_solid	0.000	0.004	0.001	0.003	0.001	0.015

Appendix C.4: Amount of Released Ions from LHS-1, LMS-1, LHS-1D into Buffer Solution

Ca	Ca	Ca	Ca	Ca	Ca	Ca	Ca
Released Ions from Simulant into Buffer Solution							
Time in hours	Unit	LHS-1, 1:100	LHS-1, 1:500	LMS-1, 1:100	LMS-1, 1:500	LHS-1D, 1:100	LHS-1D, 1:500
0.0333	mg/g_solid	1.242	1.823	0.546	1.105	1.940	2.028
0.25	mg/g_solid	1.376	1.951	0.634	1.237	2.114	2.330
0.5	mg/g_solid	1.407	1.969	0.639	1.299	2.267	2.466
1	mg/g_solid	1.411	2.033	0.671	1.269	2.396	2.567
12	mg/g_solid	1.469	2.062	0.788	1.434	2.988	3.057
24	mg/g_solid	1.491	2.039	0.837	1.490	3.208	3.310
72	mg/g_solid	1.524	2.086	0.897	1.454	3.527	3.630

Mg	Mg	Mg	Mg	Mg	Mg	Mg	Mg
Released Ions from Simulant into Buffer Solution							
Time in hours	Unit	LHS-1, 1:100	LHS-1, 1:500	LMS-1, 1:100	LMS-1, 1:500	LHS-1D, 1:100	LHS-1D, 1:500
0.0333	mg/g_solid	0.040	0.200	0.124	0.200	0.202	0.240
0.25	mg/g_solid	0.040	0.200	0.166	0.203	0.284	0.322
0.5	mg/g_solid	0.040	0.200	0.189	0.213	0.312	0.357
1	mg/g_solid	0.040	0.200	0.218	0.246	0.348	0.394
12	mg/g_solid	0.040	0.200	0.347	0.405	0.495	0.542
24	mg/g_solid	0.040	0.200	0.394	0.460	0.531	0.581
72	mg/g_solid	0.040	0.200	0.485	0.557	0.596	0.643

K	K	K	K	K	K	K	K
Released Ions from Simulant into Buffer Solution							
Time in hours	Unit	LHS-1, 1:100	LHS-1, 1:500	LMS-1, 1:100	LMS-1, 1:500	LHS-1D, 1:100	LHS-1D, 1:500
0.0333	mg/g_solid	0.200	1.000	0.200	1.000	0.306	0.358
0.25	mg/g_solid	0.200	1.000	0.200	1.000	0.491	0.447
0.5	mg/g_solid	0.200	1.000	0.200	1.000	0.396	0.460
1	mg/g_solid	0.200	1.000	0.200	1.000	0.419	0.524
12	mg/g_solid	0.200	1.000	0.200	1.000	0.535	0.594
24	mg/g_solid	0.200	1.000	0.200	1.000	0.569	0.638
72	mg/g_solid	0.200	1.000	0.200	1.000	0.613	0.657

Si	Si	Si	Si	Si	Si	Si	Si
Released Ions from Simulant into Buffer Solution							
Time in hours	Unit	LHS-1, 1:100	LHS-1, 1:500	LMS-1, 1:100	LMS-1, 1:500	LHS-1D, 1:100	LHS-1D, 1:500
0.0333	mg/g_solid	0.040	0.200	0.040	0.200	0.212	0.297
0.25	mg/g_solid	0.040	0.200	0.040	0.200	0.336	0.452
0.5	mg/g_solid	0.040	0.200	0.040	0.200	0.394	0.538
1	mg/g_solid	0.040	0.200	0.040	0.200	0.458	0.618
12	mg/g_solid	0.047	0.200	0.097	0.200	0.772	1.111
24	mg/g_solid	0.059	0.200	0.124	0.216	0.909	1.336
72	mg/g_solid	0.089	0.200	0.189	0.281	1.149	1.884

Mn	Mn	Mn	Mn	Mn	Mn	Mn	Mn
Released Ions from Simulant into Buffer Solution							
Time in hours	Unit	LHS-1, 1:100	LHS-1, 1:500	LMS-1, 1:100	LMS-1, 1:500	LHS-1D, 1:100	LHS-1D, 1:500
0.0333	mg/g_solid	0.040	0.200	0.040	0.200	0.007	0.008
0.25	mg/g_solid	0.040	0.200	0.040	0.200	0.054	0.011
0.5	mg/g_solid	0.040	0.200	0.040	0.200	0.012	0.013
1	mg/g_solid	0.040	0.200	0.040	0.200	0.015	0.015
12	mg/g_solid	0.040	0.200	0.040	0.200	0.028	0.027
24	mg/g_solid	0.040	0.200	0.040	0.200	0.028	0.028
72	mg/g_solid	0.047	0.200	0.040	0.200	0.030	0.031

Ti	Ti	Ti	Ti	Ti	Ti	Ti	Ti
Released Ions from Simulant into Buffer Solution							
Time in hours	Unit	LHS-1, 1:100	LHS-1, 1:500	LMS-1, 1:100	LMS-1, 1:500	LHS-1D, 1:100	LHS-1D, 1:500
0.0333	mg/g_solid	0.040	0.200	0.040	0.200	0.001	0.003
0.25	mg/g_solid	0.040	0.200	0.040	0.200	0.001	0.003
0.5	mg/g_solid	0.040	0.200	0.040	0.200	0.001	0.003
1	mg/g_solid	0.040	0.200	0.040	0.200	0.001	0.003
12	mg/g_solid	0.040	0.200	0.040	0.200	0.001	0.003
24	mg/g_solid	0.040	0.200	0.042	0.200	0.001	0.003
72	mg/g_solid	0.040	0.200	0.048	0.200	0.001	0.003

Al	Al	Al	Al	Al	Al	Al	Al
Released Ions from Simulant into Buffer Solution							
Time in hours	Unit	LHS-1, 1:100	LHS-1, 1:500	LMS-1, 1:100	LMS-1, 1:500	LHS-1D, 1:100	LHS-1D, 1:500
0.0333	mg/g_solid	0.010	0.050	0.010	0.050	0.167	0.335
0.25	mg/g_solid	0.010	0.050	0.016	0.052	0.217	0.425
0.5	mg/g_solid	0.010	0.050	0.025	0.066	0.258	0.493
1	mg/g_solid	0.010	0.050	0.040	0.083	0.290	0.575
12	mg/g_solid	0.012	0.050	0.102	0.189	0.469	0.889
24	mg/g_solid	0.014	0.050	0.100	0.198	0.597	1.068
72	mg/g_solid	0.015	0.053	0.069	0.175	0.749	1.446

Fe	Fe	Fe	Fe	Fe	Fe	Fe	Fe
Released Ions from Simulant into Buffer Solution							
Time in hours	Unit	LHS-1, 1:100	LHS-1, 1:500	LMS-1, 1:100	LMS-1, 1:500	LHS-1D, 1:100	LHS-1D, 1:500
0.0333	mg/g_solid	0.040	0.200	0.040	0.210	0.018	0.070
0.25	mg/g_solid	0.040	0.200	0.040	0.210	0.044	0.105
0.5	mg/g_solid	0.040	0.200	0.040	0.210	0.037	0.070
1	mg/g_solid	0.040	0.200	0.040	0.210	0.010	0.135
12	mg/g_solid	0.040	0.200	0.040	0.210	0.026	0.050
24	mg/g_solid	0.040	0.200	0.040	0.210	0.029	0.063
72	mg/g_solid	0.040	0.200	0.040	0.210	0.040	0.082

S	S	S	S	S	S	S	S
Released Ions from Simulant into Buffer Solution							
Time in hours	Unit	LHS-1, 1:100	LHS-1, 1:500	LMS-1, 1:100	LMS-1, 1:500	LHS-1D, 1:100	LHS-1D, 1:500
0.0333	mg/g_solid	0.007	0.035	0.007	0.035	0.007	0.042
0.25	mg/g_solid	0.007	0.035	0.007	0.035	0.007	0.035
0.5	mg/g_solid	0.007	0.035	0.007	0.035	0.007	0.034
1	mg/g_solid	0.007	0.035	0.007	0.035	0.007	0.042
12	mg/g_solid	0.007	0.035	0.007	0.035	0.007	0.034
24	mg/g_solid	0.007	0.035	0.007	0.035	0.007	0.034
72	mg/g_solid	0.007	0.035	0.007	0.035	0.009	0.034

Ca	Ca	Ca	Ca	Ca	Ca	Ca	Ca
		Δx	Δx	Δx	Δx	Δx	Δx
Time in hours	Unit	LHS-1, 1:100	LHS-1, 1:500	LMS-1, 1:100	LMS-1, 1:500	LHS-1D, 1:100	LHS-1D, 1:500
0.0333	mg/g_solid	0.010	0.023	0.000	0.002	0.000	0.000
0.25	mg/g_solid	0.013	0.071	0.003	0.137	0.080	0.033
0.5	mg/g_solid	0.005	0.035	0.023	0.053	0.010	0.079
1	mg/g_solid	0.003	0.164	0.006	0.024	0.030	0.045
12	mg/g_solid	0.010	0.103	0.032	0.011	0.044	0.038
24	mg/g_solid	0.022	0.065	0.042	0.048	0.048	0.143
72	mg/g_solid	0.022	0.203	0.042	0.108	0.035	0.028

Mg	Mg	Mg	Mg	Mg	Mg	Mg	Mg
		Δx	Δx	Δx	Δx	Δx	Δx
Time in hours	Unit	LHS-1, 1:100	LHS-1, 1:500	LMS-1, 1:100	LMS-1, 1:500	LHS-1D, 1:100	LHS-1D, 1:500
0.0333	mg/g_solid	0.000	0.000	0.004	0.000	0.000	0.000
0.25	mg/g_solid	0.000	0.000	0.002	0.005	0.003	0.001
0.5	mg/g_solid	0.000	0.000	0.000	0.021	0.001	0.002
1	mg/g_solid	0.000	0.000	0.000	0.020	0.006	0.002
12	mg/g_solid	0.000	0.000	0.007	0.027	0.000	0.001
24	mg/g_solid	0.000	0.000	0.006	0.028	0.002	0.009
72	mg/g_solid	0.000	0.000	0.010	0.034	0.001	0.003

K	K	K	K	K	K	K	K
		Δx	Δx	Δx	Δx	Δx	Δx
Time in hours	Unit	LHS-1, 1:100	LHS-1, 1:500	LMS-1, 1:100	LMS-1, 1:500	LHS-1D, 1:100	LHS-1D, 1:500
0.0333	mg/g_solid	0.000	0.000	0.000	0.000	0.000	0.000
0.25	mg/g_solid	0.000	0.000	0.000	0.000	0.162	0.023
0.5	mg/g_solid	0.000	0.000	0.000	0.000	0.006	0.024
1	mg/g_solid	0.000	0.000	0.000	0.000	0.019	0.031
12	mg/g_solid	0.000	0.000	0.000	0.000	0.002	0.023
24	mg/g_solid	0.000	0.000	0.000	0.000	0.007	0.017
72	mg/g_solid	0.000	0.000	0.000	0.000	0.002	0.011

Si	Si	Si	Si	Si	Si	Si	Si
		Δx	Δx	Δx	Δx	Δx	Δx
Time in hours	Unit	LHS-1, 1:100	LHS-1, 1:500	LMS-1, 1:100	LMS-1, 1:500	LHS-1D, 1:100	LHS-1D, 1:500
0.0333	mg/g_solid	0.000	0.000	0.000	0.000	0.000	0.000
0.25	mg/g_solid	0.000	0.000	0.000	0.000	0.010	0.013
0.5	mg/g_solid	0.000	0.000	0.000	0.000	0.004	0.012
1	mg/g_solid	0.000	0.000	0.000	0.000	0.000	0.011
12	mg/g_solid	0.001	0.000	0.003	0.000	0.005	0.002
24	mg/g_solid	0.001	0.000	0.003	0.005	0.007	0.004
72	mg/g_solid	0.002	0.000	0.006	0.006	0.008	0.046

Mn	Mn	Mn	Mn	Mn	Mn	Mn	Mn
		Δx	Δx	Δx	Δx	Δx	Δx
Time in hours	Unit	LHS-1, 1:100	LHS-1, 1:500	LMS-1, 1:100	LMS-1, 1:500	LHS-1D, 1:100	LHS-1D, 1:500
0.0333	mg/g_solid	0.000	0.000	0.000	0.000	0.000	0.000
0.25	mg/g_solid	0.000	0.000	0.000	0.000	0.061	0.000
0.5	mg/g_solid	0.000	0.000	0.000	0.000	0.000	0.000
1	mg/g_solid	0.000	0.000	0.000	0.000	0.001	0.001
12	mg/g_solid	0.000	0.000	0.000	0.000	0.000	0.003
24	mg/g_solid	0.000	0.000	0.000	0.000	0.001	0.004
72	mg/g_solid	0.002	0.000	0.000	0.000	0.001	0.004

Ti	Ti	Ti	Ti	Ti	Ti	Ti	Ti
		Δx	Δx	Δx	Δx	Δx	Δx
Time in hours	Unit	LHS-1, 1:100	LHS-1, 1:500	LMS-1, 1:100	LMS-1, 1:500	LHS-1D, 1:100	LHS-1D, 1:500
0.0333	mg/g_solid	0.000	0.000	0.000	0.000	0.000	0.000
0.25	mg/g_solid	0.000	0.000	0.000	0.000	0.000	0.000
0.5	mg/g_solid	0.000	0.000	0.000	0.000	0.000	0.000
1	mg/g_solid	0.000	0.000	0.000	0.000	0.000	0.000
12	mg/g_solid	0.000	0.000	0.000	0.000	0.000	0.000
24	mg/g_solid	0.000	0.000	0.002	0.000	0.000	0.000
72	mg/g_solid	0.000	0.000	0.002	0.000	0.000	0.000

Al	Al	Al	Al	Al	Al	Al	Al
		Δx	Δx	Δx	Δx	Δx	Δx
Time in hours	Unit	LHS-1, 1:100	LHS-1, 1:500	LMS-1, 1:100	LMS-1, 1:500	LHS-1D, 1:100	LHS-1D, 1:500
0.0333	mg/g_solid	0.000	0.000	0.000	0.000	0.000	0.000
0.25	mg/g_solid	0.000	0.000	0.000	0.003	0.017	0.058
0.5	mg/g_solid	0.000	0.000	0.001	0.001	0.009	0.052
1	mg/g_solid	0.000	0.000	0.002	0.003	0.008	0.038
12	mg/g_solid	0.000	0.000	0.004	0.023	0.019	0.029
24	mg/g_solid	0.001	0.000	0.002	0.016	0.035	0.019
72	mg/g_solid	0.001	0.004	0.009	0.010	0.041	0.048

Fe	Fe	Fe	Fe	Fe	Fe	Fe	Fe
		Δx	Δx	Δx	Δx	Δx	Δx
Time in hours	Unit	LHS-1, 1:100	LHS-1, 1:500	LMS-1, 1:100	LMS-1, 1:500	LHS-1D, 1:100	LHS-1D, 1:500
0.0333	mg/g_solid	0.000	0.000	0.000	0.010	0.000	0.000
0.25	mg/g_solid	0.000	0.000	0.000	0.010	0.046	0.049
0.5	mg/g_solid	0.000	0.000	0.000	0.010	0.035	0.007
1	mg/g_solid	0.000	0.000	0.000	0.010	0.002	0.099
12	mg/g_solid	0.000	0.000	0.000	0.010	0.002	0.006
24	mg/g_solid	0.000	0.000	0.000	0.010	0.008	0.004
72	mg/g_solid	0.000	0.000	0.000	0.010	0.008	0.003
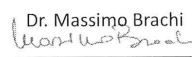
S	S	S	S	S	S	S	S
		Δx	Δx	Δx	Δx	Δx	Δx
Time in hours	Unit	LHS-1, 1:100	LHS-1, 1:500	LMS-1, 1:100	LMS-1, 1:500	LHS-1D, 1:100	LHS-1D, 1:500
0.0333	mg/g_solid	0.000	0.000	0.000	0.000	0.000	0.000
0.25	mg/g_solid	0.000	0.000	0.000	0.000	0.000	0.003
0.5	mg/g_solid	0.000	0.000	0.000	0.000	0.000	0.000
1	mg/g_solid	0.000	0.000	0.001	0.000	0.000	0.012
12	mg/g_solid	0.000	0.000	0.000	0.000	0.000	0.000
24	mg/g_solid	0.000	0.000	0.000	0.000	0.000	0.000
72	mg/g_solid	0.000	0.000	0.001	0.000	0.000	0.000

Appendix D.1: Data Sheet of pH Meter

• *Datasheet*

EN		Series 7 Vio
pH		**pH 7 Vio - PC 7 Vio**
Measuring range		0 … 14
Resolution / Accuracy		0.1, 0.01 / $\pm$0.02
Recognized calibration points and buffers		**AUTO:** 1…3 / USA, NIST **CUS:** 2 user values
Buffers indication		Yes
Calibration report		Yes
Automatic DHS recognition		Yes
Stability filter		Low – Med - High
mV		**pH 7 Vio - PC 7 Vio**
Range / Resolution		Range: -1000 … +1000 / Resolution: 1
ORP		**pH 7 Vio - PC 7 Vio**
Calibrations points		1 point / 475 mV
Conductivity		**COND 7 Vio - PC 7 Vio**
Range / Resolution		0,00 – 20,00 – 200,0 – 2000 µS / 2,00 – 20,00 – 200,0 mS Automatic scale
Recognized calibration points and buffers		1…4 / 84, 147, 1413 µS, 12.88, 111.8 mS, 1 user value
Reference temperature		15…30 °C
Temperature coefficient		0,00…10,00 %/°C
TDS		**COND 7 Vio - PC 7 Vio**
Measuring range / Temperature coefficient		0,1 mg/l / 200,0 g/l 0.40…1.00
Temperature		**pH 7 Vio - COND 7 Vio - PC 7 Vio**
Measuring range		0…100 °C
Resolution / Accuracy		0,1 / ± 0,5°C
Temperature compensation ATC (NTC30KΩ) and MTC		pH: 0…100 °C Cond: 0…100 °C
System		
Display		High definition colours LCD
Brightness and contrast management		Manual
Sleep mode		Yes
Auto-Off		Yes, after 20 minutes
IP protection		IP 57
Power supply		AA 1,5 V – 3 batteries
Sound level during standard operation		< 80 dB
Environmental operating conditions		0 … +60 °C
Maximum permissible humidity		< 95 % non-condensing
Maximum altitude of use		2000 m
System dimensions		185 x 85 x 45 mm
System weight		400 g

8

UM Serie 7Vio EN rev.1 19.05.2020

Appendix D.2: Calibration Certificate of pH Meter

Test Report
Rapporto di prova
Prüfnachweis
Rapport d'essai
Informe de la prueba

Instrument Strumento Gerät Instrument Instrumento	Serial number Numero di serie Serienmumer Numéro de série Número de serie	Test date Data del test Testdatum Date du test Fecha de la prueba
pH 7 Vio	*205032085*	*11/12/2020*

The measurement results reported in this report were obtained following the internal procedure PT-10.	I risultati delle misurazioni riportati in questo rapporto sono stati ottenuti applicando la procedura interna PT-10.	Die in diesem Bericht angegebenen Messergebnisse wurden nach dem internen Verfahren PT-10 erhalten.	Les résultats de mesure rapportés dans ce rapport ont été obtenus à la suite de la procédure interne PT-10.	Los resultados de la medición informados en este informe se obtuvieron siguiendo el procedimiento interno PT-10.

Hardware Test	Passed / Approvato / Bestanden / Réussi / Aprobado
Visual inspection	✓
Display	✓
Keypad	✓
DHS	✓

Legend:
✓ Yes / Si / Ja / Oui / Si
✗ No / No / Nein / Non / No

pH/ORP Input - Ingresso Ph ORP pH/ORP Eingang - Entrée pH/ORP– Entrada pH/ORP		
pH/ORP input *	Tolerance / Tolleranza / Toleranz / Tolérance / Tolerancia	Passed / Approvato / Bestanden / Réussi / Aprobado
-900 mV	-900 $\pm$ 1 mV	✓
0 mV	0 $\pm$ 1 mV	✓
+900 mV	+900 $\pm$ 1 mV	✓

Temperature Input - Ingresso temperatura - Temperatur Eingang - Entrée température - Entrada de temperatura		
Temp. input/ATC *	Tolerance / Tolleranza / Toleranz / Tolérance / Tolerancia	Passed / Approvato / Bestanden / Réussi / Aprobado
0 °C	0 $\pm$ 0.5 °C	✓
50 °C	50 $\pm$ 0.5 °C	✓

* Nominal value / valore nominale / nennwert / valeur nominale / valor nominal

The performed tests certify the proper functioning of the instrument and its compliance to the specifications.	I test eseguiti certificano il corretto funzionamento dell'apparecchiatura in oggetto e la sua conformità alle caratteristiche costruttive.	Die durchgeführten Tests bestätigen die ordnungsgemäße Funktion des Instruments und die Einhaltung der Spezifikationen.	Les tests effectués certifient le bon fonctionnement de l'instrument et sa conformité aux spécifications.	Las pruebas realizadas certifican el correcto funcionamiento del instrumento y su conformidad con las especificaciones.

Date of release Data di emissione Erscheinungsdatum- Date de sortie Fecha de lanzamiento	Test performed by Test realizzati da Test durchgeführt von Test réalisé par Prueba realizada por	Quality Manager Responsabile Qualità Quality Manager Responsable Qualité Gerente de Calidad	**XS Instruments®** Via della Meccanica n.25 41012 Carpi (MO) ITALY www.xsinstruments.com
11/12/2020	L'operatore	Dr. Massimo Brachi	

TR-01 test report Ph 7 rev.0 05.05.2020

Appendix D.3: Data Sheet of Oxygen Meter

11. Technical specifications

OXY 7

The Future Starts Now

Technical specifications	OXY 7 (polarographic sensor)	OXY 70 (optical sensor)
Dissolved Oxygen measuring range	0,00…19,99 mg/l-ppm / 20,0…	0,00…19,99 mg/l-ppm / 20,0…50,0 mg/l-ppm
Resolution	0,01 / 0,1	0,01 / 0,1
Accuracy (with sensor)	± 1,5% F.S.	± 0,2 up to 10 mg/l-ppm
		± 0,3 from 10 to 20 mg/l-ppm
		± 5% from 20 to 50 mg/l-ppm
Oxygen saturation measuring range	0,0…199,9 % / 200…400%	0,0…199,9 % / 200…400%
Resolution	0,1 / 1 %	0,1 / 1 %
Accuracy (with sensor)	± 10%	± 10%
Oxygen points of calibration	1 o 2 automatic	1 o 2 automatic
Barometric air pressure measuring range	0,0…1100 mbar	0,0…1100 mbar
Resolution	1 mbar	1 mbar
Accuracy	± 0,5%	± 0,5%
Automatic air pressure compensation	Yes	Yes
Temperature measuring range	0,0… 60,0 °C	0,0… 60,0 °C
Resolution	0,1 °C	0,1 °C
Accuracy	± 0,5 °C	± 0,5 °C
Automatic and manual temperature compensation	Yes	Yes (only automatic)
Salinity measuring range	0…50 ppt	0…50 ppt
Salinity compensation	Yes manual	Yes manual
GLP system	No	Yes
Display	LCD	LCD backlight
Data memory	No	Man / Auto 500 Data with date and time
Data logger function	No	Yes
Date and time	No	Yes
Memory data of calibration	No	Yes
CAL DUE (calibration timer)	No	Yes
IP protection class	Waterproof IP 57	Waterproof IP 57
Auto power off	Yes (after 20 min)	Yes (after 20 min)
Inputs	BNC / RCA (cinch)	DIN multipin
Communication interface	No	USB
Power supply	3 x 1,5V battery AA	3 x 1,5V battery AA
		AC/DC power with USB cable
Battery life	From 300 to 500 hours	From 300 to 500 hours
Dimensions / weight only meter	86 × 196 × 33 mm / 295 g	86 × 196 × 33 mm / 300 g
Dimensions / weight with carrying case	385 x 300 x 115 mm / 1720 g	385 x 300 x 115 mm / 1725 g

Specifications subject to change without notice

12

127

Appendix D.4: Calibration Certificate of Oxygen Meter

Calibration certificate

Instrument	Serial number	Production date
Portable meter OXY7	191231021	03/04/2019

Herewith we certify that the above mentioned instrument has been tested and comply to the technical specifications below:

Hardware test:

Verification	Result
Visual inspection	o.k.
Display	o.k.
Keypad	o.k.

Measurement test DO:

O_2 saturation	Result
0 %	o.k.
100 %	o.k.

Measurement test temperature / ATC:

Temp. input / ATC	Tolerance	Result
0 °C	0 ± 0.5 °C	o.k.
50 °C	50 ± 0.5 °C	o.k.

Date: 03/04/2019

Signature:

Calibration certificate v2.1_12/2017

Appendix D.5: Data Sheet of Turbidity Meter

Lovibond® Water Testing

Tintometer® Group

TB 211 IR

mit USB-Schnittstelle

- USB-Schnittstelle
- Messbereich von 0,01 - 1100 NTU
- Messungen gemäß EN ISO 7027
- Messungen mittels Infrarot im Winkel von 90 °

Bestell-Nr.: 266030

Das kompakte Lovibond® Infrarot-Trübungsmessgerät TB 211 IR für die schnelle und exakte Vor-Ort-Analyse. Gemessen wird, wie in der EN ISO 7027 vorgesehen, das Streulicht im Winkel von 90 °.
Der weite Messbereich von 0,01 bis 1100 TE/F = NTU = FNU bei einer Nachweisgrenze von 0,01 NTU ermöglicht den Einsatz des Gerätes
in verschiedenen Bereichen, von Trinkwasser bis hin zu Abwasser.
Da die Messungen mittels Infrarotlicht erfolgen, können sowohl gefärbte als auch farblose Wasserproben vermessen werden.
Eine direkte Übertragung der Messergebnisse an einen PC ist durch die USB-Schnittstelle beim TB 211 IR einfach einzurichten. Das notwendige USB-Kabel ist bereits Teil des Lieferumfangs.

Industrie

Chemische Industrie | Industrien sonstige | Kommunen | NGO | Ölindustrie | Schifffahrt | Schwimmbad öffentlich | Schwimmbadservice

Applikation

Abwasserbehandlung | Beckenwasserkontrolle | Schwimmbadwasseraufbereitung | Trinkwasseraufbereitung

TB 211 IR

Ein kompaktes Messgerät für die zuverlässige und einfache Bestimmung der Trübung. Eine USB Schnittstelle für die Datenübertragung und ein Ringspeicher mit 125 Speicherplätzen erleichtern die Messdatenverwaltung.

Messbereich

Test Name	Messbereich
Trübung	0,01 - 1100 NTU

Technische Daten

Optik	Temperaturkompensierte LED (860 nm) und Photosensorenverstärker in geschützter Messschachtanordnung.
Messprinzip	Nephelometrisch (90° Streulicht)
Messbereich	0,01-1100 NTU (Autorange)
Genauigkeit	± 2,5 % des Messwertes, oder ± 0,01 NTU, je nachdem was größer ist, im Bereich von 0,01 - 500 NTU ; ± 5 % des Messwertes im Bereich von 500 - 1000 NTU
Display	Hintergrund beleuchtetes LCD
Schnittstellen	Micro-USB
Bedienung	Bedingt säure- und lösungsmittelbeständige Polycarbonatfolie
Auto – OFF	Ja
Justierung	Softwaregestütze Anwenderjustierung und Verwendung von T-CAL-Standards
interner Speicher	interner Ringspeicher für 125 Datensätze
Stromversorgung	9 V-Block
Uhr	Echtzeituhr und Datum
Tragbarkeit	Tragbar
Umgebungsbedingungen	5 - 40 °C bei einer rel. Luftfeuchtigkeit 30 - 90 % (nicht kondensierend)
Konformität	CE
Abmessungen	110 x 55 x 190 mm
Gewicht mit Verpackung	(Basisgerät)

Lieferumfang

- Gerät im Kunststoffkoffer
- 4 Trübungsstandards (< 0,1, 20, 200 und 800 NTU)
- 9 V Blockbatterie
- 2 Küvetten (ø 24 mm) mit Deckeln
- USB-Kabel 1,5 m
- Gewährleistungserklärung
- Certificate of Compliance
- Bedienungsanleitung

Zubehör

Titel	Bestell-Nr.
Satz Trübungsstandards T-CAL (<0,1, 20, 200, 800 NTU)	194150
Block-Batterie 9 V	1950012
Reinigungstuch	197635
Messküvetten mit schwarzem Deckel, Höhe 55 mm, ø 24 mm, 12er Set	197655
Messschacht-Deckel	19801119
USB-Kabel 3m	19802509
T-CAL®-Standard, 4000 NTU, 125 ml	48012912
T-CAL®-Standard, 4000 NTU, 500 ml	48012950
Werkskalibrierzertifikat ISO 9001 für TB210 IR/TB 211 IR/ TB300 IR	999765

Appendix D.6: Data Sheet of Precision Balance PCB 350-3

KERN	PCB 200-2	PCB 250-3	PCB 350-3	PCB 400-2	PCB 400-1
Ablesbarkeit (d)	0,01 g	0,001 g	0,001 g	0,01 g	0,1 g
Wägebereich (Max)	200 g	250 g	350 g	400 g	400 g
Tarierbereich (subtraktiv)	200 g	250 g	350 g	400 g	400 g
Reproduzierbarkeit	0,01 g	0,001 g	0,001 g	0,01 g	0,1 g
Linearität	± 0,02 g	±0,003 g	±0,003 g	±0,03 g	±0,2 g
Mindeststückgewicht bei Stückzählung	0,02 g	0,002 g	0,002 g	0,02 g	0,2 g
Anwärmzeit	30 Min.	2 Std.	2 Std.	2 Std.	10 Min.
Referenzstückzahlen bei Stückzählung	5, 10, 20, 25, 50				
Wägeeinheiten	Details **„Wägeeinheiten"** siehe Kap. 9.3				
Empf. Justiergewicht, nicht bei-gegeben (Klasse) Details zur **„Auswahl des Jus-tiergewichtes"** s. Kap. 9.3	200g (M1)	200g (F1)	300g (F1)	400g (F2)	400g (M 2)
Einschwingzeit (typisch)	3 sec.				
Betriebstemperatur	+ 5° C .... + 35° C				
Luftfeuchtigkeit	max. 80 % (nicht kondensierend)				
Gehäuse (B x T x H) mm	163 x 245 x 79 ohne Windschutz 163 x 245 x 123 mit Windschutz				
Windschutz mm	-	Ø 90, Höhe 53	Ø 90, Höhe 53	-	-
Wägeplatte mm	Ø 105	Ø 81	Ø 81	Ø 105	130 x 130
Gewicht kg (netto)	1,1				1,4
Stromversorgung	220V-240V AC, 50 Hz / 9 V, 300 mA				
Batteriebetrieb	9 V-Blockbatterie (optional)				
Akku (optional)	Betriebsdauer mit Anzeigenhinterleuchtung 24 h Betriebsdauer ohne Anzeigenhinterleuchtung 48 h Ladezeit 8 h				
Schnittstelle	RS 232				
Unterflurwägeeinrichtung	serienmäßig				

Deutsch

5   PCB-BA-d-0914

131

Appendix D.7: Date Sheet of Optisens Cond 7200

2.1 Technische Daten

Messsystem

Messprinzip	Konduktive Leitfähigkeit
Messbereich	0,05...10 µS/cm (c=0,01) 0,001...1 mS/cm (c=0,1)

Werkstoffe

Aufbau	Gehäuse: Edelstahl 1.4435 (ähnlich wie 316 L, pharmazeutische Ausführung) Zelle: Edelstahl 1.4435 (ähnlich wie 316 L, pharmazeutische Ausführung)
Sensoroptionen	Mit integriertem Pt100 Temperaturfühler
Prozessanschluss	Clamp DN 25

Messgenauigkeit

Genauigkeit der Leitfähigkeit:	+/-10% vom Nennwert ①

Einsatzbedingungen

Temperaturbereich	0...+135°C / +32...+275°F
Max. Betriebsdruck	16 bar bei +25°C, 9 bar bei +60°C / 232 psi bei +77°F, 130,5 psi bei +140°F

① Je nach Produktionsbedingungen kann die Zellkonstante vom Nennwert abweichen. Diese Abweichung kann im Messumformer kompensiert werden.

Elektrischer Anschluss

Kabel	Kabel COND-W 7200	Kabel COND-W 1200
Sensor-Kabelanschluss	M12 Stecker	4-poliger Stecker (Hirschmann)
Kabellänge	10 m / 33 ft	5 m / 16,5 ft, 10 m / 33 ft, 15 m / 49,5 ft, 20 m / 66 ft
Kabeloptionen	Aderendhülsen	

2 TECHNISCHE DATEN   OPTISENS COND 7200

2.2 Abmessungen
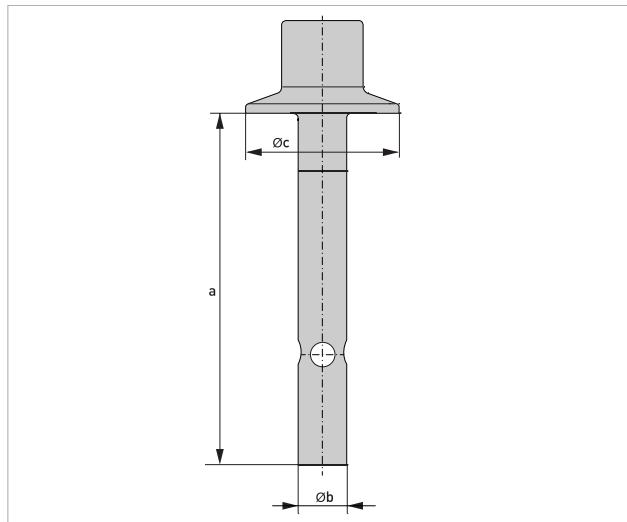
Abbildung 2-1: OPTISENS COND 7200

	Abmessungen [mm]	Abmessungen [Zoll]
a	115	4,53
b	Ø 16	Ø 0,63
c	Ø 50,5	Ø 1,99
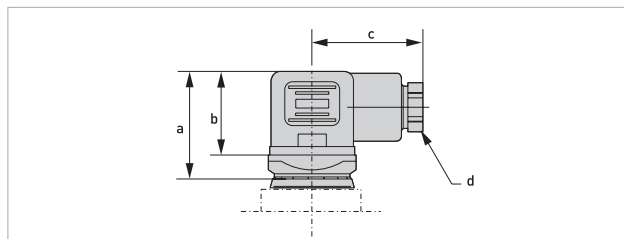
Abbildung 2-2: Winkelstecker (Hirschmann)

	Abmessungen [mm]	Abmessungen [Zoll]
a	34	1,34
b	27	1,06
c	35	1,38
d	Pg 9	

Appendix D.8: Data Sheet of Optisens pH 8100

134

② TECHNISCHE DATEN

OPTISENS PH 8100

Einsatzbedingungen

Temperaturbereich	0…+130°C / +32…+266°F
Max. Betriebsdruck	10 bar / 145 psi (absolut)
Mindestleitfähigkeit	> 2 µS/cm

Einbaubedingungen

Prozessanschluss	PG 13,5
Eintauchhalterung	SENSOFIT IMM 1000
Durchflusshalterung	SENSOFIT FLOW 1000
Einbau-Einschraubadapter	SENSOFIT INS 1000
Wechselarmatur	SENSOFIT RET 1000/2000 (in Vorbereitung)

Werkstoffe

Sensorschaft	Glas
Messelektrode	H-Glas
Innenpuffer	pH 7,0
Bezugselektrolyt	Polisolve Plus
Diaphragma	2 x offen
Dichtung	EPDM

Elektrischer Anschluss

Stecker	VP 8,0
Kabel	Kabel pH/ORP-W VP 8.0
Kabellänge	5 m / 16,4 ft oder 10 m / 32,8 ft

Bitte wenden Sie sich für weitergehende Informationen an Ihr regionales Vertriebsbüro.

134
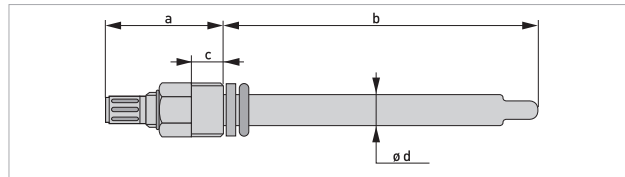
2.2 Dimensions

Abbildung 2-1: Abmessungen des OPTISENS PH 8100

	Dimensions [mm]	Dimensions [inch]
a	52	2.0
b	120	4.7
c	12	0.5
d	Ø 12	Ø 0.5
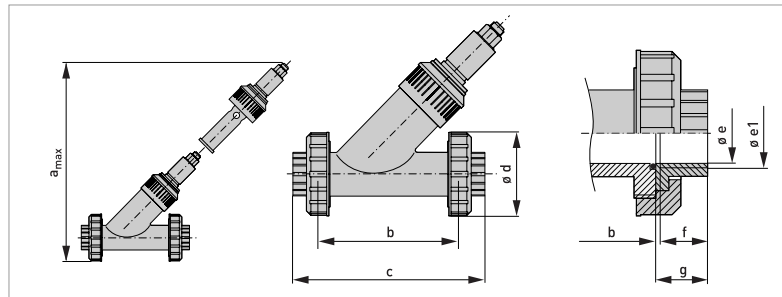
Abbildung 2-2: Abmessungen SENSOFIT FLOW 1000

	Abmessungen [mm]	Abmessungen [Zoll]
a_{max}	165	6,5
b	142,5	5,61
c	178,5	7,03
d	Ø 75	Ø 2,95
e	Ø 21	Ø 0,83
e1	G1	G1
f	19,1	0,75
g	22	0,87

135

Appendix D.9: Data Sheet of OLS7

Sensata
Technologies

| OLS7 SERIES
OPTICAL LIQUID LEVEL SENSOR 1/4"NPT MOUNT

The OLS7 series is a liquid level sensor for single point liquid level detection.

The sensor has an infra-red emitter and detector aligned within an accurately shaped cone to give good optical coupling when the sensor is in air. This coupling is greatly reduced, when the sensor is immersed in liquid, as the infra-red light escapes through the liquid rather than being reflected back to the detector.

The sensor has a transistor output, so can be configured by the user for particular applications.

Features

- Low cost sensors for general liquid sensing
- High reliability optical sensing
- External mount via 1/4"NPT thread
- Standard temperature range -25ºC to +80ºC
  Extended temperature range -40ºC to +125ºC
- High and Low output versions
- Resistant to false triggering caused by foaming

SPECIFICATIONS

Technical

Mounting Style	External
Mounting Thread	1/4" NPT
Body Material	Polysulfone UDEL 1700
Temperature Range	-25 to +80ºC/-40º to +125ºC
Maximum Pressure	7bar
Tightening Torque for Fixing	1.5Nm/13.26lbs in
Cable Length - Standard	25cm
Wire Size	24AWG
Cable Conductor Material	Tinned copper
Wire Sheath Material	PTFE
Wire Temperature Rating	125ºC
Sealing Gasket	Not supplied

Electrical

Supply Voltage (Vs)	**Vdc**	4.5 to 15.4 or 10 to 28
Supply Current Max (Is)	**mA**	2.5 (Vs = 15.4Vdc)
Output Type		Voltage High or Low
Output Voltage (Vout) @ Iout =100mA		Output High Vout = Vs-1V max Output Low Vout = 0.5Vmax
Output Sink & Source Current Iout		100mA max or 1A
Sensor Connections		Red= supply + ve, Blue= common(0V), Green= Output (see wiring diagrams overleaf)

Page 1

cynergy³

STANDARD PARTS

	Mount	Temp Range °C	Supply Volts V	Output	
OLS700D3SH	1/4"NPT	-25 to +80	5 to 15dc	High in air	Volts
OLS700D3LSH	1/4"NPT	-25 to +80	5 to 15dc	Low in air	Volts
OLS710D3SH	1/4"NPT	-40 to +125	5 to 15dc	High in air	Volts
OLS710D3LSH	1/4"NPT	-40 to +125	5 to 15dc	Low in air	Volts
OLS710D324-003	1/4"NPT	-40 to +125	10 to 28dc	High in air	Open drain
OLS710D3L24-003	1/4"NPT	-40 to +125	10 to 28dc	Low in air	Open drain

Custom versions can be made for particular applications. Please contact Sensata with your requirements.

DIMENSIONS

All dimensions are in millimeters.

1/4"NPT Thread
Ø 10.40
9.40
23.40

19 AF

1/4"NPT Thread
Ø 10.40
003 Open Drain version
9.40
18   15

INSTALLATION
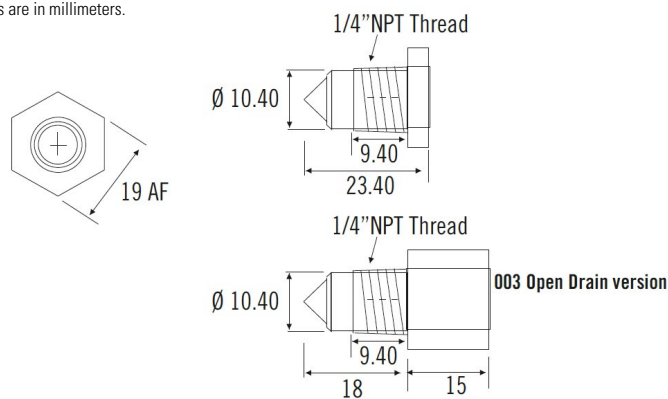
Installation in 1/4"NPT socket

The sensor can be mounted in either the side or the bottom of a tank. It must not be mounted in the top of a tank with the cone downwards.

This sensor requires a 1/4"NPT thread connection.

The sensor should be screwed into a 1/4"NPT socket and should not be overtightened.

1/4"NPT socket

Red wire =+Vs
Green wire =Output
Blue wire = 0V

Page 2

www.sensata.com

cynergy3
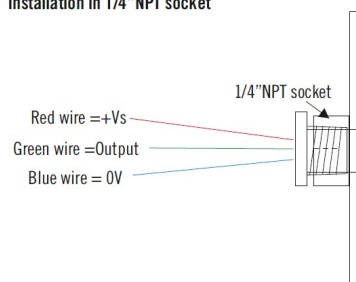
Appendix E.1: Data Sheet of Vacuum Controller

IKA

designed for scientists

VC 10 lite
/// Datenblatt

Drehzahlgeregelter, universeller Vakuumcontroller für das kontrollierte Evakuieren von Luft (Gas) aus Laborgeräten, sowie für klassische Trenn-, Filtrations- oder Trocknungsaufgaben im Labor. Der Controller ist für zahlreiche Anwendungen einsatzbereit und lässt sich einfach installieren.

Der VC 10 lite ist nur mit der Vakuumpumpe VACSTAR digital kompatibel. Eine Kabelverbindung zwischen Pumpe und Controller ist erforderlich.
Manueller und programmierbarer Modus verfügbar.

Features:
- Ventilreinigungsfunktion für lange Standzeiten
- Hohe Energieeffizienz dank Gerät-zu-Gerät Kommunikation: Steuerung des Umwälzkühlers durch Verbindung des

IKAworldwide   IKAworldwide /// #lookattheblue   @IKAworldwide

www.ika.com

Technische Änderungen vorbehalten

IKA

designed for scientists

Vakuumcontrollers mit PC 1.3 Datenkabel (als Zubehör erhältlich)

- Integriertes Belüftungsventil für einfachen Druckausgleich und Belüftung mit Inertgas nach Prozessende
- VENT-Kurztaste ermöglicht Druckausgleich während eines laufenden Prozesses
- Programmfunktion: Es können bis zu zehn benutzerdefinierte Programme mit bis zu zehn Druck-/Zeitsequenzen gespeichert werden
- USB / RS232 Schnittstellen zur Verbindung mit der Laborsoftware labworldsoft®
- Elektronisches Steuerungssystem für verbesserte Prozesseffizienz und höhere Lösemittelrückgewinnungsrate
- Hohe Energieeffizienz durch Gerät-zu-Gerät Kommunikation (Vakuum-Controller zu Umlaufkühler)

Für zusätzliche Sicherheit für Anwender und Umwelt empfiehlt sich der Einsatz des
Vakuum-Sicherheits-Emissionskondensators VSE 1, der verhindert, dass Lösungsmittel in die Raumluft abgegeben werden. Der VSE 1 ist als Zubehör erhältlich.

IKAworldwide   IKAworldwide /// #lookattheblue   @IKAworldwide

www.ika.com
Technische Änderungen vorbehalten

IKA

designed for scientists

Technische Daten

Anschlussdurchmesser Saugseite [mm]	8
Anschlussdurchmesser Druckseite [mm]	8
Anschlussdurchmesser Belüftung [mm]	8
Eingangsdruck [mbar]	1 - 1050
Analog-Drehzahl-Vakuum-Regelung	ja
Anzeige	TFT
Druckeinheit	mbar, hPa, mmHg, Torr
Vakuumsensor	ja
Vakuumsensortyp	Keramik Al2O3
Druck max. am Drucksensor [bar]	1.6
Messbereich (absolut) [mbar]	1 - 1100
Regelbereich [mbar]	1 - 1100
Auflösung [mbar]	1
Messunsicherheit [mbar]	1
Mediumstemperatur (Gas) [°C]	5 - 40
Belüftungsventil	ja
Messbereich Temperatur max. [°C]	200
Auflösung Temperaturmessung [K]	1
Messgenauigkeit Temperatur [K]	±1
Zeitschaltuhr	ja
Zeiteinstellung min. [s]	1
Zeiteinstellung max. [min]	6000
Schnittstelle Vakuum Drehzahlregelung	VACSTAR
Produktberührendes Material	Al2O3, PTFE, FPM, PPS
Gehäusewerkstoff	PBT
Befestigung	Stativ / Klemme
Befestigungsdurchmesser [mm]	16
Modus Manuell	ja
Modus Programm	ja
Graph Funktion	ja
Kühleransteuerung	ja
Vakuum leckage Test	ja
Abmessungen (B x H x T) [mm]	95 x 150 x 110
Gewicht [kg]	1.284
Zulässiger Umgebungstemperaturbereich [°C]	5 - 40
Zulässige Relative Feuchte [%]	80
Schutzart nach DIN EN 60529	IP 20
RS 232 Schnittstelle	ja
USB Schnittstelle	ja
Spannung [V]	100 - 240
Frequenz [Hz]	50/60
Geräteaufnahmeleistung [W]	24
Geräteaufnahmeleistung Standby [W]	2
Gleichspannung [V=]	24
Stromaufnahme [mA]	1000

IKAworldwide   IKAworldwide /// #lookattheblue   @IKAworldwide

www.ika.com
Technische Änderungen vorbehalten

Appendix E.2: Data Sheet of Vacuum Pump

VACSTAR digital
/// Datenblatt

Die 4-Kammer Membran Vakuumpumpe überzeugt durch eine hohe Saugleistung, geringen Platzbedarf und hohe Servicefreundlichkeit. Die Parametereinstellung erfolgt mittels Dreh-Drückknopf über ein digitales Drehzahl Display. Automatische Prozesse können mit dem als Zubehör erhältlichen Vakuumcontroller VC 10 gesteuert werden. Ein für die Verbindung erforderliches Analogkabel ist im Lieferumfang der Vakuumpumpe enthalten. Zusätzlich empfohlen ist die Verwendung des VSE 1 Vakuum Sicherheitsemmissionskondensators, der verhindert, dass Lösungsmittel an die Raumluft abgegeben wird.

Die Vacstar digital wird für trockene und ölfreie Anwendungen im Laboralltag eingesetzt. Ihre Membranen sind besonders chemieresistent.

IKAworldwide   IKAworldwide /// #lookattheblue   @IKAworldwide

www.ika.com
Technische Änderungen vorbehalten

IKA

designed for scientists

Technische Daten

Förderleistung max. (50/60Hz) [m³/h]	1.32
Förderleistung max. (50/60Hz) [l/min]	22
Enddruck ohne Gasballast [mbar]	2
Saugstufen	4
Zylinder	4
Anschlussdurchmesser Saugseite [mm]	8
Anschlussdurchmesser Druckseite [mm]	8
Eingangsdruck [mbar]	2 - 1030
Zweipunktregelung	ja
Analog-Drehzahl-Vakuum-Regelung	ja
Einstellmöglichkeit Drehzahl	Drehknopf
Drehzahlbereich [rpm]	285 - 1200
Anzeige	LED
Lautstärke bei min. Druck [dB(A)]	54
Produktberührendes Material	Al2O3; PTFE; FFPM; PPS; NBR
Gehäusewerkstoff	Alu-Guss beschichtet / thermoplastischer Kunststoff
Abmessungen (B x H x T) [mm]	150 x 375 x 370
Gewicht [kg]	11.5
Zulässiger Umgebungstemperaturbereich [°C]	5 - 40
Zulässige Umgebungsbedingungen	80% (bis 31°C), linear abnehmend bis max. 50% (@40°C)
Schutzart nach DIN EN 60529	IP 20
RS 232 Schnittstelle	ja
USB Schnittstelle	ja
Spannung [V]	100 - 240
Frequenz [Hz]	50/60
Geräteaufnahmeleistung [W]	130
Geräteaufnahmeleistung Standby [W]	3

IKAworldwide   IKAworldwide /// #lookattheblue   @IKAworldwide

www.ika.com
Technische Änderungen vorbehalten

Appendix E.3: Data Sheet of Precision Pump

KNF

DOSIERPUMPE FÜR FLÜSSIGKEITEN

SIMDOS 10

▷ Intuitive Bedienung
▷ Einfache Kalibrierung
▷ Einstellbar auf die Flüssigkeitscharakteristik
▷ Selbstansaugend, trockenlaufsicher
▷ Analoge und Impulsansteuerung (RC)
▷ Strahlwassergeschützt IP65
▷ Kleine Baugrösse

Anwendungsgebiete

• Chemie
• Organische synthetische Chemie
• Pharmakologie
• Lösemittel für Haftmittel und Klebstoffe
• Polymere Beschichtungen
• Lebensmitteltechnologie
• Reinigungs- und Lösungsmittel

Leistungsbereich

Förderleistung	Dosiervolumen	Max. Saughöhe	Max. Druck
1 - 100 ml/min	1 - 999 ml	3 mWS	6 bar

Chemische Resistenz

Code	Pumpenkopf	Membrane	Ventile	Filter [1]
KT	PP	PTFE beschichtet	FFKM Kalrez®	PEEK
TT	PVDF	PTFE beschichtet	FFKM Kalrez®	PVDF
FT	PTFE	PTFE beschichtet	FFKM Kalrez® *	PEEK
ST	EDELSTAHL	PTFE beschichtet	FFKM Kalrez®	PEEK

*Auf Projektbasis FFKM Chemraz®
[1] Material von Gehäuse und Gewebe

Ausführungsversionen

S-Version	RC-Version		RC Plus-Version
• Manueller Betrieb	• Manueller Betrieb • Analoge Ansteuerung: 0-5 V, 0-10 V, 0-20 mA, 4-20 mA, von 1 bis 100% • Start/Stopp über Logik Eingang (TTL)	• Reset/Befüllen über Logik Eingang (TTL) • Ausgangssignal für Fehlermeldung • Kabel für externe Steuerung	• Entspricht der RC Version • Plus RS 232

Technische Daten

• Stromversorgung 100 - 240 V / 50 - 60 Hz
• Zulässige Umgebungstemperatur +5 bis +40° C
• Zulässige Flüssigkeitstemperatur +5 bis +80° C
• Maximal zulässige Viskosität 150 cSt
• Genauigkeit +/-2% (Nominalwert)
• Wiederholgenauigkeit +/-1%

• Leistungsaufnahme 24 W
• Schutzart IP65
• Abmessungen: 150 x 93 x 144 mm
• Gewicht: 0.9 kg
• Hydraulische Anschlüsse 4/6 mm

www.knf.com

ZUBEHÖR

Ventil-Kit

	ID-Nr.
Chemraz® Spezialventile für ausgesuchte Chemikalien	168037

⚠ Special Valves CHEMRAZ®

Membran-Druckhalteventil für Speicherbehälterposition über der Pumpe

	ID-Nr.
Komplettsatz KT	166283
Komplettsatz TT	166284
Komplettsatz FT	166285

Filter

Typ	Material[1]	Anschluss	ID-Nr.
FS 25 T	PVDF	Für Schlauch ID 3.2 und 4 mm	165211
FS 25 X	PEEK	Für Schlauch ID 3.2 und 4 mm	165213

[1] Material von Gehäuse und Gewebe

Pulsationsdämpfer kann nur bei kontinuierlichem Fördern angewendet werden, von 30 bis 100 ml/min

	ID-Nr.
FPD KT	167817
FPD TT	167818
FPD FT	167819

Befestigungsplatte

	ID-Nr.
zur Wandmontage	160473

Stativhalterung

	ID-Nr.
	160474

Fussschalter

	ID-Nr.
für Einzelstart und -stopp	155872

www.knf.com

KNF Flodos AG, Technische Änderungen vorbehalten DB_SIMDOS10_DE_02_168047

KNF

Appendix E.4: Data Sheet of Heating Bath

IKA

designed for scientists

HBR 4 control

/// Datenblatt

Das Heizbad zeichnet sich aus durch:
- Zylindrische Badform
- In den Badboden integrierte Heizelemente
- Wahlweise niederviskoses Öl (50 mPas) oder Wasser als Wärmeträger
- Nutzvolumen: ca. 4 l
- Heizleistung: 1000 W
- Zwei Tragegriffe
- Stufenlos einstellbarer Sicherheitstemperaturbegrenzer nach DIN 12877
- Schutz vor Verbrennung durch Doppelmantel
- Digitalanzeige für Soll-, Ist- und Sicherheitstemperatur sowie Drehzahl
- Integrierter Magnetrührantrieb zum Umwälzen der Temperierflüssigkeit, dadurch bessere Wärmeverteilung im Bad

IKAworldwide   IKAworldwide /// #lookattheblue   @IKAworldwide

www.ika.com

Technische Änderungen vorbehalten

IKA

designed for scientists

- RS 232-Schnittstelle
- Heizbad kann mit einem externen Temperaturfühler zur Temperierung direkt im Medium betrieben werden

IKAworldwide   IKAworldwide /// #lookattheblue   @IKAworldwide

www.ika.com
Technische Änderungen vorbehalten

IKA

designed for scientists

Technische Daten

Heizleistung [W]	1000
Heiztemperaturbereich [°C]	Raumtemp. - 200
Einstellmöglichkeit Heiztemperatur	Stufenlos
Einstellgenauigkeit Solltemperatur [K]	±1
Reglerschwankung (3l Wasser / 90 °C) [K]	±1
Reglerschwankung (3l Siliconöl / 50mPas / 150°C) [K]	±2
Drehzahlanzeige	LCD
Einstellmöglichkeit Drehzahl	Stufenlos
Drehzahlbereich [rpm]	150 - 800
Motorleistung Aufnahme [W]	5
Motorleistung Abgabe [W]	1
Füllvolumen max. [l]	4
Füllhöhe min. [mm]	20
Produktberührendes Material	Edelstahl 1.4301
Anschluss für ext. Temperaturmessfühler	PT1000
Sicherheitskreis einstellbar [°C]	50 - 210
Klassenbezeichnung nach DIN 12876	II
Außendurchmesser [mm]	250
Innendurchmesser [mm]	200
Außenhöhe [mm]	250
Innenhöhe [mm]	160
Abmessungen (B x H x T) [mm]	340 x 250 x 340
Gewicht [kg]	5.6
Zulässige Umgebungstemperatur max. [°C]	40
Zulässige Relative Feuchte [%]	80
Schutzart nach DIN EN 60529	IP 20
RS 232 Schnittstelle	ja
Spannung [V]	230
Frequenz [Hz]	50/60
Geräteaufnahmeleistung [W]	1020

IKAworldwide   IKAworldwide /// #lookattheblue   @IKAworldwide

www.ika.com

Technische Änderungen vorbehalten

Appendix E.5: Data Sheet of Chiller

IKA

designed for scientists

RC 2 lite
/// Datenblatt

Kompakter Umwälzkühler mit starker 400 Watt Kälteleistung, konzipiert für einfache Kühlaufgaben bis -10 °C.

Der RC 2 lite ist das perfekte Peripheriegerät zur Kühlung von Rotationsverdampfern, Rückflusskühlern oder als Kühlquelle für Geräte, die mit Hilfe eines Wärmetauschers Wärme abführen (z.B. Doppelwandmahlbehälter, gekühlte Inkubatoren, Laborreaktoren, Kühlschlangen).

Der gut zugängliche und leicht zu reinigende Maschenfilter aus Edelstahl stellt eine gleichbleibend hohe Kühlleistung über Jahre hinweg sicher. Dank des geringen Füllvolumens von nur einem Liter können mit dem RC 2 lite besonders schnell niedrige Temperaturen erreicht werden. Das große Arbeitsvolumen von 2,5 Litern ermöglicht eine Vielzahl von externen Anwendungen ohne Nachfüllen von Flüssigkeit. Der Füllstand im Reservoir kann besonders übersichtlich über das große beleuchtete Schauglas im Blick behalten werden.

IKAworldwide   IKAworldwide /// #lookattheblue   @IKAworldwide

www.ika.com
Technische Änderungen vorbehalten

IKA

designed for scientists

Die kraftvolle Druck- und Saug-Pumpe ermöglicht den gleichzeitigen Betrieb von mehreren kleinen Applikationen sowie externen Anwendungen in offenen Bädern in Kombination mit einem Levelcontroller. Durch das natürliche Kältemittel R290 ist der RC 2 lite besonders umweltfreundlich und bestens vorbereitet auf die Zukunft.

IKAworldwide   IKAworldwide /// #lookattheblue   @IKAworldwide

www.ika.com
Technische Änderungen vorbehalten

IKA

designed for scientists

Technische Daten

Gerätetyp	Kälte-Umwälzthermostat
Klassenbezeichnung nach DIN 12876	I
Kennzeichnung nach DIN 12876	NFL
Kältemittel	R290
Kältemittelmenge [g]	70
Kältemittel Druck max. [bar]	21
Kälteleistung (@20°C) [W]	400
Kälteleistung (@10°C) [W]	350
Kälteleistung (@0°C) [W]	250
Kälteleistung (@-10°C) [W]	140
Arbeitstemperatur [°C]	-10 - Raumtemp.
Betriebstemperatur min. [°C]	-10
Betriebstemperatur max. (mit Fremdheizung) [°C]	70
Temperaturanzeige	ja
Temperaturregelung	PID
Arbeitstemperaturfühler	PT1000
Arbeitstemperaturanzeige	LED
Temperaturkonstanz DIN 12876 [K]	±0.5
Anzeigeauflösung [K]	0.1
Einstellgenauigkeit Solltemperatur [K]	±0.1
Füllvolumen [l]	1 - 3.5
Pumpentyp	Druck- / Saugpumpe
Pumpendruck max. (0 Liter Förderstrom) [bar]	0.35
Pumpendruck (Saugseite) max. (0 Liter Förderstrom) [bar]	0.15
Förderstrom max. (0 bar Gegendruck) [l/min]	18
Pumpenanschlüsse	M16x1
Zulässige Einschaltdauer [%]	100
Geräuschpegel [dB(A)]	51
Abmessungen (B x H x T) [mm]	225 x 385 x 430
Gewicht [kg]	24.5
Zulässiger Umgebungstemperaturbereich [°C]	5 - 32
Zulässige Relative Feuchte [%]	80
Schutzart nach DIN EN 60529	IP 21
RS 232 Schnittstelle	ja
USB Schnittstelle	ja
Spannung [V]	230
Frequenz [Hz]	50/60
Geräteaufnahmeleistung [W]	250

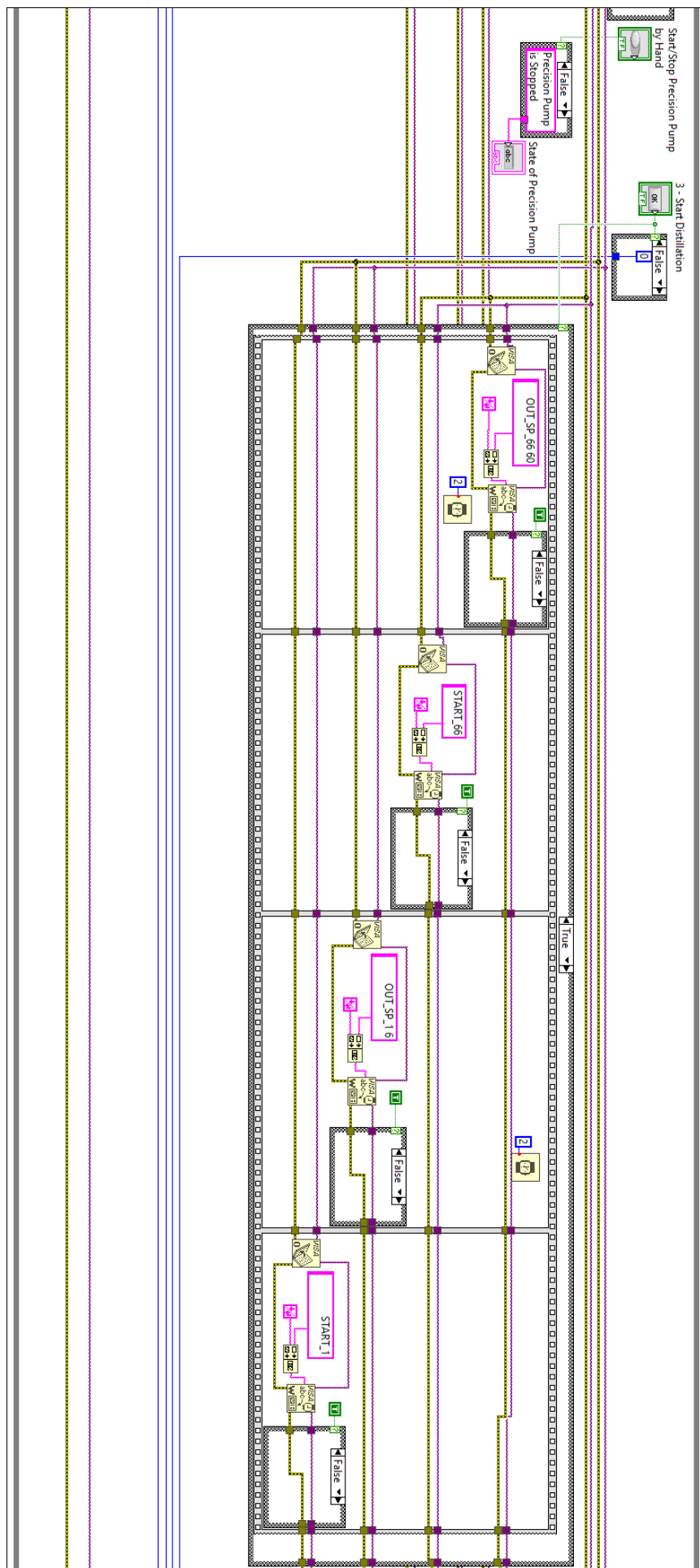IKAworldwide   IKAworldwide /// #lookattheblue   @IKAworldwide

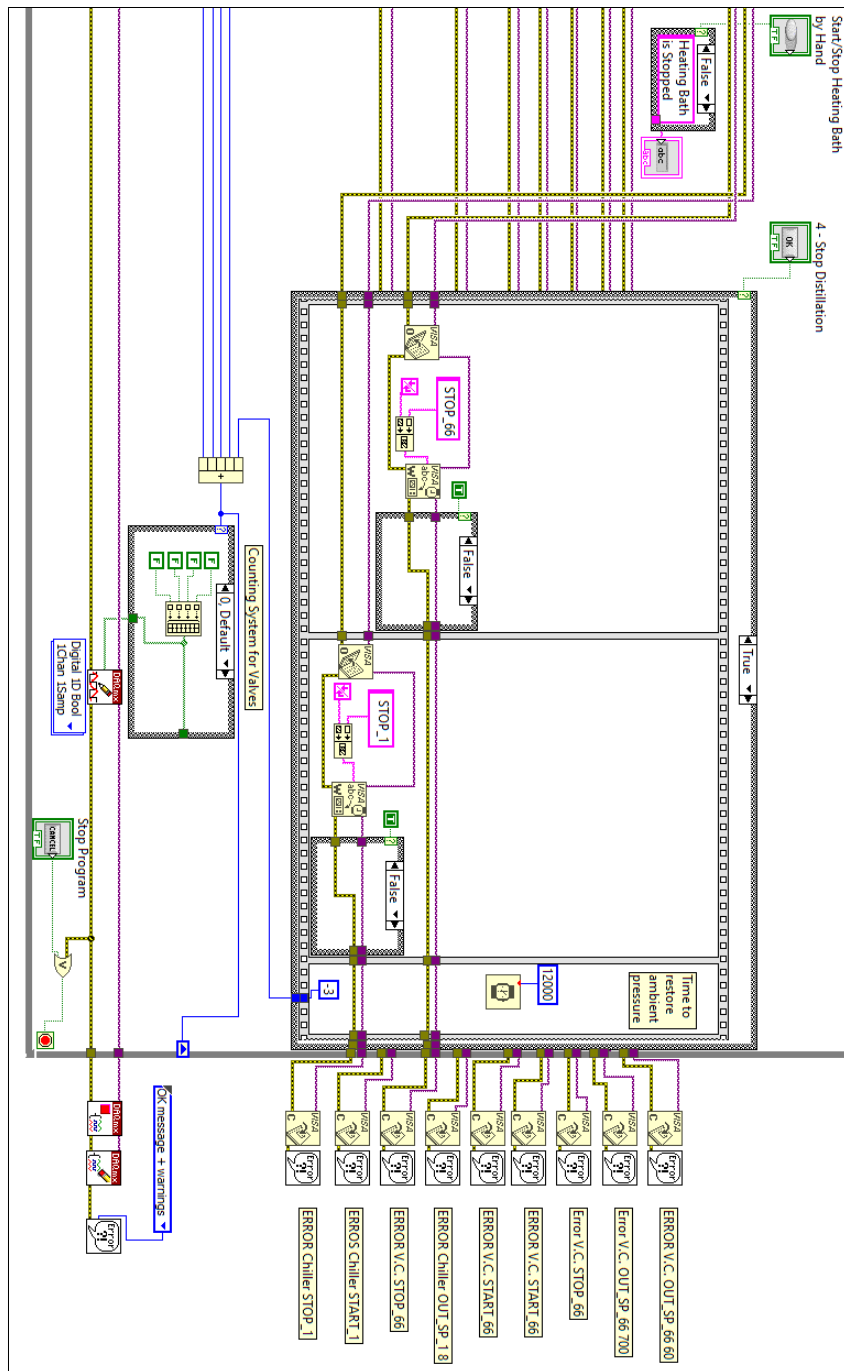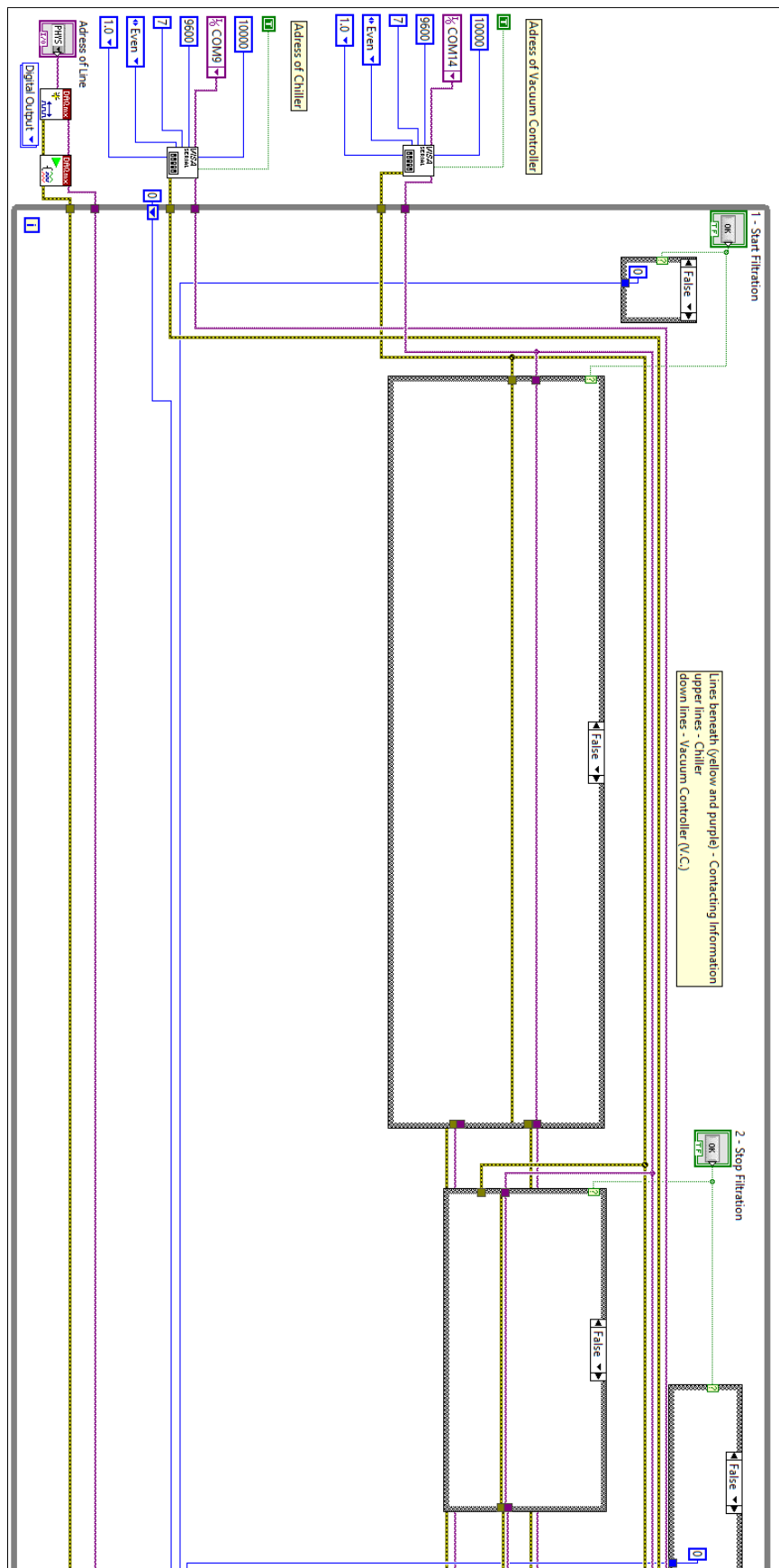**www.ika.com**
Technische Änderungen vorbehalten

Appendix F.1: Program with Inner "False" Cases
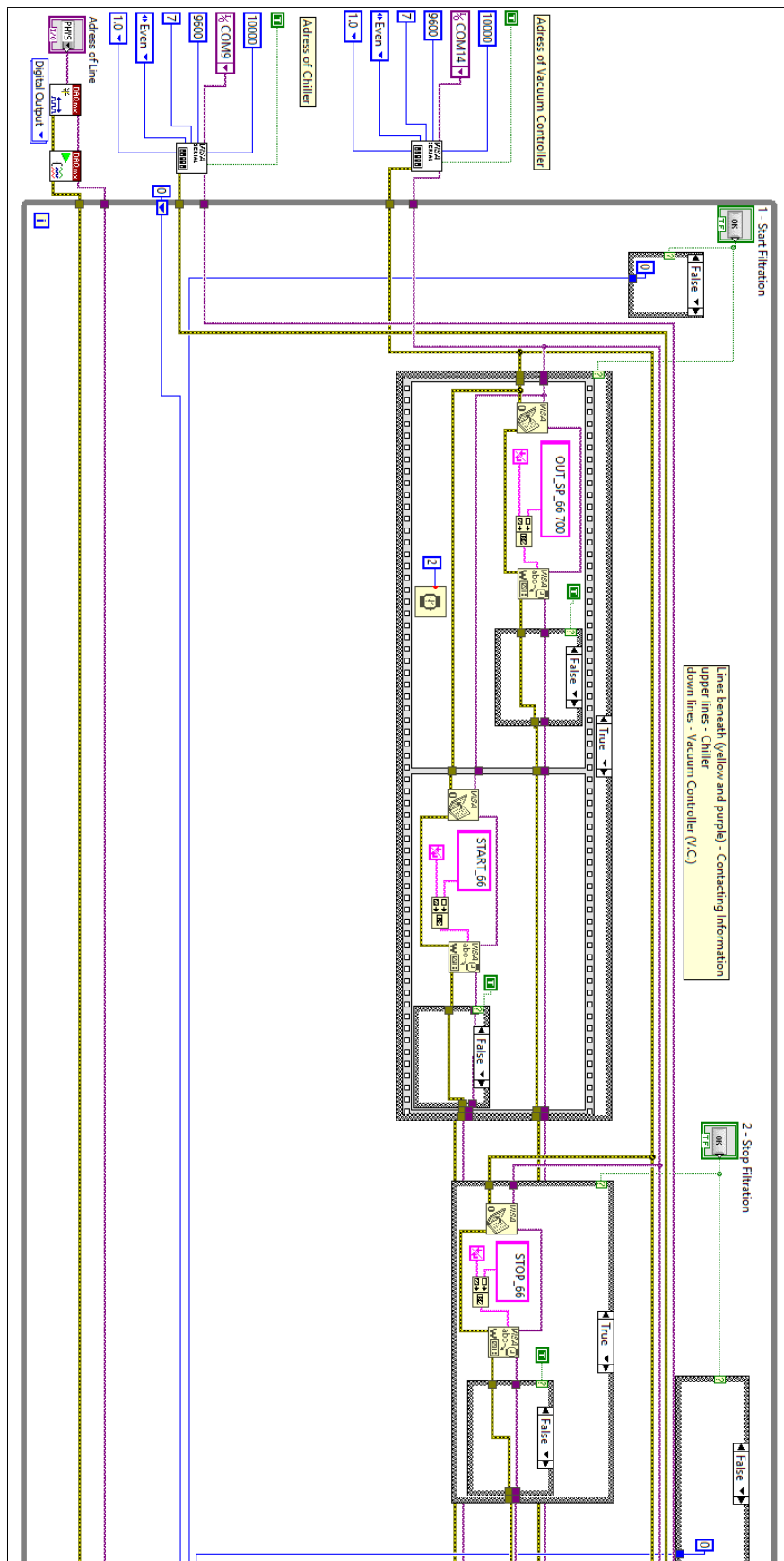
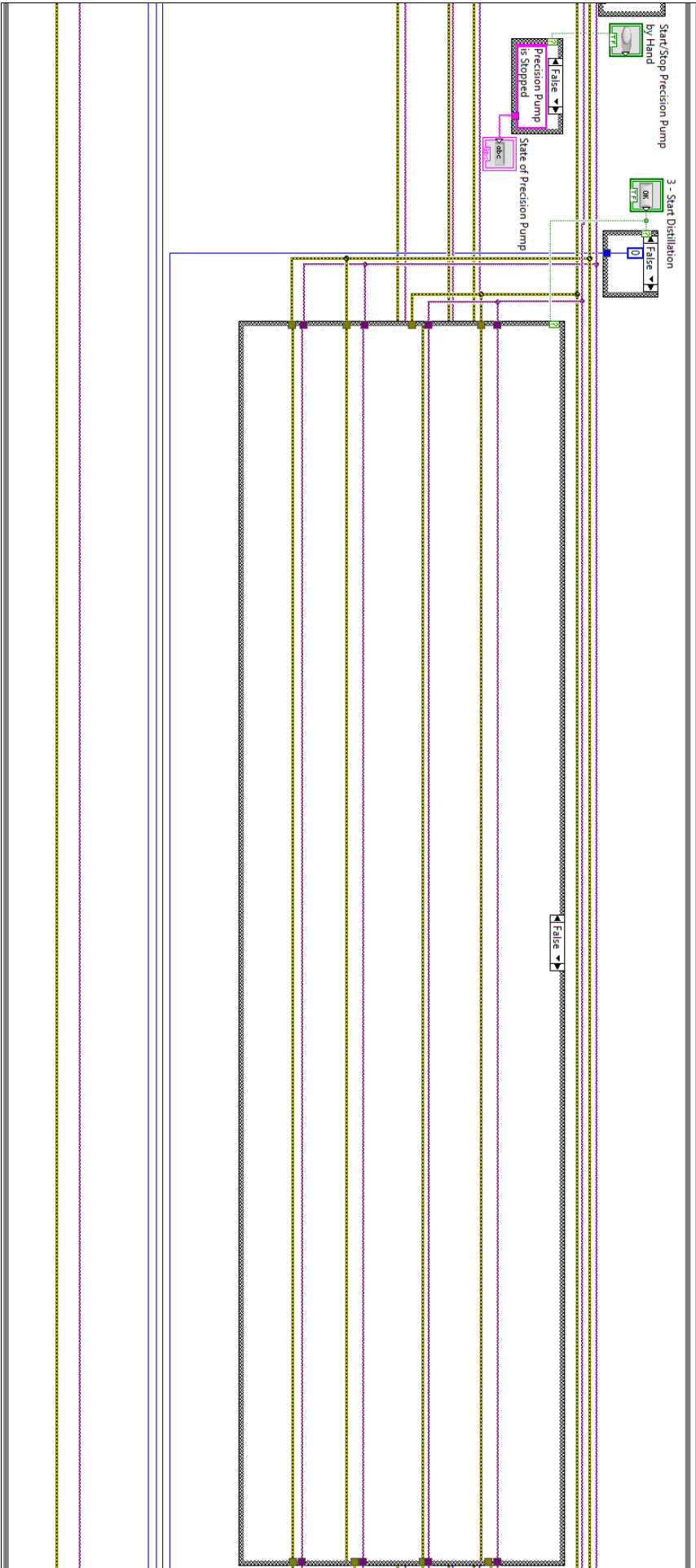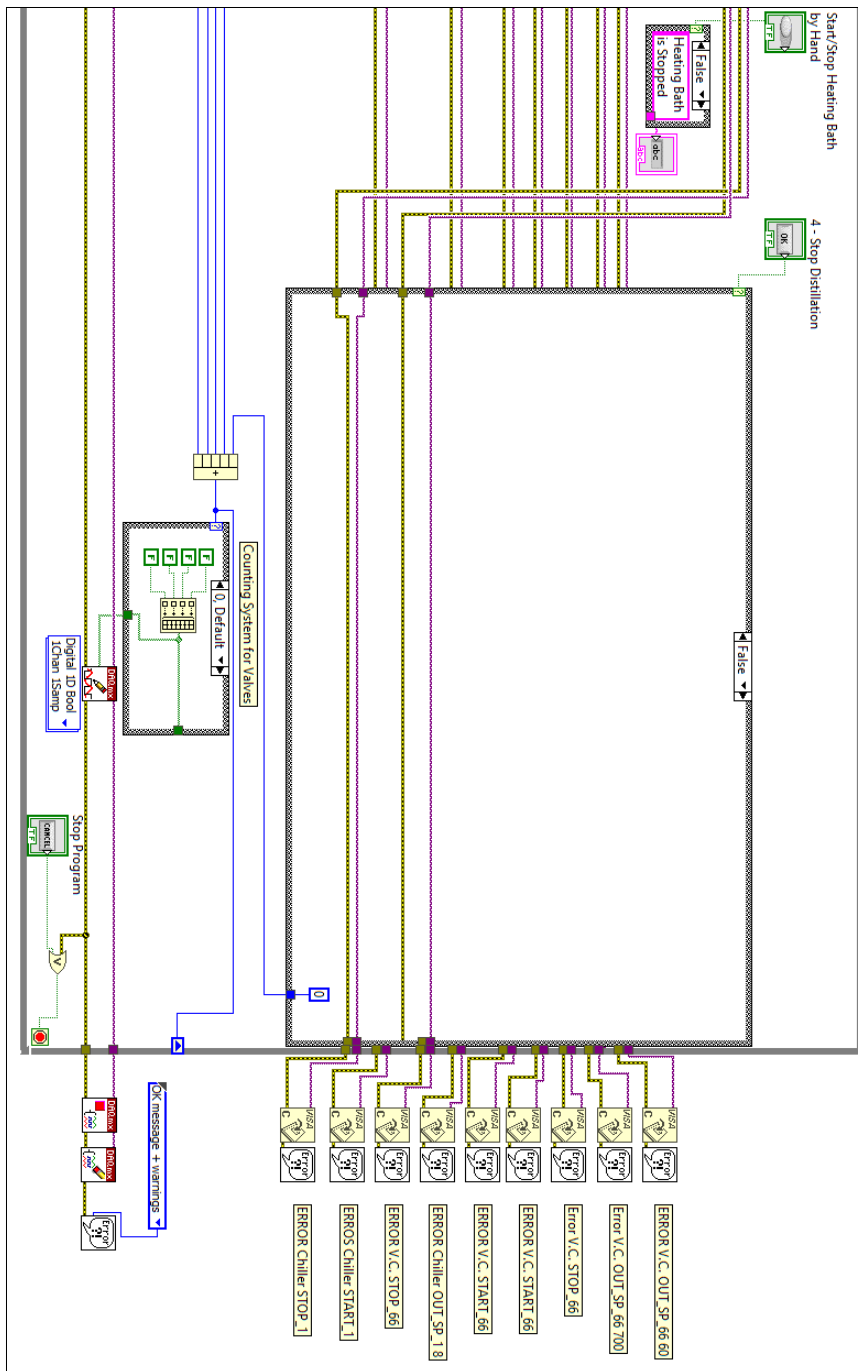# Appendix F.2: Program with Outer "False" Cases

Appendix G.1: Optimised *LabVIEW* Program

Appendix G.2: Optimised *LabVIEW* Program with Inner "False" Cases

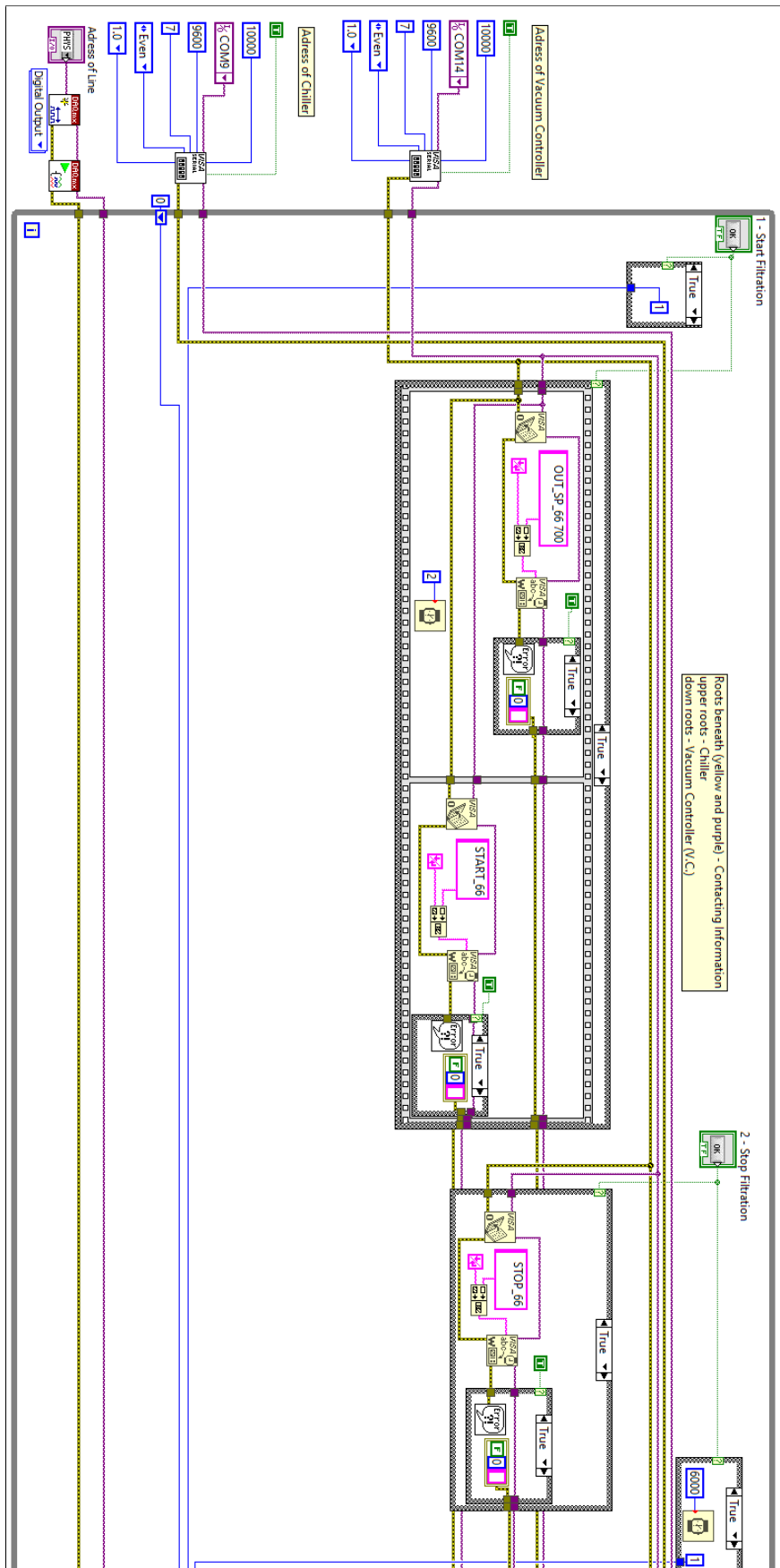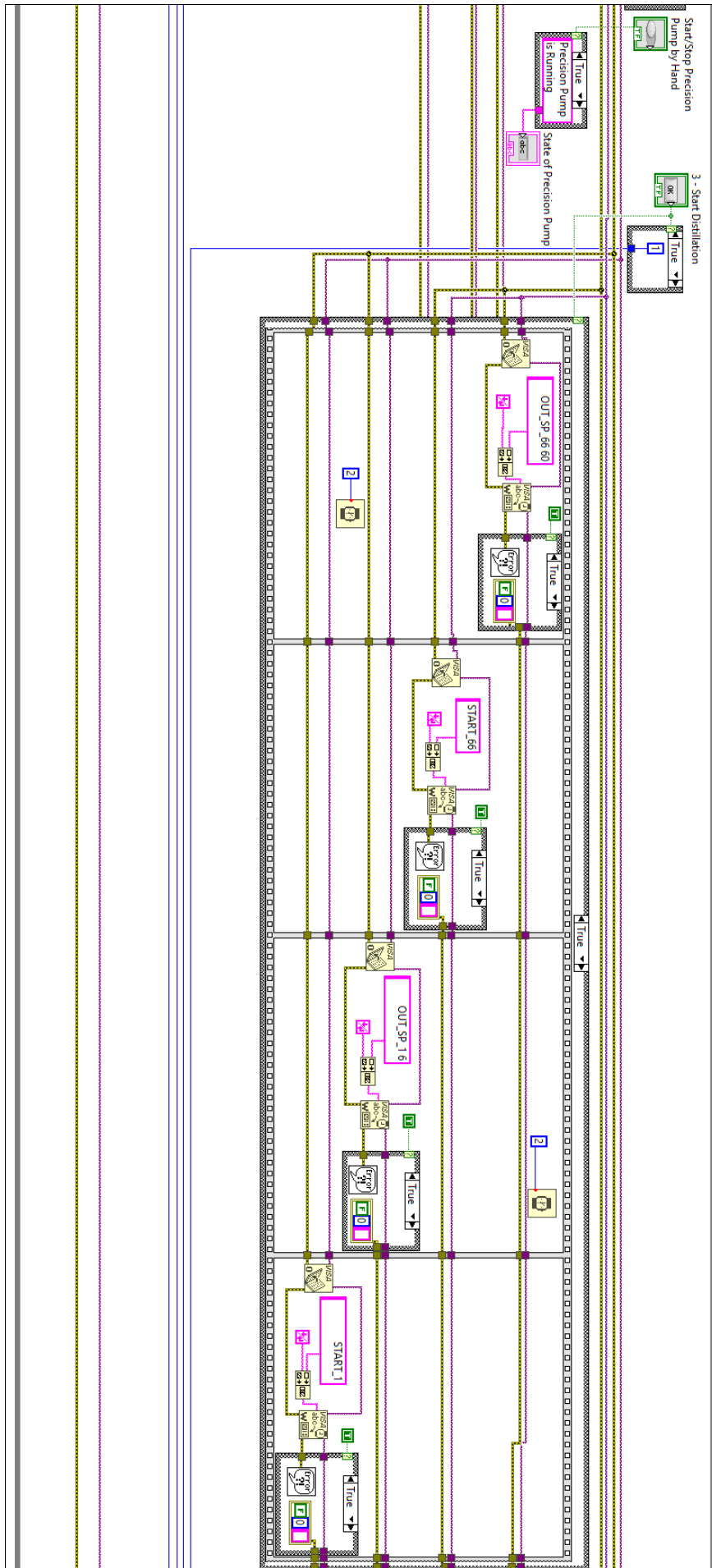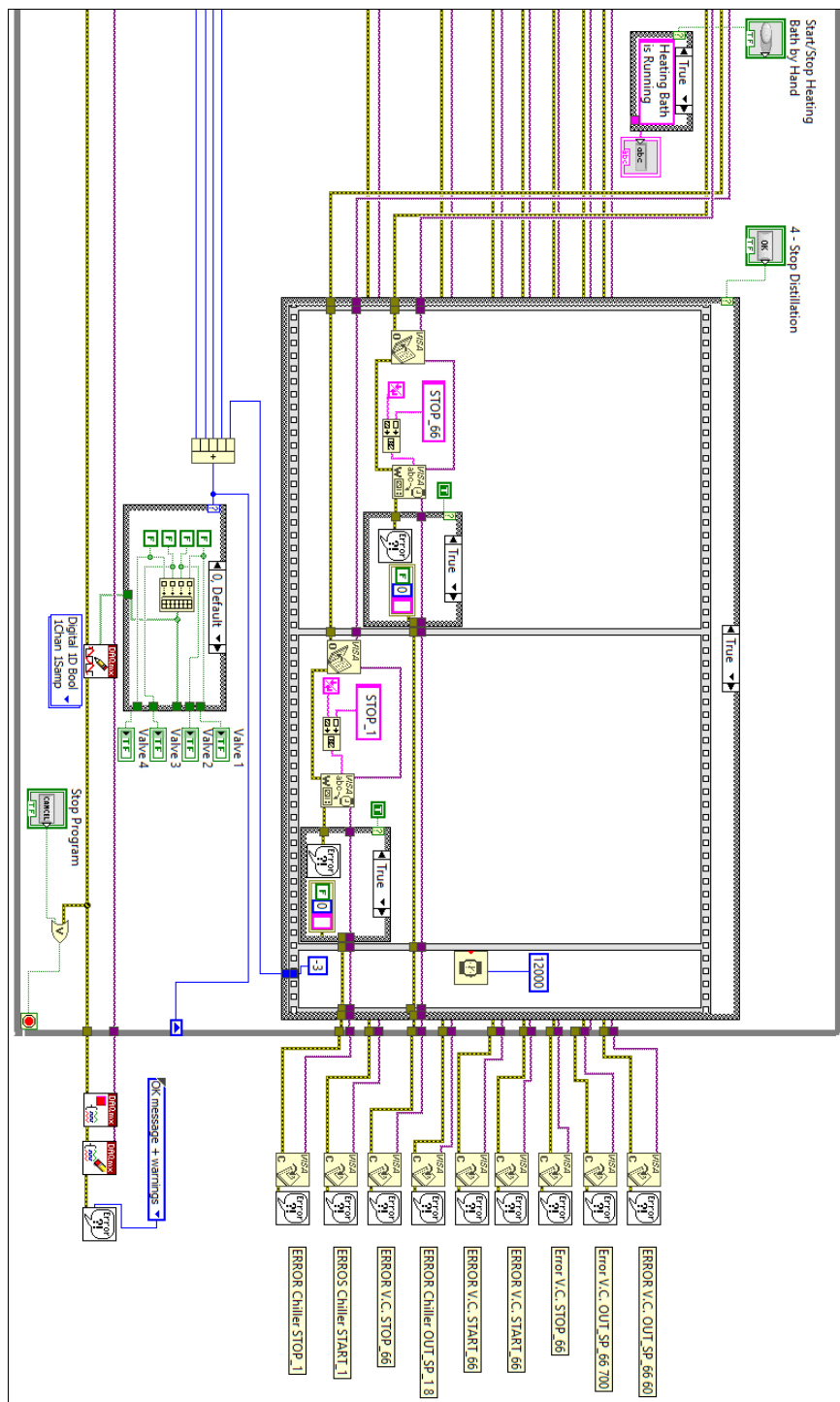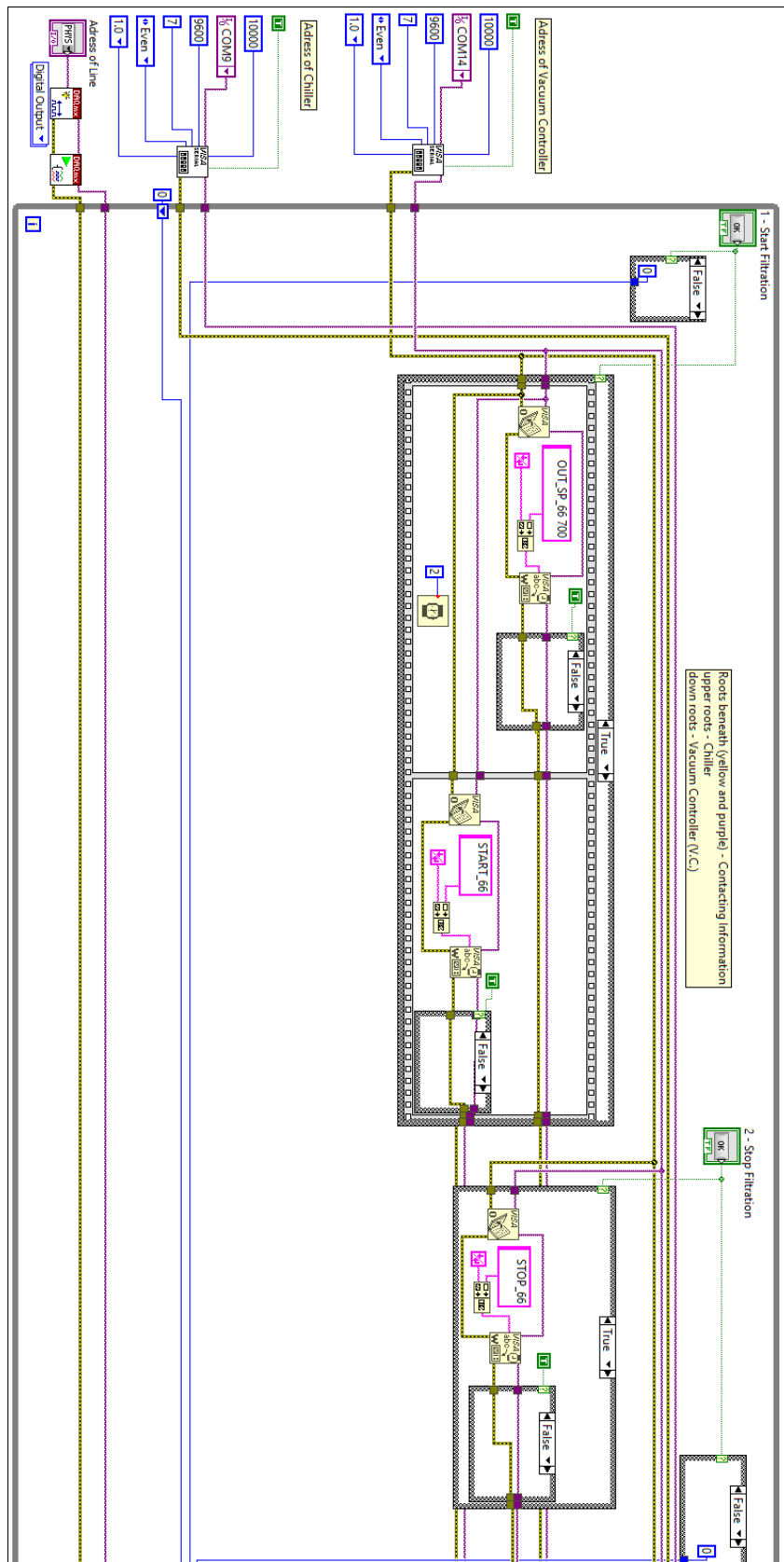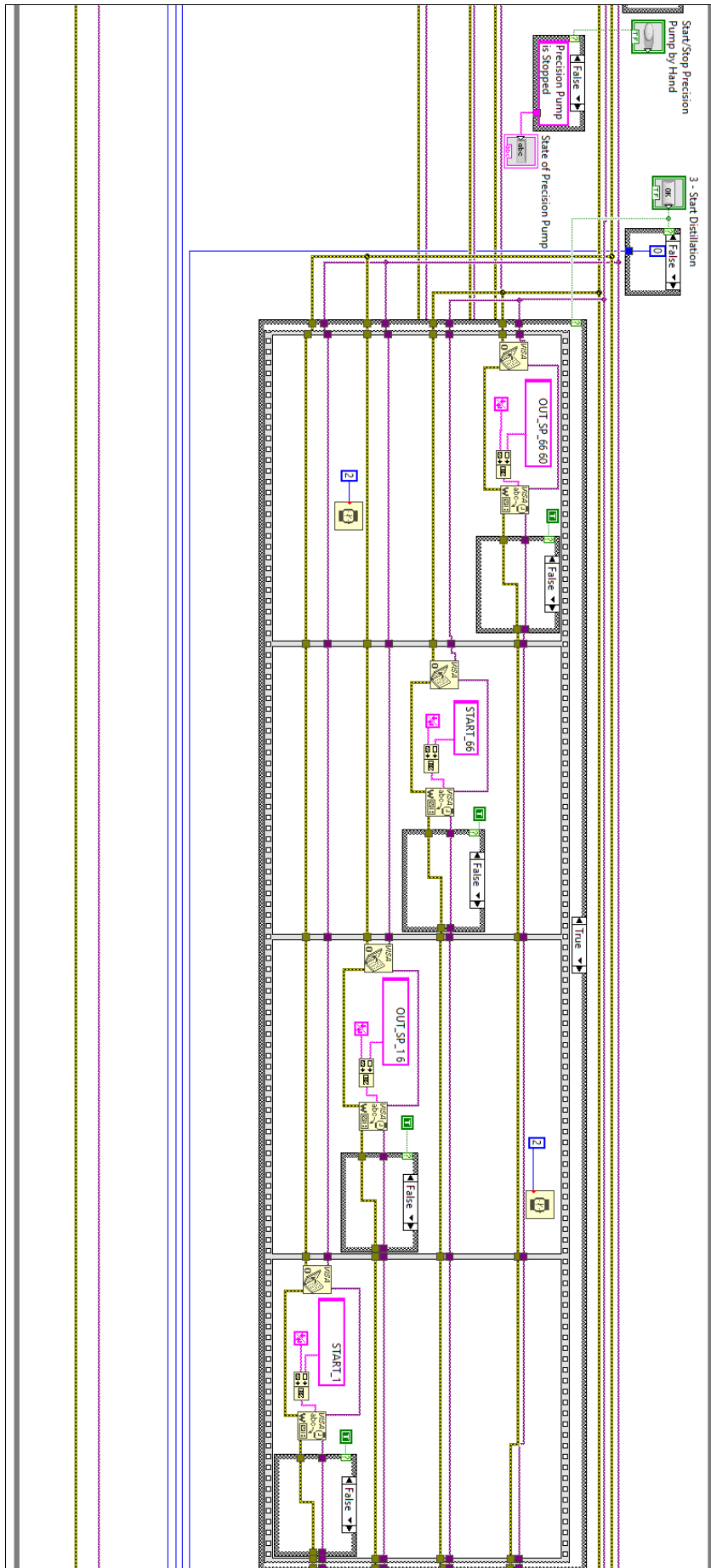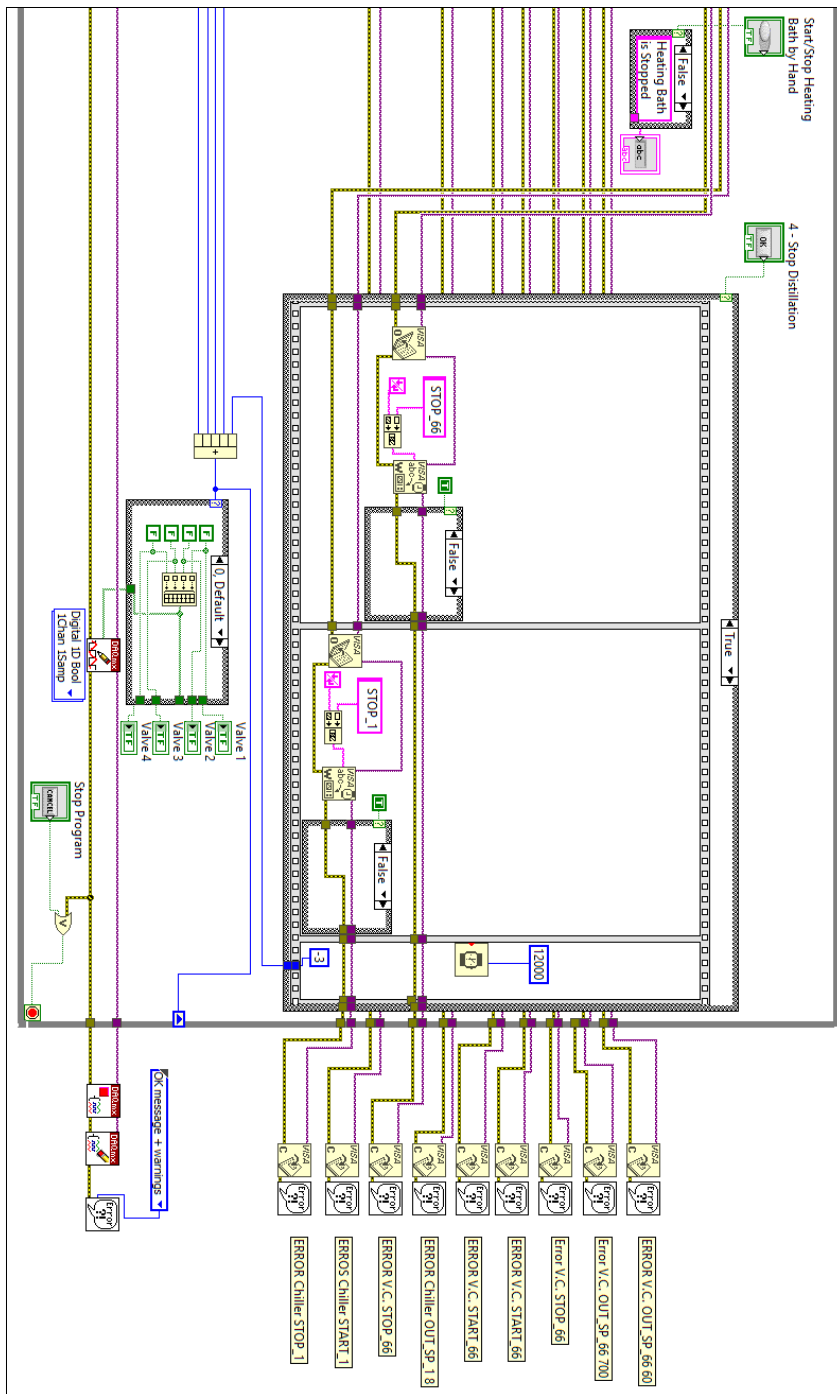# Appendix G.3: Optimised *LabVIEW* Program with Outer "False" Cases
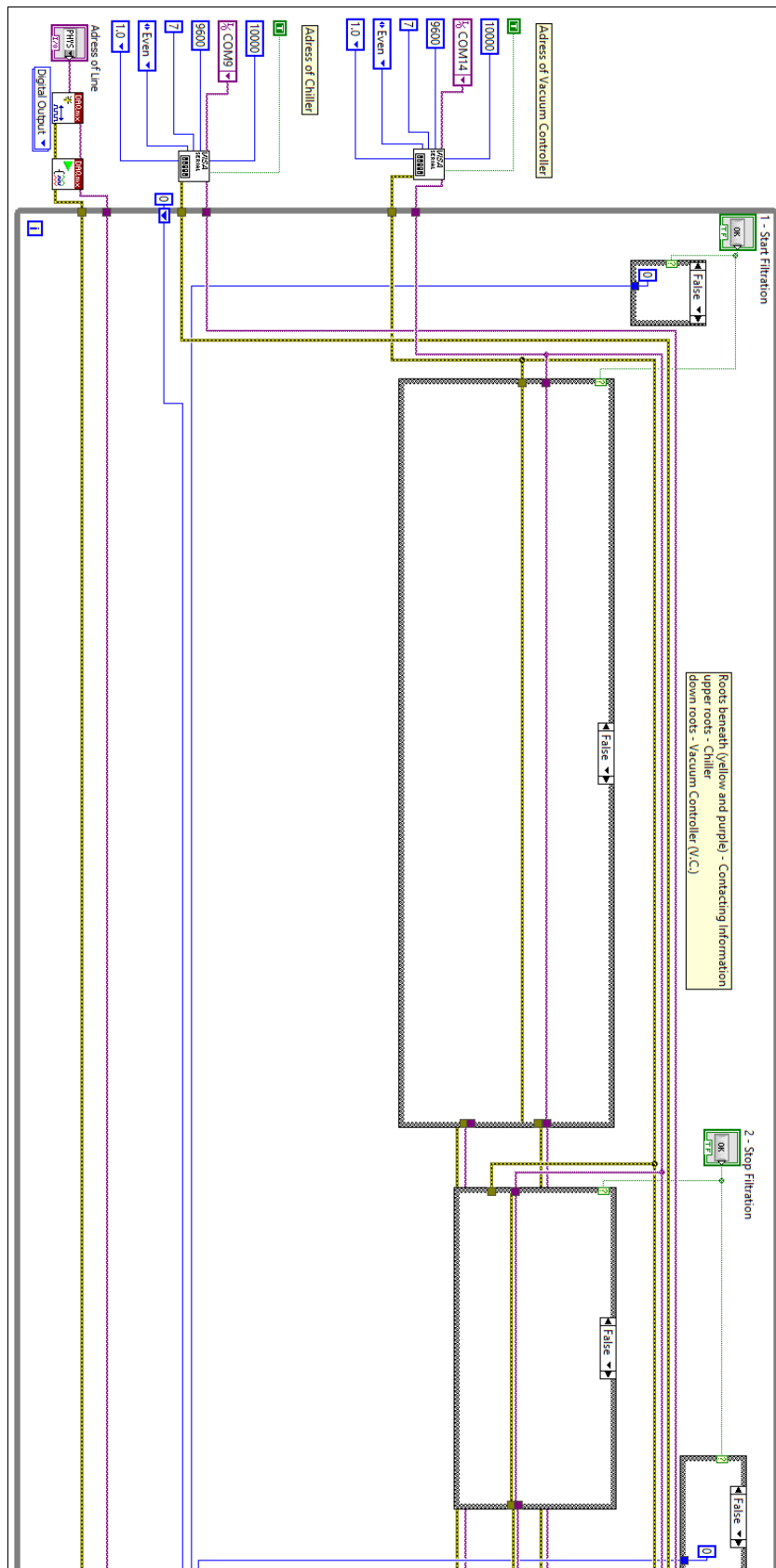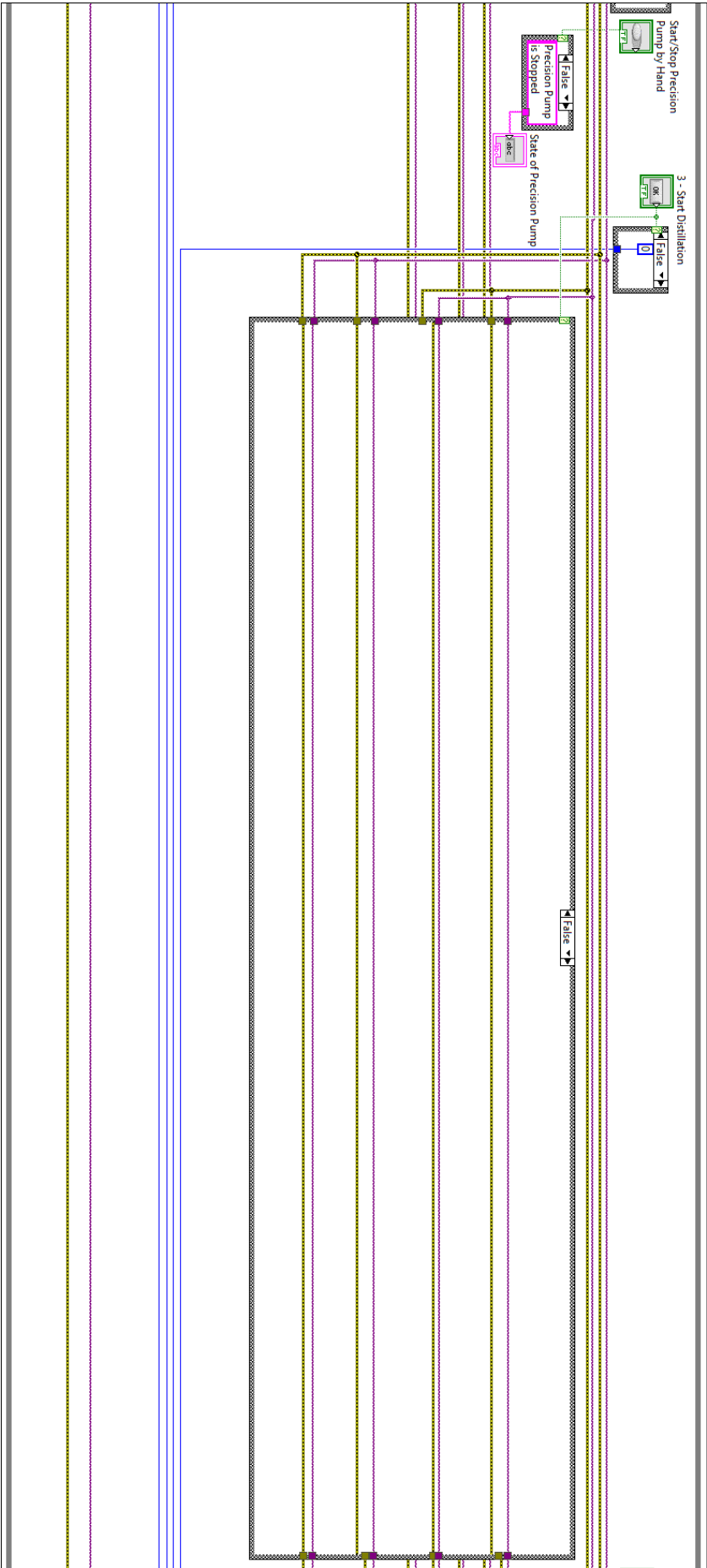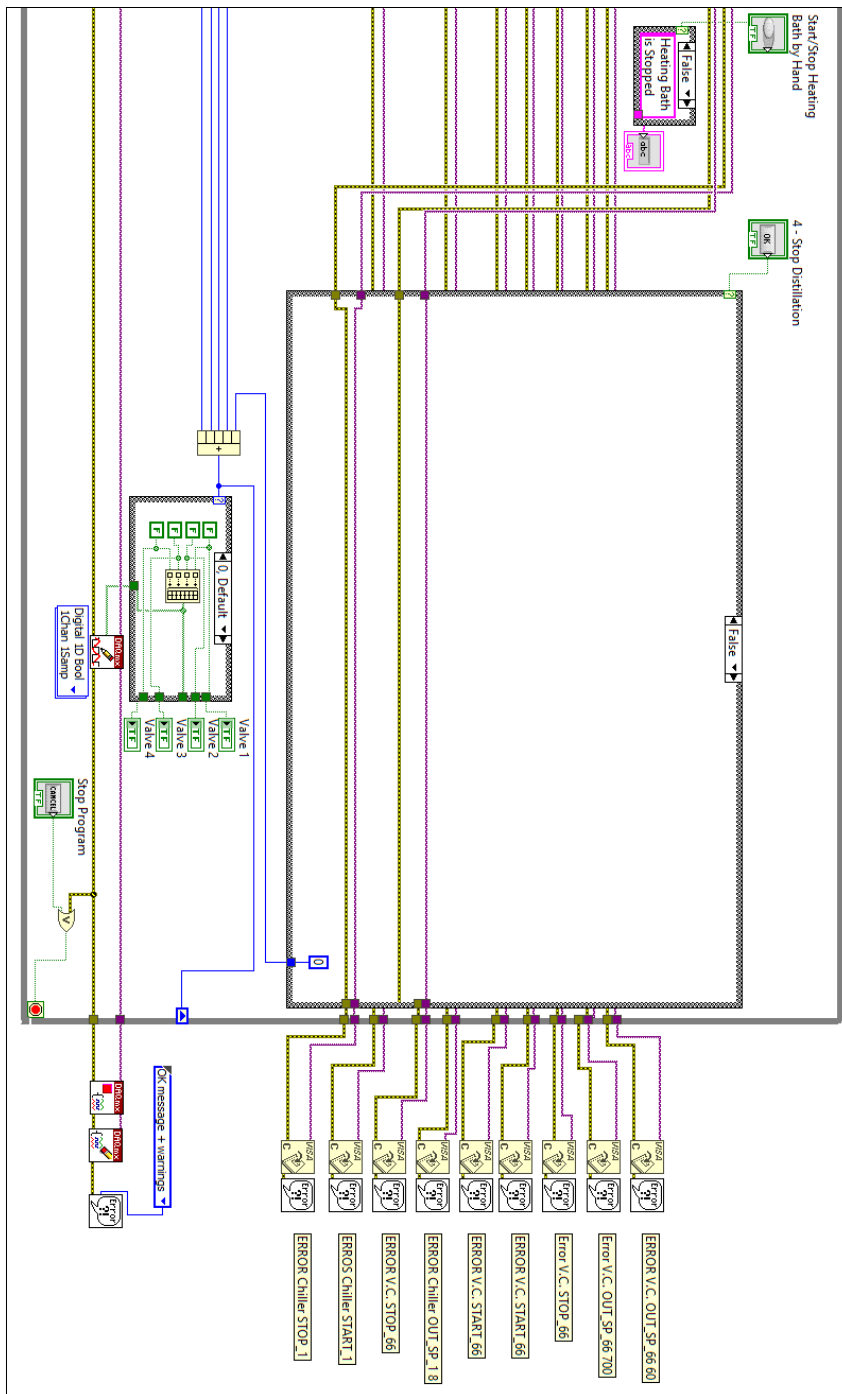
Appendix H.1: Test Procedure Check List

Number	Task	√
Preparation		
1.1.	Organise Environment	
1.2.	Clean Small Measuring Cup with Ultra-Pure Water	
1.3.	Clean Glass Pipette No.1 for samples with LHS-1	
1.4	Clean Glass Pipette No.2 for samples with LMS-1	
1.5	Clean Measuring Cylinder with Ultra-Pure Water	
1.6.	Label Wastewater Cup	
1.7.	Calibrate pH Meter	
1.8.	Calibrate Oximeter	
1.9.	Print Excel Sheet with Experiment Variables	
1.10.	Label Tubes: Mixture Ratio, Simulant, Extraction Time, With/Without Buffer	
Ultra-Pure Water		
2.1.	Fill 1l Ultra-Pure Water into 1l Glass Bottle	
2.2.	Insert Magnetic Stirring Bar	
2.3.	Letting it Mix on Magnetic Stirrer for 1 Hour	
Buffer Solution		
3.1.	Put 26.978 g of Ammonium Acetate into Measuring Cup	
3.2.	Add Ultra-Pure Water until 500 ml Volume is Reached	
3.3.	Wait until Ammonium Acetate is Totally Dissolved in Water	
3.4.	Transfer Solution into 2.5 l Measuring Cup	
3.5.	Fill 50 ml of Ultra-Pure Water into Second Measuring Cup	
3.6.	Put Tip on Precision Pipette	
3.7.	Put on Protective Gloves for Handling Acetic Acid	
3.8.	Add 2.86 ml Acetic Acid to This Second Cup with Precision Pipette	
3.9.	Fill Second Cup with Ultra-Pure Water until a Volume of 500 ml	
3.10.	Transfer Solution from Second Cup to 2.5 l Measuring Cup with Ammonium Acetate Water Solution	
3.11.	Add 1 l of Ultra-Pure Water	
Regolith Water		
4.1.	Measure Temperature, pH Level of Ultra-Pure Water with pH meter	
4.2.	Add 250 ml of Ultra-Pure Water to Plastic Container (8 times)	
4.3.	Label the Plastic Containers	
4.4.	2.5 g (2 times) or 0.5 g (2 times) of LHS-1 are Measured in Weighing Boat	
4.5.	2.5 g (2 times) or 0.5 g (2 times) of LMS-1 are Measured in Weighing Boat	
4.6.	Simulant is Added to Specific Container	
4.7.	Put Containers on Shaker (8 Containers)	
4.8.	Start Shaker	
4.9.	Start Stopwatch	
4.10.	Ensure 20 Rotations per Minute Mixing on Shaker	

	At 2 Minutes:	
4.11.	Stop Shaker for Water Extraction after 2 Minutes	
4.12.	Get Containers out of Shaker	
4.13.	Repeat following Steps for each Container	
4.14.	Extract approximately 10 ml with Glass Pipette	
4.15.	Fill into First Probe Tube	
4.16.	Put Container Back in Shaker	
4.17.	Start Shaker Again	
4.18.	Measure pH Level of Water Probe	
4.19.	Write pH Level into Printed Excel Sheet	
4.20.	Centrifuge all Probe Tubes for 10 Minutes	
4.21.	5 to 6 ml is Filled from Probe Tube into Measuring Cup while Trying to let Sediment Sit in First Probe Tube	
4.22.	5 to 6 ml Extracted from Measuring Cup with Syringe	
4.23.	Filter is Screwed on top of Syringe	
4.24.	Water is Filtrated into Second Probe Tube	
	At 15 Minutes:	
4.25.	Stop Shaker for Water Extraction after 15 Minutes	
4.26.	Get Containers out of Shaker	
4.27.	Repeat following Steps for each Container	
4.28.	Extract approximately 10 ml with Glass Pipette	
4.29.	Fill into First Probe Tube	
4.30.	Put Container Back in Shaker	
4.31.	Start Shaker Again	
4.32.	Measure pH Level of Water Probe	
4.33.	Write pH Level into Printed Excel Sheet	
4.34.	Centrifuge all Probe Tubes for 10 Minutes	
4.35.	5 to 6 ml is Filled from Probe Tube into Measuring Cup while Trying to let Sediment Sit in First Probe Tube	
4.36.	5 to 6 ml Extracted from Measuring Cup with Syringe	
4.37.	Filter is Screwed on top of Syringe	
4.38.	Water is Filtrated into Second Probe Tube	
	At 30 Minutes:	
4.39.	Stop Shaker for Water Extraction after 30 Minutes	
4.40.	Get Containers out of Shaker	
4.41.	Repeat following Steps for each Container	
4.42.	Extract approximately 10 ml with Glass Pipette	
4.43.	Fill into First Probe Tube	
4.44.	Put Container Back in Shaker	
4.45.	Start Shaker Again	
4.46.	Measure pH Level of Water Probe	
4.47.	Write pH Level into Printed Excel Sheet	
4.48.	Centrifuge all Probe Tubes for 10 Minutes	
4.49.	5 to 6 ml is Filled from Probe Tube into Measuring Cup while Trying to let Sediment Sit in First Probe Tube	
4.50.	5 to 6 ml Extracted from Measuring Cup with Syringe	

4.51.	Filter is Screwed on top of Syringe	
4.52.	Water is Filtrated into Second Probe Tube	
	At 60 Minutes:	
4.53.	Stop Shaker for Water Extraction after 60 Minutes	
4.54.	Get Containers out of Shaker	
4.55.	Repeat following Steps for each Container	
4.56.	Extract approximately 10 ml with Glass Pipette	
4.57.	Fill into First Probe Tube	
4.58.	Put Container Back in Shaker	
4.59.	Start Shaker Again	
4.60.	Measure pH Level of Water Probe	
4.61.	Write pH Level into Printed Excel Sheet	
4.62.	Centrifuge all Probe Tubes for 10 Minutes	
4.63.	5 to 6 ml is Filled from Probe Tube into Measuring Cup while Trying to let Sediment Sit in First Probe Tube	
4.64.	5 to 6 ml Extracted from Measuring Cup with Syringe	
4.65.	Filter is Screwed on top of Syringe	
4.66.	Water is Filtrated into Second Probe Tube	
	At 720 minutes (12 hours):	
4.67.	Stop Shaker for Water Extraction after 720 Minutes	
4.68.	Get Containers out of Shaker	
4.69.	Repeat following Steps for each Container	
4.70.	Extract approximately 10 ml with Glass Pipette	
4.71.	Fill into First Probe Tube	
4.72.	Put Container Back in Shaker	
4.73.	Start Shaker Again	
4.74.	Measure pH Level of Water Probe	
4.75.	Write pH Level into Printed Excel Sheet	
4.76.	Centrifuge all Probe Tubes for 10 Minutes	
4.77.	5 to 6 ml is Filled from Probe Tube into Measuring Cup while Trying to let Sediment Sit in First Probe Tube	
4.78.	5 to 6 ml Extracted from Measuring Cup with Syringe	
4.79.	Filter is Screwed on top of Syringe	
4.80.	Water is Filtrated into Second Probe Tube	
	At 1440 minutes (24 hours):	
4.81.	Stop Shaker for Water Extraction after 1440 Minutes	
4.82.	Get Containers out of Shaker	
4.83.	Repeat following Steps for each Container	
4.84.	Extract approximately 10 ml with Glass Pipette	
4.85.	Fill into First Probe Tube	
4.86.	Put Container Back in Shaker	
4.87.	Start Shaker Again	
4.88.	Measure pH Level of Water Probe	
4.89.	Write pH Level into Printed Excel Sheet	

4.90.	Centrifuge all Probe Tubes for 10 Minutes	
4.91.	5 to 6 ml is Filled from Probe Tube into Measuring Cup while Trying to let Sediment Sit in First Probe Tube	
4.92.	5 to 6 ml Extracted from Measuring Cup with Syringe	
4.93.	Filter is Screwed on top of Syringe	
4.94.	Water is Filtrated into Second Probe Tube	
	At 4320 minutes (72 hours):	
4.95.	Stop Shaker for Water Extraction after 4320 Minutes	
4.96.	Get Containers out of Shaker	
4.97.	Repeat following Steps for each Container	
4.98.	Extract approximately 10 ml with Glass Pipette	
4.99.	Fill into First Probe Tube	
4.100.	Put Container Back in Shaker	
4.101.	Start Shaker Again	
4.102.	Measure pH Level of Water Probe	
4.103.	Write pH Level into Printed Excel Sheet	
4.104.	Centrifuge all Probe Tubes for 10 Minutes	
4.105.	5 to 6 ml is Filled from Probe Tube into Measuring Cup while Trying to let Sediment Sit in First Probe Tube	
4.106.	5 to 6 ml Extracted from Measuring Cup with Syringe	
4.107.	Filter is Screwed on top of Syringe	
4.108.	Water is Filtrated into Second Probe Tube	
Regolith Buffer		
5.1.	Measure Temperature, pH Level of Buffer Solution with pH meter	
5.2.	Add 250 ml of Buffer Solution to Plastic Container (8 times)	
5.3.	Label the Plastic Containers	
5.4.	2.5 g (2 times) or 0.5 g (2 times) of LHS-1 are Measured in Weighing Boat	
5.5.	2.5 g (2 times) or 0.5 g (2 times) of LMS-1 are Measured in Weighing Boat	
5.6.	Simulant is Added to Specific Container	
5.7.	Put Containers on Shaker (8 Containers)	
5.8.	Start Shaker	
5.9.	Start Stopwatch	
5.10.	Ensure 20 Rotations per Minute Mixing on Shaker	
	At 2 Minutes:	
5.11.	Stop Shaker for Water Extraction after 2 Minutes	
5.12.	Get Containers out of Shaker	
5.13.	Repeat following Steps for each Container	
5.14.	Extract approximately 10 ml with Glass Pipette	
5.15.	Fill into First Probe Tube	
5.16.	Put Container Back in Shaker	
5.17.	Start Shaker Again	
5.18.	Measure pH Level of Water Probe	
5.19.	Write pH Level into Printed Excel Sheet	
5.20.	Centrifuge all Probe Tubes for 10 Minutes	

5.21.	5 to 6 ml is Filled from Probe Tube into Measuring Cup while Trying to let Sediment Sit in First Probe Tube	
5.22.	5 to 6 ml Extracted from Measuring Cup with Syringe	
5.23.	Filter is Screwed on top of Syringe	
5.24.	Water is Filtrated into Second Probe Tube	
	At 15 Minutes:	
5.25.	Stop Shaker for Water Extraction after 15 Minutes	
5.26.	Get Containers out of Shaker	
5.27.	Repeat following Steps for each Container	
5.28.	Extract approximately 10 ml with Glass Pipette	
5.29.	Fill into First Probe Tube	
5.30.	Put Container Back in Shaker	
5.31.	Start Shaker Again	
5.32.	Measure pH Level of Water Probe	
5.33.	Write pH Level into Printed Excel Sheet	
5.34.	Centrifuge all Probe Tubes for 10 Minutes	
5.35.	5 to 6 ml is Filled from Probe Tube into Measuring Cup while Trying to let Sediment Sit in First Probe Tube	
5.36.	5 to 6 ml Extracted from Measuring Cup with Syringe	
5.37.	Filter is Screwed on top of Syringe	
5.38.	Water is Filtrated into Second Probe Tube	
	At 30 Minutes:	
5.39.	Stop Shaker for Water Extraction after 30 Minutes	
5.40.	Get Containers out of Shaker	
5.41.	Repeat following Steps for each Container	
5.42.	Extract approximately 10 ml with Glass Pipette	
5.43.	Fill into First Probe Tube	
5.44.	Put Container Back in Shaker	
5.45.	Start Shaker Again	
5.46.	Measure pH Level of Water Probe	
5.47.	Write pH Level into Printed Excel Sheet	
5.48.	Centrifuge all Probe Tubes for 10 Minutes	
5.49.	5 to 6 ml is Filled from Probe Tube into Measuring Cup while Trying to let Sediment Sit in First Probe Tube	
5.50.	5 to 6 ml Extracted from Measuring Cup with Syringe	
5.51.	Filter is Screwed on top of Syringe	
5.52.	Water is Filtrated into Second Probe Tube	
	At 60 Minutes:	
5.53.	Stop Shaker for Water Extraction after 60 Minutes	
5.54.	Get Containers out of Shaker	
5.55.	Repeat following Steps for each Container	
5.56.	Extract approximately 10 ml with Glass Pipette	
5.57.	Fill into First Probe Tube	
5.58.	Put Container Back in Shaker	

5.59.	Start Shaker Again	
5.60.	Measure pH Level of Water Probe	
5.61.	Write pH Level into Printed Excel Sheet	
5.62.	Centrifuge all Probe Tubes for 10 Minutes	
5.63.	5 to 6 ml is Filled from Probe Tube into Measuring Cup while Trying to let Sediment Sit in First Probe Tube	
5.64.	5 to 6 ml Extracted from Measuring Cup with Syringe	
5.65.	Filter is Screwed on top of Syringe	
5.66.	Water is Filtrated into Second Probe Tube	
	At 720 minutes (12 hours):	
5.67.	Stop Shaker for Water Extraction after 720 Minutes	
5.68.	Get Containers out of Shaker	
5.69.	Repeat following Steps for each Container	
5.70.	Extract approximately 10 ml with Glass Pipette	
5.71.	Fill into First Probe Tube	
5.72.	Put Container Back in Shaker	
5.73.	Start Shaker Again	
5.74.	Measure pH Level of Water Probe	
5.75.	Write pH Level into Printed Excel Sheet	
5.76.	Centrifuge all Probe Tubes for 10 Minutes	
5.77.	5 to 6 ml is Filled from Probe Tube into Measuring Cup while Trying to let Sediment Sit in First Probe Tube	
5.78.	5 to 6 ml Extracted from Measuring Cup with Syringe	
5.79.	Filter is Screwed on top of Syringe	
5.80.	Water is Filtrated into Second Probe Tube	
	At 1440 minutes (24 hours):	
5.81.	Stop Shaker for Water Extraction after 1440 Minutes	
5.82.	Get Containers out of Shaker	
5.83.	Repeat following Steps for each Container	
5.84.	Extract approximately 10 ml with Glass Pipette	
5.85.	Fill into First Probe Tube	
5.86.	Put Container Back in Shaker	
5.87.	Start Shaker Again	
5.88.	Measure pH Level of Water Probe	
5.89.	Write pH Level into Printed Excel Sheet	
5.90.	Centrifuge all Probe Tubes for 10 Minutes	
5.91.	5 to 6 ml is Filled from Probe Tube into Measuring Cup while Trying to let Sediment Sit in First Probe Tube	
5.92.	5 to 6 ml Extracted from Measuring Cup with Syringe	
5.93.	Filter is Screwed on top of Syringe	
5.94.	Water is Filtrated into Second Probe Tube	
	At 4320 minutes (72 hours):	
5.95.	Stop Shaker for Water Extraction after 4320 Minutes	
5.96.	Get Containers out of Shaker	

5.97.	Repeat following Steps for each Container	
5.98.	Extract approximately 10 ml with Glass Pipette	
5.99.	Fill into First Probe Tube	
5.100.	Put Container Back in Shaker	
5.101.	Start Shaker Again	
5.102.	Measure pH Level of Water Probe	
5.103.	Write pH Level into Printed Excel Sheet	
5.104.	Centrifuge all Probe Tubes for 10 Minutes	
5.105.	5 to 6 ml is Filled from Probe Tube into Measuring Cup while Trying to let Sediment Sit in First Probe Tube	
5.106.	5 to 6 ml Extracted from Measuring Cup with Syringe	
5.107.	Filter is Screwed on top of Syringe	
5.108.	Water is Filtrated into Second Probe Tube	
Acidification (Only Water Probes)		
6.1.	Put on Protective Gloves for Handling Nitric Acid	
6.2.	Put Tip on Precision Pipette No.1	
6.3.	Fill 5 ml of every Probe into Third Probe Tube using Precision Pipette No.1	
6.4.	Put Tip on Precision Pipette No.2	
6.5.	Put on Protective Gloves for Handling Nitric Acid	
6.6.	Add 0.2 ml of Nitric Acid into third Probe Tube with Precision Pipette No.2	
6.7.	Repeat for all Probes	
Post-Processing		
7.1.	Bundle Probe Tubes and Pack into Box for Transport to Hamburg	